Catalysis Reviews: Science and Engineering
Publication details, including instructions for authors and subscription information:
http://www.tandfonline.com/loi/lctr20

Steady-State and Dynamic Reactor Models for Hydrotreatment of Oil Fractions: A Review

Fabián S. Mederos [a], Ignacio Elizalde [b] & Jorge Ancheyta [a c]
[a] Instituto Mexicano del Petróleo, Eje Central Lázaro Cárdenas Norte 152, Col. San Bartolo Atepehuacan, México D.F. 07730, México
[b] Facultad de Química, UNAM, Ciudad Universitaria, México D.F. 04510, México
[c] Escuela Superior de Ingeniería Química e Industrias Extractivas (ESIQIE-IPN), UPALM, Zacatenco, México D.F. 07738, México
Version of record first published: 10 Nov 2009.

To cite this article: Fabián S. Mederos , Ignacio Elizalde & Jorge Ancheyta (2009): Steady-State and Dynamic Reactor Models for Hydrotreatment of Oil Fractions: A Review, Catalysis Reviews: Science and Engineering, 51:4, 485-607

To link to this article: http://dx.doi.org/10.1080/01614940903048612

Catalysis Reviews, 51:485–607, 2009

ISSN: 0161-4940 print 1520-5703 online
DOI: 10.1080/01614940903048612

Steady-State and Dynamic Reactor Models for Hydrotreatment of Oil Fractions: A Review

Fabián S. Mederos[1], Ignacio Elizalde[2], and Jorge Ancheyta[1,3]

[1] Instituto Mexicano del Petróleo, Eje Central Lázaro Cárdenas Norte 152, Col. San Bartolo Atepehuacan, México D.F. 07730, México
[2] Facultad de Química, UNAM, Ciudad Universitaria, México D.F. 04510, México
[3] Escuela Superior de Ingeniería Química e Industrias Extractivas (ESIQIE-IPN), UPALM, Zacatenco, México D.F. 07738, México

The modeling of catalytic hydrotreatment reactors for petroleum fractions have been classified in several ways, for example steady-state and dynamic, pseudohomogeneous, and heterogeneous, and so on. Depending on the system to be modeled, operating conditions and type of feedstock, these approaches could exhibit some advantages and disadvantages, wide scopes and limitations. In this review, the discussion about those modeling aspects, already published, is used to develop a generalized reactor model, which can be simplified in order to derive each single model previously reported. Some guides to estimate model parameters are also given.

Keywords Hydrotreatment, Modeling, Reactor design, Trickle-bed reactors

1. INTRODUCTION

The catalytic hydrotreatment (**HDT**), a hydrogen addition process which increases hydrogen/carbon ratio of a hydrocarbon feed, has become one of the fundamental processes in the petroleum-refining industry from technical, economic, and environmental points of view, requires of constant technological research (1). The HDT process is essential to obtain fuels with improved quality and low polluting compounds content (sulfur, nitrogen, aromatics, etc.). This process has gained significant attention due to the environmental

Received April 25, 2008; Accepted February 27, 2009.
Address correspondence to Jorge Ancheyta, Instituto Mexicano del Petróleo, Eje Central Lázaro Cárdenas Norte 152, Col. San Bartolo Atepehuacan, México D.F. 07730 México. E-mail: jancheyt@imp.mx

restrictions during combustion of fossil fuels such as emissions of sulfur oxides (**SOx**), nitrogen oxides (**NOx**) and volatile organic matter (**VOM**) such as aromatics and olefins (1, 2).

Except for hydrotreating of naphtha, in which a gas-solid fixed-bed reactor (**FBR**) is used, three-phase reactors employed for HDT applications operate in trickle-bed flow. Three-phase catalytic reactors (**TPCR**) are vessels where three phases are present: gas, liquid, and solid (the catalyst is solid phase), e.g. trickle beds, or with mobile solid particles, such as mechanically stirred slurry reactor, slurry bubbling reactor and ebullated bed reactor. In most fixed bed systems, the flowing phases (gas and liquid) move cocurrently. The countercurrent flow, though possible, is rarely used (3). With the mobile solid particles, continuous addition and withdrawal of solid particles in the reactor is presented. The catalyst particle size in fixed beds of TPCRs is more or less one order of magnitude higher than those when the solid particles are mobile. Regardless of particle size in TPCRs, there is resistance to mass transfer in both gas-liquid and liquid-solid interphases, and the latter is often rate controlling (4).

The trickle-bed reactor (**TBR**) is extensively applied in hydroprocessing of petroleum fractions for removal of impurities i.e. sulfur, nitrogen and other hetero-atoms, for hydrocracking (**HCR**) of heavy or residual oil stocks to produce lower boiling range materials and to improve the quality of the feed for subsequent processing, hydrofinishing, or hydrotreatment of lubricant oils (5, 6). When the main purpose of an HDT plant is to remove sulfur compounds from petroleum fractions without significant changes in boiling point distribution, the process is normally called hydrodesulfurization (**HDS**). A TBR is a type of packed bed reactor (**PBR**) where a gas phase and a liquid phase flow cocurrently downward through the porous catalyst packing (solid phase), as fixed bed, in which different reactions take place (7). In the trickle flow regime, the liquid reactant (dispersed phase) flows downward through the reactor in the form of thin laminar film, rivulets and droplets around the solid catalyst. The gas reactant (continuous phase) fills the remaining void space of the catalyst bed and flows separately. The trickle flow regime occurs at relatively low gas and liquid flow rates, that is why it is classified as low-interaction-regime of TPCR systems (8–10).

It is envisaged that new regulations for automotive fuels will be applied worldwide, for instance the so-called ultralow sulfur (**ULS**) specifications (10 ppm in gasoline and diesel) (11, 12). Therefore, apart from modifications in catalyst formulation, reactor design and process configuration, the refineries will need to increase the severity in the operating conditions of the HDT reactor in order to accomplish the more stringent specifications (13–15). These new conditions will alter the performance of HDT commercial units. One way to cope up with this situation is by modeling and simulation which allows for

understanding the phenomena occurring in the reactor with the main purpose of establishing the optimal operating conditions.

Up until now articles dealing with the general aspects of TBRs modeling can easily be found in the literature but critical reviews that specifically treat steady-state and dynamic (unsteady-state) modeling and simulation of TBRs for hydrotreatment of oil fractions are scarce (7, 16–25). Among the different approaches for modeling chemical reactors sustaining HDT reactions, the most common are those that perform the analysis based on local average behavior of molecules (average models). These models allow for using differential calculus and other related mathematical tools in the analysis of the reactor performance.

The objective of this review is the description and analysis of the main average reactor models for HDT of oil fractions reported in the literature up to date in order to examine their advantages and disadvantages, so a general deterministic HDT reactor model can be structured.

2. MODELING OF TRICKLE-BED REACTORS PERFORMANCE

For decades, different models have been developed to understand, design, simulate or optimize the performance of the TBRs employed in HDT units for production of high quality fuels. This development has been parallel to the need for more detailed prediction capability motivated by continuous changes in HDT process conditions (nature of feedstocks, new reactor and catalyst design, reaction conditions, etc.). In this first part an attempt has been made to organize the different model classifications and a few criteria are suggested for the proper selection of a reactor model.

A. Classification

Few classifications of TBR models have been reported in the literature, based on their different level of sophistication. For instance Shinnar (26) proposed a simple classification which distinguishes between "learning" and "predictive" models. The former are of neuronal networks type, and the latter can be sub-classified as deterministic and stochastic models as illustrated in Fig. 1.

On the one hand, in deterministic models, continuous models (i.e., Fickian, dispersion, diffusion or effective transport models using Fick's and Fourier's laws of mass and heat dispersion, respectively) are represented by differential equations with one or more independent variables; while discrete models are finite stage models described mainly by capillary, sphere packing or cell models, the latter was introduced firstly by Deans and Lapidus in 1960 (27).

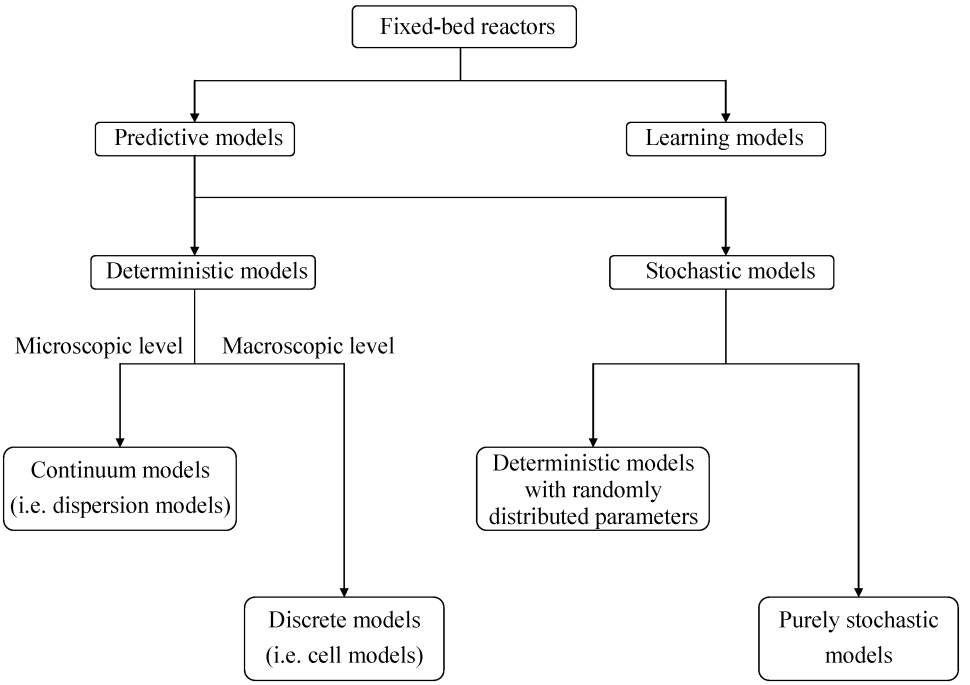

Figure 1: General classification of FBRs.

According to these authors, interstices between packing elements are idealized as perfectly stirred tanks in order to represent the dispersion behavior. On the other hand, the stochastic models are characterized by taking into account random arrangement of particles and void spaces within randomly packed beds. The purely stochastic models could be employed only if sufficient statistical information concerning the structure of packed bed, void spaces and fluid discrete paths is available. Its application in cell models, as example, may be developed by varying the cell size and choosing cell sizes to conform the size distribution of void spaces in the packed bed. However, its use seems to be doubtful due to the computational cost. An alternative option within the stochastic model type could be the use of deterministic models based upon differential equations while considering void spaces in the packing as sources of perturbations in the patterns of concentration, temperature and fluid velocity through the bed. In these models, also known as deterministic models with random perturbation, the particles and void spaces can be positioned randomly throughout the bed, and statistical properties of the patterns can be calculated. Whereas the purely stochastic models change the original conception of the dispersion models, the introduction of randomly distributed parameters in discrete models produces a large amount of model variations without changing the original character of the model. Since

deterministic models are described by differential equations, their application using model parameters randomly distributed is only appropriate for macro-scale studies, where the effect of individual void spaces on the patterns is negligible.

Crine et al. (28) defined another classification based on successive levels of modellization at various observation planes:

1. **Microscopic level**, which corresponds to large volume elements at the molecular scale but small at the bed granulometry. The transport processes are described theoretically by differential equations of continuum type.
2. **First macroscopic level** corresponding to local phenomenological observations; which assumes the volume elements large enough to consider the bed as locally homogeneous. At this level, the regionalized variables can be defined, e.g., fluid holdups, irrigation rate, etc., and all the transport processes can be described by using the concept of an elementary transport cell based on a simplified representation of the packing.
3. **Second macroscopic level** characterizing the bed as a whole, where liquid maldistribution (due to random clustering of the transport cells) has to be considered.

Froment and Bischoff (29) have introduced perhaps the most popular classification of continuous models for adiabatic and nonadiabatic FBRs, which is shown in Fig. 2. They considered that if gradients of concentration and temperature across the phase boundaries cannot be neglected, the

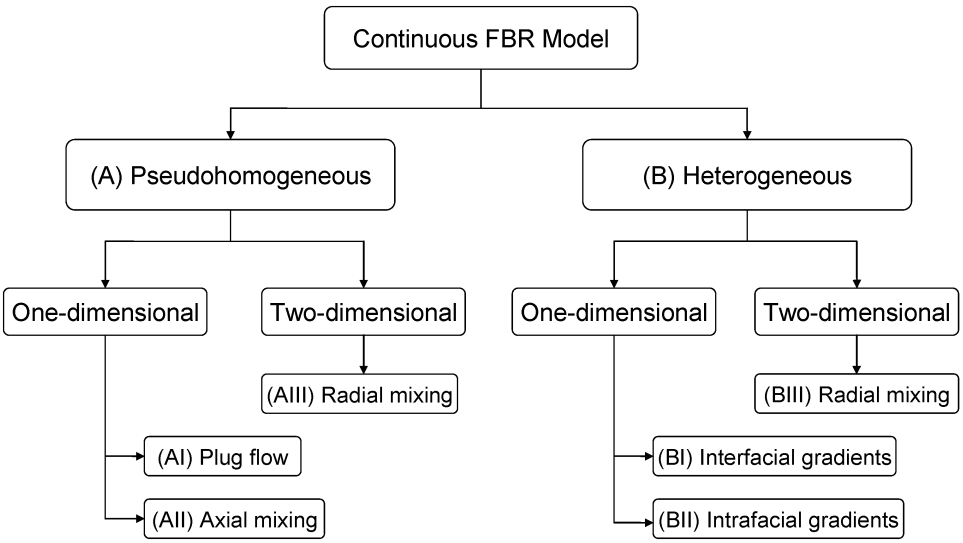

Figure 2: Classification of continuous models for FBRs.

continuum concept can be narrowed to the phases present in the reactor (heterogeneous continuum models), while if the heterogeneous fluid/particle system is regarded as a single pseudohomogeneous phase, the modeling of the FBR is drastically simplified to the state variables of a single isotropic continuum (pseudohomogeneous continuum models).

According to Iannibello (30), the simple plug flow pseudohomogeneous model proposed in the literature to predict the behavior of hydrotreatment TBRs can be grouped into two types: "kinetic" models and "hydrodynamic" models (Fig. 3). Kinetic based models are generally functions of intrinsic rates and do not account for the influence of hydrodynamics and related phenomena on the conversion rate. Hydrodynamic based models attempt to incorporate the influence of hydrodynamics on catalyst utilization, assuming generally plug flow and introducing an apparent kinetic rate constant (k_{app}). Two approaches have been followed in the development of hydrodynamic models, one relates to the reactor overall efficiency to the external liquid mixing, and the other relates it to the liquid-solid contacting efficiency, which can be determined with the liquid holdup or with the irrigation rate of the bed (28).

The pseudohomogeneous models consider the bed as a pseudocontinuum, while heterogeneous models distinguish between temperatures and concentrations in the bulk gas phase and at the surface of the catalyst. Each category can be considered with one- (**1D**) or two-dimensional (**2D**) models to account in less or more detail for temperature and concentration gradients inside the reactor (Fig. 4).

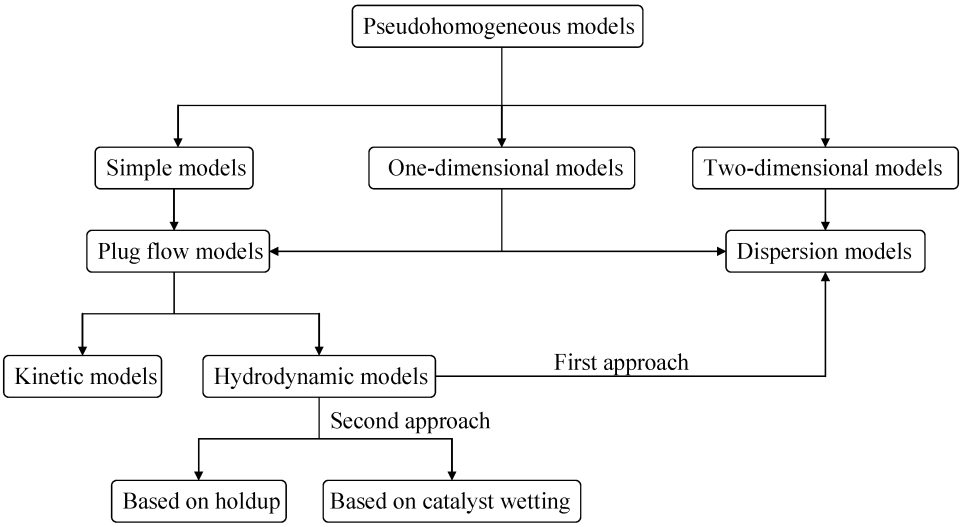

Figure 3: Classification of continuum pseudohomogeneous models for FBRs.

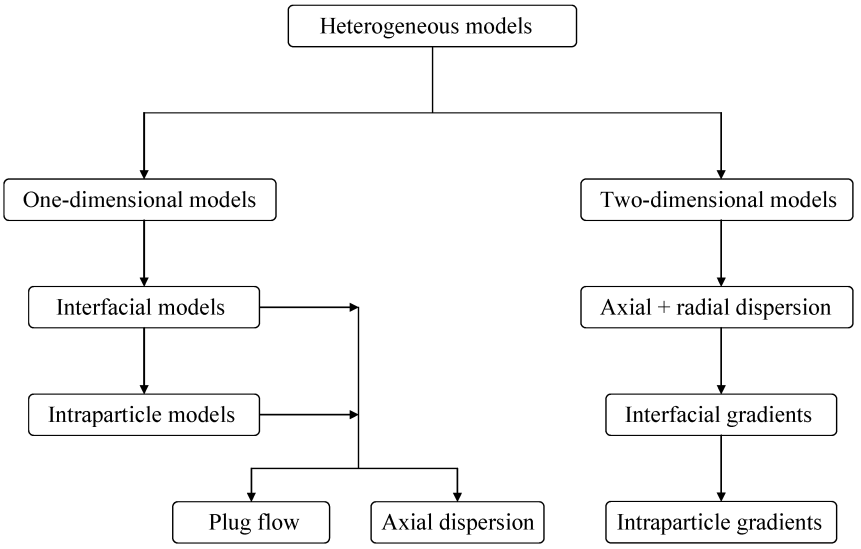

Figure 4: Classification of continuum heterogeneous models for FBRs.

B. Selection of Model Complexity

The level of sophistication and complexity of a reactor model depends mainly on the purpose of the investigation and need of prediction capabilities. On the one hand the simplest models assume either perfect mixing or plug-flow, i.e., the well-known extreme cases of ideality. The deviations from such ideal flow patterns are frequently accounted for by using axial dispersion coefficients. On the other hand the most sophisticated models resolve the fluid dynamics clearly with direct numerical solution of the Navier-Stokes equations and superimpose the kinetics on it; e.g. computational fluid dynamics (**CFD**) models.

Some general rules regarding the level of reactor model sophistication have been reported. For instance Feyo De Azevedo et al. (20) established that a model should not be more detailed than absolutely necessary for the particular purpose involved. Glasscok and Hale (31) reported 80% of benefit with only 20% of model complexity, and concluded that the obligation to develop complex models may be avoided as the only via to properly simulate the behavior of a reactor. Dudukovic et al. (7) stated that in the definition of the sophistication level for reactor modeling, the flow pattern and mixing should be commensurate with the level of modeling used to understand the kinetics. Whenever that is not the case, the modeling effort yields less than maximum benefits since kinetics ultimately drives the reactor performance.

There is not a magic rule for establishing the complexity of a model, however the best practice is to consider the simplest model with

all the main relevant phenomena and then add complexity to reduce the error between experimental and calculated data (24). The model equations complexity is strongly determined by flow conditions, but for FBRs the plug flow hypothesis, i.e. relatively simple equations, is often satisfactory (32).

In general, to describe all physical and chemical phenomena in a PBR, a model should have the following characteristics:

1. it must be a conservative system;
2. it should not predict backmixing of material over large distances; and
3. it should produce the correct asymptotic (steady state) solution.

C. Hydrotreatment Reactor Types

The multiphase catalytic packed-bed reactors are operated either with a continuous gas and a distributed liquid phase (trickle operation), where the main mass transfer resistance is located in the gas or with a distributed gas and a continuous liquid phase (bubble operation) (17), where the main mass transfer resistance is located in the liquid phase. The modes of operation generally used in three-phase are: Trickle- or packed-bed reactors, in which the catalyst is stationary; and slurry reactors, in which the catalyst is suspended in the liquid phase. The former are typically used in HDT process.

According to the reactor design, gas and liquid move cocurrently downflow or gas is fed countercurrently upflow. In the most applied cocurrent downflow configuration of commercial reactors, the liquid phase flows mainly through the catalyst particles in the form of films, rivulets, and droplets as shown schematically in Fig. 5 (21).

Based on the direction of the fluid flow multiphase catalytic packed reactors can then be classified as trickle bed reactors with cocurrent gas-liquid downflow, trickle-bed reactors with countercurrent gas-liquid flow, and packed-bubble reactors where gas and liquid are contacted in cocurrent upflow. When a fixed bed reactor is chosen the frequently asked question is whether to use an upflow or downflow mode of operation. A detailed knowledge of the possibilities of a reactor is critical to properly make the catalyst and reactor selection and process design.

In the case of catalytic packed beds with two-phase flow, such as those used for straight-run naphtha hydrodesulfurization, from a reaction engineering perspective, large catalyst to liquid volume ratio and plug-flow of both phases are preferred, and catalyst deactivation is very slow or negligible, which facilitates reactor modeling and design. However, for three-phase catalytic reactors (a system in which gas and liquid phases

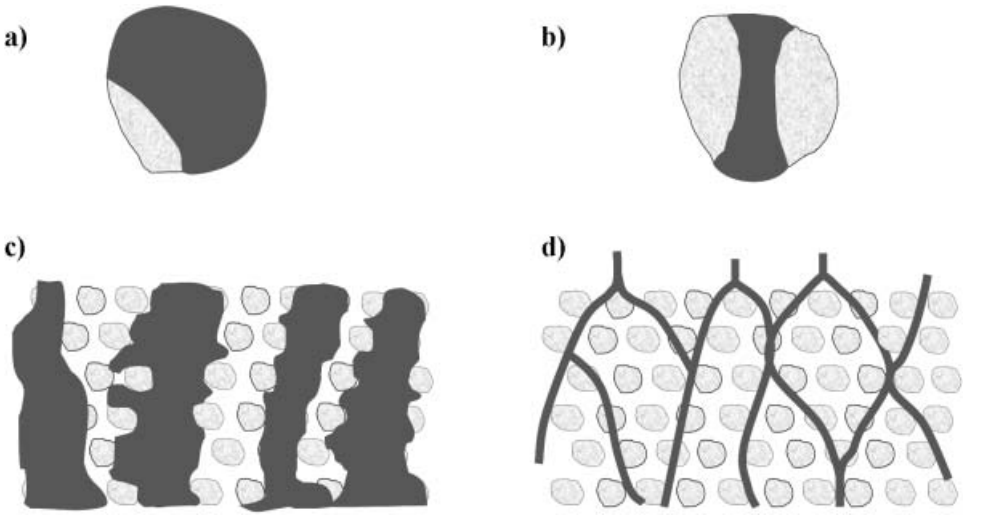

Figure 5: Schematic representation of liquid flow textures encountered during trickle-flow regime in TBRs: a) Particle-scale film flow, b) Particle-scale rivulet flow, c) Bed-scale film flow, and d) Bed-scale rivulet flow.

are in contact with a solid phase, the catalyst), which are frequently employed for hydrotreatment of middle distillates and heavy petroleum fractions, the reaction occurs between the dissolved gas and the liquid-phase reactant at the surface of the catalyst, and the choice of upflow versus downflow operation can be based on rational considerations such as the limiting reactant at the operating conditions of interest (7).

In a TBR the catalyst bed is fixed, the flow pattern is much closer to plug flow, and the ratio of liquid to solid catalyst is small. If heat effects are substantial, i.e., highly exothermic reactions such as in the case of hydrotreatment of unsaturated feeds (LCO, light cycle oil from fluid catalytic cracking units) they can be controlled by recycling of liquid product stream although this may not be practical if the product is not relatively stable under reaction conditions or if very high conversion is desired, as in HDS, since light recycle rate causes the system approaching to the continuous stirred tank reactor (**CSTR**) behavior. For such high increases of temperature the most preferred solution is quenching with hydrogen although the use of other streams have also been reported (33, 34). Even when completely vapor-phase reaction in a fixed catalyst bed may be technically feasible, a TBR may be preferred for saving energy costs due to reactant vaporization (i.e., HDS of naphtha). The limiting reactant may be essentially all in the liquid phase or in both liquid and gas phases and the distribution of reactant and products between gas and liquid phases may vary with conversion (6).

1. Conventional Trickle-Bed Reactors with Cocurrent Gas-Liquid Downflow

A TBR consists of a column that may be very high (above 10–30 m), that is equipped with one or several fixed beds of solid catalysts, throughout which gas and liquid move concurrent downflow. Fig. 6 shows the typical film flow texture found during trickle-flow regime in TBRs (21). In this mode, gas is the continuous phase and liquid holdup is lower. This operation is the most often used in practice, since there are less severe limitations in throughput than in countercurrent operation (17).

For gas-limited reactions (high liquid reactant flux to the catalyst particle, low gas reactant flux to the particle), especially at partially wetted conditions, a downflow reactor is preferred as it facilitates the transport of the gaseous reactant to the catalyst (7).

Opposed to commercial TBR, the bench-scale trickle bed reactors operate at equivalent space velocity and both, the liquid velocity and the catalyst bed length have important effects on the performance of the reactor (35). The main advantages and disadvantages of TBRs with concurrent operation are given elsewhere (6, 7, 21, 25, 36, 37, 38).

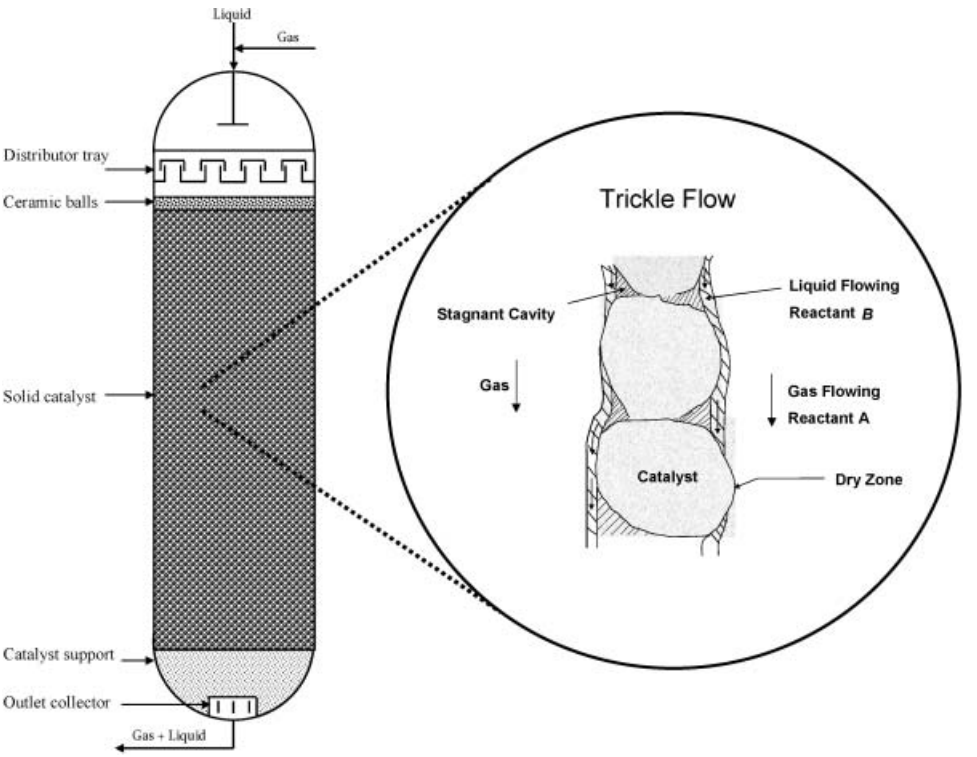

Figure 6: Schematic illustration of trickle-flow regime in a TBR (21).

2. TBRs with Countercurrent Gas-Liquid Flow (Packed Beds with Countercurrent Flow or Countercurrent Catalytic Packed Bed Reactors)

TBRs operating in countercurrent gas-liquid flow provide the opportunity for selective removal of by-products that may act as inhibitor, e.g. in hydrodesulfurization where hydrogen sulfide has an inhibitory effect.

The introduction of FBRs with countercurrent flow in a number of refining operations is likely either via re-design of existing reactors or by introduction of new technology. The goal is not an improvement in reactant (hydrogen) mass transfer, which is not rate limiting, but enhancing the removal of inhibitory by-products or *in situ* product separation. That is why countercurrent flow will be preferred for processes that suffer from by-product catalyst inhibition (7).

A catalytic packed bed reactor, with countercurrent mode where reaction takes place and large surface area/volume ratio, is a suitable alternative to TBRs. However, the main problems of the countercurrent reactor in commercial hydroprocessing applications are due to hardware limitations. The catalyst loading is 20–25% by volume in countercurrent operation (though less catalyst volume is necessary for the countercurrent operation for getting the same conversion), whereas in cocurrent TBR, the catalyst loading is 60–70% by volume. There is, therefore, a need to develop improved hardware configurations allowing for countercurrent contact of gas and liquid in the presence of small size catalyst particles and also when the catalyst loading is above 50% by volume (25). The advantages and disadvantages of these reactors are reported elsewhere (7, 25, 36).

3. Packed Bubble-Flow Reactors (Upflow Reactors, Upflow Cocurrent HDS Reactors, Packed-Bubble Columns, Upflow Packed Bubble Columns, Flooded Bed Reactors, or Submerged Upflow Reactors) with Cocurrent Gas-Liquid Upflow

In bubble flow operation, a continuous liquid phase together with a dispersed gas phase moves upward cocurrently through the packed bed. Such an operation would be recommended in cases where liquid reactants are treated with a relatively small amount of gas, as in hydration of nitrocompounds and olefins, or where a relatively large liquid residence time is required for the desired degree of conversion. These reactors are used when it is necessary to assure complete external wetting of the catalyst and at the same time have high liquid holdup. In this mode the liquid is typically the continuous phase.

The bubble operation is also advantageous when the reactor diameter/particle diameter ratio is relatively small, because the liquid catalyst contact is more effective than in trickle operation. Compared with empty bubble

columns, the packed bed has the advantage of reducing substantially the backmixing in the flowing phases as well as the coalescence of gas bubbles. Under any condition the wall heat transfer coefficient should also be higher than in trickle operation (17).

For liquid-limited reactions (low liquid reactant flux to the catalyst particle, high gas reactant flux to the particle), an upflow reactor should be preferred as it provides for complete catalyst wetting and for the fastest transport of the liquid reactant to the catalyst (7).

For a very shallow catalyst bed it has also been shown that upflow operation gives much better conversions than downflow operation under the same reaction conditions.

The gas and liquid flow rates typically used in a bench-scale downflow trickle bed HDS reactor are such that, when they are used in a cocurrent upflow operation, a bubble flow regime will be generated. The performance of a reactor under this hydrodynamic flow condition should be considerably different from the one obtained under trickle flow conditions. In an upflow system the low-boiling components, which are generally more reactive, pass into the vapor phase and are swept out more rapidly than the high boiling material which progresses relatively slowly through the bed. This superior performance of upflow processing is attributed to the fact that it maximizes the residence time of the heavy liquid fractions, but a more important factor may have been the very low liquid flows used (6).

When both gas and liquid flow upward, maldistribution of liquid or incomplete catalyst wetting should not be very important, particularly when the hydrodynamic conditions of bubble flow prevail within the reactor.

The gas and liquid flow rates, which are normally used in pilot-scale HDS, TBR, may result in bubble flow conditions when the gas and liquid are passed cocurrently upwards in the same reactor.

In very shallow catalyst beds, an HDS reactor performs better with cocurrent (gas + liquid) upflow operation than with cocurrent (gas + liquid) downflow operation. These results are not time dependent, which shows that this difference is not simply a transient phenomenon (35).

An upflow (flooded bed) reactor, which should give good solid-liquid contacting, could be used instead of an autoclave to obtain information on the intrinsic kinetics (6). The advantages and disadvantages of packed bubble-flow reactors have been given elsewhere (6, 7, 35).

D. Models for Trickle Bed Reactors

The analysis of multiphase catalytic fixed-bed reactors is a challenging task, as the reactor performance in most cases not only depends on the chemical reaction rate but also strongly on fluid dynamics and several

transport processes. In order to combine these factors quantitatively, reactors models with different level of sophistication have been developed.

The simplest model for globally taking into account fluid dynamics of the flowing liquid in trickle-bed reactors is the **1D** dispersion model (**PD**). This model has been used by numerous authors for determining particle Bodenstein number (Bo_p) for the spreading of a tracer as a function of operating conditions. In general, Bo_p defined in this way is significantly lower for trickling conditions than in single-phase flow through packed beds (39), i.e., the dispersion in the liquid phase is higher. The PD model does not explicitly take into account *stagnant zones* which make them noticeable by marked tailing in tracer experiments, particularly with porous catalysts. Therefore a model in which the liquid phase is divided into a stagnant (inactive) and a free-flowing (active) fraction is considerably more realistic. Such a model is known as cross-flow (**PE**) or cross-flow dispersion (**PDE**) model. Figure 7 shows the presence of stagnant zones in adjacent catalyst particles in TBRs. It is also shown in the zoom of this figure that the stagnant regions contribute to the capture of fines.

In spite of all information available on fluid dynamics and mass transfer, the *a priori* design of TBR is still far removed from a chemical reaction engineering routine. For robust modeling, correlations for the dependence of model parameters on operating variables are still lacking, as well as peformance of model complexity to predict the degree of conversion with sufficient accuracy. In this situation extensive use of analogies and similarities between the various models must be made in order to make optimal use of the available data (17).

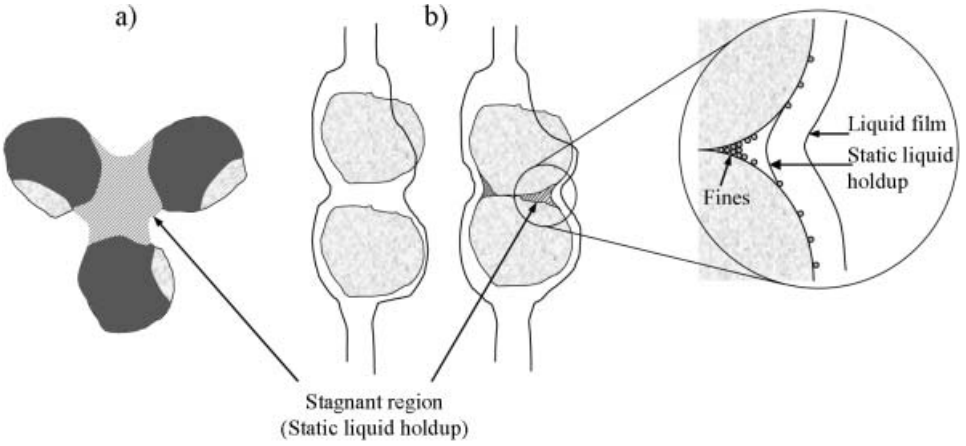

Figure 7: Schematics of stagnant liquid zones between catalyst particles in TBRs: a) Liquid pocket, and b) Pendular ring.

The nonsteady-state methods permit more detailed kinetic analysis of elementary steps. The determination of reaction rate constants and mechanisms has been frequently done from the analysis of the transient behavior of multiphase reactors (40).

In the past, catalyst development drove the selection of an appropriate multiphase reactor type. This sequential approach is increasingly being replaced by a parallel method for catalyst and reactor selection. This approach requires quantitative models for the flow patterns, phase contacting, and transport in various multiphase reactor types. The proper selection of the reactor type and its efficiency of operation greatly impact the total capital and manufacturing costs of the whole process (7).

1. *Simple Pseudohomogeneous Models*

The earliest models reported in the literature to simulate, design and optimize HDT reactors were of pseudohomogeneous type, which may be considered to be very simple since they only take into account inlet and outlet data of the reactor. Of course, they were not used alone but also experimental and commercial experiences with similar reactors were and continue to be employed for such purposes. These models are based on various assumptions that lead to drastically simplified equations. In some cases the models were so over-simplified that nowadays only books of chemical reactor design at undergraduate level used them for academic purposes.

According to Iannibello et al. (30), pseudohomogeneous models can be broadly categorized into two types: kinetic models and hydrodynamic models. The former do not consider the influence of hydrodynamics and related phenomena on conversion and are generally based on intrinsic rates of reactions (k_{in}). They describe the performance of the process generally in terms of a first order or nth order kinetics. Due to its importance over other hydrotreatment reactions, hydrodesulfurization has been traditionally the most studied reaction, so that these models have been mainly developed for HDS, whose kinetic order has been reported to range between 1.0–2.5 (41, 42). For HDS, sometimes two parallel reactions of non-refractory and refractory compounds are assumed (43), both following first-order kinetics. This type of models has found its major application when testing and evaluating catalysts in small-scale reactors, but surely they cannot be used alone for scale-up purposes, because hydrodynamics effects are neglected. Furthermore, the comparison of different catalysts may suffer from uncertainty due to the superimposition of kinetic and hydrodynamic effects. The frequent reason given by experimentalist to justify the use of these models when supporting catalyst screening results is that all catalyst samples are subject to more or less the same hydrodynamic behavior so that kinetics can be compared. This

condition can be reached by employing both same size and catalysts which are compared in the same reactor system.

On the other hand hydrodynamic models attempt to incorporate the influence of hydrodynamics on catalyst utilization. These models emphasize some other aspects of the reactor such as external liquid holdup, catalyst wetting, axial dispersion, etc. They generally assume plug flow pattern with first-order kinetics, and introduce an apparent kinetic rate constant (k_{app}) in place of the intrinsic rate constant to account for the effects of hydrodynamics. It has been shown that the incorporation of a hydrodynamic parameter in reaction rate equations improves the performance of the model in terms of data fitting, and thus providing more appropriate basis for scale-up of pilot-plant data by adding chemical and physical complexities in the kinetic analysis of HDT reactions.

Crine et al. (28) assumed that the development of hydrodynamic models followed two approaches: in one, the overall reactor efficiency is related to the external liquid mixing (i.e., D_a^f, D_r^f, λ_a^f, λ_r^f, etc.), whereas in the other, it is related to the liquid-solid contacting efficiency (i.e., ε_{TL}, ε_L, f_w, η_{CE}, etc.).

1.1. Models Based on Kinetics

Many authors have reported that pore diffusion effects can be taken into account within the framework of an effective or apparent reaction rate constant (i.e., multiplying intrinsic reaction rate constant by effectiveness factor), in order to formulate a pseudohomogeneous basic plug flow model which is sufficient to describe the progress of chemical reactions in the liquid phase of a TBR (5, 6, 17, 44). The suppositions of this model are:

1. Plug flow pattern of the liquid phase.
2. No evaporation or condensation occurs from or into the liquid phase.
3. No mass or heat transfer limitations between gas-liquid and liquid-solid interfaces.
4. The liquid is saturated with gas at all times.
5. First-order isothermal, irreversible reaction with respect to the liquid reactant.
6. No homogeneous reaction.
7. Gaseous reactant present in large excess.
8. Reaction occurs only at the catalyst surface.

The analysis of TBR performance under such ideal circumstances and the assumption of simple first-order power law kinetics can be easily approximated by an expression analogous to that of the well-known and widely used

piston-flow reactor design equation with a single reactant phase. This approach provides a quick initial analysis of real cases.

The final integrated equation is represented by a logarithmic dependence of the degree of conversion on apparent rate constant and mean liquid residence time or space time ($\tau_L = 1/LHSV$). The derivation of such an equation is typically reported in chemical reaction engineering text books (29, 45, 46) and can be obtained from the mass balance of the limiting reactant in the reaction (say sulfur, S, in HDS reaction) in a differential element of reactor volume in steady-state operation, as is described next:

$$[\textbf{input}] = [\textbf{output}] + [\textbf{disappearance by reaction}] + [\textbf{accumulation}] \tag{1}$$

$$[F_S] = [F_S + dF_S] + [(-r_S)dV] \tag{2}$$

since $F_S = C_S^L \upsilon_L$,

$$(-r_S)dV = -dC_S^L \upsilon_L \tag{3}$$

after variables separation, integration, and inclusion of space-velocity concept ($LHSV = \upsilon_L/V$), for instance, for first order kinetics $(-r_S) = \eta k_{in} C_S^L$, the final equation is:

$$\ln\left(\frac{(C_S^L)_0}{(C_S^L)_f}\right) = \frac{\eta k_{in}}{LHSV} \tag{4}$$

The chemical complexity of the reaction may be reasonably taken into account by assuming nth order kinetics $\left(-r_S = \eta k_{in}(C_S^L)^n\right)$, with $n \neq 1$. The final equation for this case is:

$$\frac{1}{n-1}\left[\frac{1}{(C_S^L)_f^{n-1}} - \frac{1}{(C_S^L)_0^{n-1}}\right] = \frac{\eta k_{in}}{LHSV} \tag{5}$$

In 1967, Frye and Mosby (47) derived an isothermal reactor equation (or kinetic equation) for desulfurization of light catalytic cycle oil applicable over a wide range of conditions. The equation has one adjustable parameter dependent on physical properties, considering liquid feed vaporization, phase equilibrium, first-order with respect to each sulfur compound and hydrogen, and the effect of H_2S and aromatic hydrocarbon adsorption. The model was able to predict the total HDS percent of the feedstock by using the equation

developed for model compounds with acceptable accuracy. This approach could be enhanced by considering more than a lump for prediction of HDS. Further analysis about the effect of gas-to-oil rate on the vapor-liquid equilibrium (**VLE**) in a deep diesel HDS reactor was performed by Hoekstra in 2007 (48), using the same model of Frye and Mosby (47).

Papayannakos and Georgiou (49) presented a simple kinetic model for hydrogen consumption during residue catalytic HDS, including the effects of reactor conditions and catalyst type, size and age. The intrinsic reaction rates for hydrogen consumption were described by using a second-order kinetic equation, and the intraparticle diffusional effects were discussed by means of the effective diffusivity. Strong pore diffusion limitations were observed for commercial-size catalyst particles. The differential mass balance equation for the remaining hydrogen demand and sulfur compounds was given by Eq. (5), where the total hydrogen reaction rate was found to be of second order ($n = 2$), while the reaction order for the HDS reaction was 2.5.

Many other authors have used either Eq. (4) or (5) to model experimental isothermal reactors at different scales for different purposes such as catalyst screening, effect of feedstock properties, evaluation of commercial catalysts, etc. Some of these studies were summarized by Ancheyta et al. (41, 42, 50).

Kinetic models are usually employed for catalyst testing at laboratory scale and also for obtaining intrinsic parameters of any rate of reaction. Several experimental techniques such as reduction of catalyst size, variation of amount of catalyst and flowrate in order to maintain a specific LHSV, fill up the catalyst bed with inert fines, etc. are necessary to properly compare different catalysts. The main drawback of PBRs for kinetic studies is the fact that they are integral reactors, that is, the concentrations gradients may be significant. The only way to obtain kinetic information is to assume a kinetic model and adjust its parameters by comparing model results with experimental ones (51). It must be performed iteratively in order to find the best set of parameters. Having the effective constant rate, the intrinsic parameters can be obtained providing an accurate effectiveness factor. The main advantage of this type of reactors in kinetic studies over batch reactor is that the former allow for determining the deactivation of catalyst, although it is difficult to decouple the kinetic model from deactivation phenomenon (52).

1.2. Models Based on Hydrodynamics

To account for hydrodynamics and other physical effects, an apparent kinetic rate constant can be introduced: $k_{app} = k_{in} \cdot f(\text{hydrodynamics})$. Therefore, to obtain the hydrodynamic model, for instance for $n = 1$, Eq. 4 can be rewritten as (note that k_{app} is used instead of ηk_{in}):

$$\ln\left(\frac{(C_S^L)_0}{(C_S^L)_f}\right) = \frac{k_{app}}{LHSV} \tag{6}$$

where k_{app} depends on catalyst utilization. The interparticle and intraparticle physical phenomena may be accounted separately by means of the following equation:

$$k_{app} = k_{in}(1-\in_B)\eta\psi(u_L) \tag{7}$$

where k_{in} is based on catalyst pellet volume and hence a factor $(1-\in_B)$ appears, which is the fraction of reactor volume occupied by the catalyst undiluted, η is the catalyst effectiveness factor, and $\psi(u_L)$ is a function of the superficial liquid velocity (u_L) that considers the variation of the degree of utilization of the catalyst due to hydrodynamic phenomena (30). Substituting Eq. (7) into Eq. (6) the general hydrodynamic model is obtained, Eq. (25), which is given in Table 1.

Satterfield (6) reported a simple first order kinetic model for analysis of TBRs performance employed in HDT of gas oils under ideal conditions. The model only takes into consideration the liquid phase as a single homogeneous phase, assumes plug flow pattern of the liquid flow rate, no mass transfer limitation, irreversible reaction with respect to the liquid reactant, no reaction heat effects, no homogeneous reaction, total wetting of catalyst pellets, and a pseudo rate constant for reactor design. For a more realistic approach, this author suggested to include the effect of liquid-solid contacting effectiveness (f_w *or* η_{CE}) defined as k_{app}/k_{in} using the correlation presented by Bondi (53) [Eq. (10)]. It was found that k_{app} increased, approaching to k_{in}, as the liquid flow rate tends to infinity. Furthermore, in accordance to experimental observations, the value of the exponent α in the relationship given by Eq. (26) in Table 1 proposed by several authors was found to vary substantially depending on the flowrate region being considered. At substantially high superficial liquid velocities, where liquid contacting becomes essentially complete and liquid maldistribution is no longer a problem, the exponent α should approach zero (54). The relationship between inlet and outlet concentrations of the liquid reactant is given by Eq. (6).

1.2.1. Models based on liquid holdup

Since it is normally assumed that reactions take place in all the catalyst particles inside the reactor, the total volume of catalyst is employed to calculate the LHSV. Otherwise, there must be some means for correcting this inefficiency if the true conversion severity needs to be determined. To solve

Table 1: Generalized hydrodynamic models.

1) General hydrodynamic model

$$\ln\left(\frac{(C_S^L)_0}{(C_S^L)_f}\right) = \frac{k_{in}(1-\epsilon_B)\eta\psi(u_L)}{LHSV} \tag{25}$$

2) First approach model (related to liquid-solid contacting efficiency)

$$\ln\left(\frac{(C_S^L)_0}{(C_S^L)_f}\right) = \frac{\kappa k_{in}(1-\epsilon_B)\eta(L_B)^{\alpha}}{(LHSV)^{1-\alpha}}(d_{pe})^{\beta}\left(\frac{\mu_L}{\rho_L}\right)^{\gamma}\left(\frac{\sigma_c}{\sigma}\right)^{\omega} \tag{26}$$

3) Second approach model (related to external liquid mixing)

$$\ln\left(\frac{(C_S^L)_0}{(C_S^L)_f}\right) = \frac{k_{in}(1-\epsilon_B)\eta}{(LHSV)} - \frac{[k_{in}(1-\epsilon_B)\eta]^2}{(LHSV)^2}\frac{d_{pe}}{L_B Pe_d} \tag{27}$$

when Peclet number is related to *LHSV* and L_B by an empirical correlation of the following type:

$$Pe_d = \kappa(LHSV)^{\alpha}L_B{}^{\alpha} \tag{28}$$

with $1 > \alpha \geq 0.5$, then Eq. 27 arrives to the following expression:

$$\ln\left(\frac{(C_S^L)_0}{(C_S^L)_f}\right) = \frac{k_{in}(1-\epsilon_B)\eta}{(LHSV)} - \frac{[k_{in}(1-\epsilon_B)\eta]^2 d_{pe}}{\kappa(LHSV)^{2+\alpha}L_B{}^{1+\alpha}} \tag{29}$$

this problem it has been considered that catalyst utilization depends on the liquid volume within the reactor (44, 55), which is called liquid holdup.

Ross (55) was the first author who published holdup data for commercial reactors, more than 40 years ago. He measured the liquid residence time distributions by using the pulse technique in different size trickle hydrotreaters (**HDTs**) containing the same reactants and catalyst and operating under the same reaction conditions. It was found that liquid holdup in commercial reactor was only about two-thirds that of the pilot reactor, which indicated that those commercial units were less efficient than the pilot plant reactors in spite of using higher linear liquid and gas velocities. This seemed to have been caused by poorer liquid distribution over the catalyst bed (poor catalyst utilization), and/or by mass transport of reactants through the liquid film on the catalyst. It was reported that for reactors larger than about 1 in. diameter, liquid distribution becomes an important problem (44).

The uniformity of liquid distribution improves considerably with increasing liquid velocity. The greater liquid and gas velocities in commercial units the greater turbulence in the liquid film, which in turn would increase the transfer of reactants through the film. On the basis of these results it was considered that the total (external plus intraparticle) liquid holdup (ε_{TL}) could be used as a measure of liquid-catalyst contacting. Therefore, when analyzing data from commercial and pilot plant HDS reactors, k_{app} was assumed to be proportional to ($k_{in}\ \varepsilon_{TL}$), that means ($1-\in_B$) = 1, η = 1, and $\psi(u_L) = \kappa\varepsilon_{TL}$ as indicated in Eq. (25) given in Table 1, in which liquid space time (or total residence time of the liquid) is the basic parameter in reactor performance. Therefore, this model takes into account both external and internal wetting of catalyst (30, 56).

Henry and Gilbert (44) extended the model reported by Ross (55) to use (ε_L/LHSV) as the space time for correlating pilot plant and full-scale hydrotreating performances. Their modified plug flow model is based on the external holdup of the liquid (ε_L) with negligible backmixing effects (assuming that holdup effects were controlling), and it was used to analyze the kinetic data with undiluted catalyst bed obtained by Mears (57). The external liquid holdup is considered a parameter that, although empirically, accounts for the external effective wetting of the catalyst pellets.

This model, also known as the holdup model, can be employed to correlate catalyst activity with parameters such as liquid mass velocity, liquid hourly space velocity, catalyst size, and catalyst bed length. It has been shown that the liquid velocity and the catalyst bed length have important effects on the performance of the reactor. These effects (i.e., maldistribution of liquid) have been explained in terms of volume of liquid in the reactor or holdup. For instance, a higher liquid holdup (higher space time) in the catalyst bed appears to be the key to increase catalyst utilization.

When reaction rate is indeed proportional to free-drainage holdup (or dynamic liquid holdup) and this holdup is proportional to ${u_L}^{1/3}$ (28), for the laminar film model ε_L is proportional to ${d_{pe}}^{-2/3}$ and to $v^{1/3}$ where $v = \mu/\rho$, thus the Henry and Gilbert (44) correlation would become that given by Eq. 26 with α = 1/3, β = −2/3, γ = 1/3, and ω = 0. This latter equation predicts that decreasing catalyst size will increase conversion, but the same general effect would be produced by varying catalyst size if diffusion limitations within catalyst particles were significant.

It has been pointed out by Henry and Gilbert (44) and Satterfield (6) that for certain combinations of liquid and gas flow rates the gas flow reduces the liquid holdup, that is, very high gas flow rates could be detrimental to catalyst utilization. In the development of Henry and Gilbert's model, the influence of gas flow rates over catalyst utilization was not analyzed; therefore, the expression derived can be only applied for a constant gas flow. Furthermore,

because this model does not consider the effect of the pore diffusion limitations at high temperatures it cannot be reliable for predictions under typical conditions employed in HDT reactions.

Paraskos et al. (5) evaluated the effects of backmixing and flow behavior (e.g., liquid holdup, incomplete catalyst wetting) on the mass transfer resistance in hydrotreatment of gas oils in a pilot plant TBR. The effect of varying LHSV on conversions of sulfur, metals, and nitrogen showed that the percentage of HDS should be dependent on catalyst bed length, and backmixing and liquid holdup or incomplete catalyst wetting reduce the efficiency of the TBR; so it was established that larger catalyst bed length minimizes the effects of liquid holdup or incomplete catalyst wetting.

The function $\psi(u_L)$, on an empirical basis, was assumed to be proportional to the liquid-solid contacting effectiveness (η_{CE}) in order to correlate experimental results of HDT. The following correlation was used for the liquid-solid contacting effectiveness:

$$\eta_{CE} = \kappa(u_L)^{\alpha} \tag{8}$$

Eq. (8) correlates the liquid–solid contacting efficiency with the superficial liquid velocity. Using Eq. (26) (Table 1), it was also found that the power-law coefficient in the holdup or the effective catalyst wetting–LHSV relationship (α) might be dependent on the reaction conditions (e.g. temperature, LHSV, H_2 partial pressure, etc.) as well as on the nature of the feed and reaction. First-order kinetics represents well HDS, hydrodenitrogenation (**HDN**), and hydrodemetallization (**HDM**) reactions when either liquid holdup or catalysts wetting effects are taken into account. However, when these effects are neglected, the apparent order of reaction undergoes a change as the conversion level increases. For small deviations from plug flow with first-order reactions the relation between outlet and inlet concentrations were expressed by Eq. (27).

1.2.2. Models based on catalyst wetting

Experiments in bench-scale TBRs have shown that distribution of liquid over catalyst particle bed can be extremely nonuniform at the low-liquid space velocities prevailing in bench-scale reactors as compared with commercial-scale reactors. This liquid maldistribution within the catalyst bed causes an ineffective use of catalyst active sites also known as "incomplete catalyst wetting." This effect can be reduced considerably by improving the uniformity of liquid distribution with increasing superficial liquid velocity and reducing catalyst particles size. In catalyst-wetting based models, the catalyst utilization is assumed to be proportional to the fraction of the outside catalyst

surface effectively wetted by the flowing liquid also known as "effective catalyst wetting," which is defined as the ratio of external wetted area to total area of catalyst particle.

Murphree et al. (58) presented the application of liquid residence-time distribution studies in order to examine the deviations of downflow two-phase FBRs from plug flow by calculating the contacting efficiency, defined as the ratio of real reactor performance to ideal plug flow reactor performance. The ability of the model to estimate the reaction rate constant was also reported. These authors concluded that any difference in conversion of these two units at the same operating conditions must be attributed to differences in contacting between catalyst and fluid existing in the two units. The model presented by the authors seems to be the first attempt to separate chemical and physical effects on HDS conversion, in an easy manner, in any reactor by measuring the effects of fluid-catalyst external contacting efficiency.

Bondi (53) presented a simple procedure by which it is possible to separate chemical kinetics from physical conversion resistances that are present in TBRs. The procedure to calculate chemical reaction rate constants from conversion data on bench- and pilot-scale TBRs was reported to be useful for any other reactor system. An empirical parameter is introduced which characterizes the conversion resistance depending on liquid and gas velocities, and is valid only for the particular experiments. The low flow rates, which are characteristic of experimental reactors, can magnify poor oil-catalyst contacting and cause low conversion rates that vary with liquid velocity.

The empirical relationship developed by Bondi (53) can be used to reduce the gap between conversion data obtained in batch reactors and those from small-scale TBRs that often perform poorly. His empirical correlation for HDS of heavy gas oil, given by Eq. (9), relates the space time required to achieve 50% conversion (or conversion half time, $\tau_{1/2}$), to the analogous space time at complete wetting ($\tau_{1/2,c}$), and to the linear superficial liquid velocity.

$$\tau_{1/2} = \tau_{1/2,\,c} + \frac{A'}{{u_L}^{b'}} \tag{9}$$

where A' and b' are empirical constants. According to Satterfield (6) this relationship can also be expressed by Eq. (10) in terms of reaction rate constants.

$$\frac{1}{k_{app}} = \frac{1}{k_{in}} + \frac{A'}{{G_{mL}}^{b'}} \tag{10}$$

It is important to point out that Bondi (53) also found an insignificant positive gas flow effect which was neglected in his model.

The effect of backmixing in the presence of liquid holdup and incomplete catalyst wetting was discussed by Mears (59), who proposed a relationship between $\ln\left(\left(C_S^L\right)_0 \Big/ \left(C_S^L\right)_f\right)$ and L_B based on the effective catalyst wetting effects in order to show that for a bench-scale TBR the liquid velocity and the catalyst bed length have important effects on the performance of the reactor; in other words, he postulated the hypothesis that the utilized fraction of catalyst (and hence k_{app}) is proportional to the true constant of completely wetted catalyst (k_{in}), to the catalyst effectiveness factor (η) and to the contacting efficiency η_{CE} (or f_w), that is, to the fraction of the external catalyst area wetted by liquid:

$$k_{app} = k_{in}\eta f_w \tag{11}$$

where f_w (or a_w/a_S) is the fraction of the external pellets area that is effectively wetted. By incorporating the correlation of the effectively wetted area (a_w) proposed by Puranik and Vogelpohl (60), which was developed for incomplete contacting in absorption towers packed with different packing size and shape, Mears (59) arrived to Eq. 26 with $\alpha = 0.32$, $\beta = 0.18$, $\gamma = -0.15$, and $\omega = 0.21$.

If Onda's correlation is used, the following model equation can be derived (59):

$$-\log\left(\frac{\left(C_S^L\right)_f}{\left(C_S^L\right)_0}\right) = \left(\frac{k_{in}\eta}{LHSV}\right)\left[1-\exp\left(-\kappa L_B^{0.4} LHSV^{0.4}\right)\right]. \tag{12}$$

Mears' approach is more acceptable from a physical point of view than that of Henry and Gilbert (44), since it considers reaction rate to be proportional to the effectively (freshly) wetted area of the catalyst, instead of to the liquid volume (61). Mears also found that even when a fraction of his data (57) was satisfactorily explained by the holdup model of Henry and Gilbert (44), data with diluted bed could not be evaluated with this model.

Dudukovic (56) suggested that catalyst effectiveness factor and partial surface-wetting effects, being coupled local phenomena in TBRs, are a function of the Thiele modulus for nonvolatile liquid reactants in liquid-phase reactant-limited reactions, considering both incomplete external wetting and fractional pore fill-up (or internal partial wetting). Fractional pore fill-up will depend on the catalyst pore structure and physical properties (particularly on surface tensions) of the gas-liquid-solid system involved. This trickle bed effectiveness factor model is based on the following formulation for partially wetted catalyst pellet in TBR (η_{TB}) with a reaction occurring only in the liquid filled pore region of the pellet

$$\eta_{TB} = \eta_i \eta^* \tag{13}$$

where η_i represents the fraction of the particle internal volume wetted (pore filling), and η^* is the effectiveness factor of a pellet partially wetted (inside and outside), defined as

$$\eta^* = \frac{\tanh(\Phi_{TB})}{\Phi_{TB}} = \frac{\tanh\left(\frac{\eta_i}{\eta_{CE}}\Phi_T\right)}{\frac{\eta_i}{\eta_{CE}}\Phi_T} \tag{14}$$

The effectiveness factor in TBRs is then obtained by substituting Eq. (14) into Eq. (13)

$$\eta_{TB} = \eta_{CE}\frac{\tanh\left(\frac{\eta_i}{\eta_{CE}}\Phi_T\right)}{\Phi_T} \tag{15}$$

Eq. (15) reduces to the following relationship as that used by Mears (59) only if $\Phi_T \gg 1$ (very fast reaction) or $\eta_i/\eta_{\mathrm{CE}} \approx 1$:

$$\eta_{TB} = \eta_{CE}\eta \tag{15a}$$

For very low values of Thiele modulus, that is very slow reactions, by expanding *tanh* in a Maclaurin series and dropping out the terms with order higher than cubic, Eq. (15) is reduced to

$$\eta_{TB} \approx \eta_i\left[1 - \frac{1}{3}\left(\frac{\eta_i}{\eta_{CE}}\Phi_T\right)^2\right] \tag{15b}$$

The reactor design equation for first-order reaction based on assumed plug flow of the liquid is equal to Eq. (25) considering $\eta\psi(u_L) = \eta_{TB}$.

Crine et al. (28) presented a phenomenological description of the hydrodynamic and mass transfer processes occurring in a TBR. The proposed model, which accounts for the random and discontinuous nature of the packed bed, has been verified with experimental hydrotreating data. These data may be correlated using a single wetting parameter (L_m) introduced on physical ground, which is independent of the temperature and nature of the reaction system investigated. It varies only with the fluid properties and the catalyst size, and exhibits a logical dependence with the operating conditions. Crine's model was developed in order to take into account the discontinuous and random nature of the bed, relating the TBR global efficiency (η_G) to the particle effectiveness factor (η) as (56):

$$\eta_G = \eta_E \cdot \eta_{CE}\frac{\tanh\left(\frac{\eta_i}{\eta_{CE}}\Phi_T\right)}{\Phi_T} \tag{16}$$

Due to capillary forces and high molecular weight of the liquid reactants, η_i is commonly assumed to be unity (61, 62). The relative contributions of the films and of the contacted liquid pockets are taken into account in η_E and η_{CE}. The proposed reactor design model is equal to Eq. (25) considering $\eta\psi(u_L) = \eta_G$.

Iannibello et al. (63) observed that pore filling of the catalyst can be considered as total, even at very low liquid flow rates and hence very low intraparticle holdup, and at relatively high temperature. The partial catalyst utilization is probably due to intraparticle diffusivity phenomena rather than to partial pore filling. Rate of reactions of large molecules containing sulfur and metals was reported to be strongly affected by intraparticle mass transport phenomena. The decrease on the apparent kinetic constant may be ascribed to the reduction of the apparent intraparticle diffusivity of reactants. These authors validated the correlation for predicting the contacting effectiveness suggested by Mills et al. (64), and proposed that it may be useful to evaluate the hydrodynamic conditions where the kinetic rate constant may be independent of hydrodynamics. The same group in 1985 (30) employed four models that take into consideration the physical and chemical complexity of three-phase systems in order to interpret the results obtained from a pilot trickle-bed reactor, in which the removal of sulfur and metals from a heavy residual oil was carried out. The external holdup (**EH**), total holdup (**TH**), apparent diffusivity (**AD**), and the second-order kinetic models were tested with different catalysts, and it was observed that AD and EH models gave almost the same result in terms of data fitting and a slightly better than the second-order model. The TH model seemed less attractive from an engineering point of view because the calculated reaction order differed considerably from one catalyst to another or from one reaction to another. Iannibello's group concluded that a model based on the contacting efficiency (AD model) seems to be theoretically stronger than the others. The authors also analyzed a first order reaction model that incorporates the parallel reactions of reactive and refractory fractions provided a good interpretation of experimental data concerning alumina catalyst. The model is

$$\frac{\left(C_S^L\right)_f}{\left(C_S^L\right)_0} = \alpha e^{-k'_\alpha/LHSV} + \beta e^{-k'_\beta/LHSV} \tag{17}$$

where $\beta = 1-\alpha$, $k'_\alpha = \eta_{CE} k_\alpha$, and $k'_\beta = \eta_{CE} k_\beta$.

This two-lump model, namely reactive and refractory fractions, has been used more recently in the hydrocracking of asphaltenes, providing the best data fitting (65). On the other hand, due to sieving effects caused by fine pores present in alumina based catalyst, an appropriate modeling of hydrotreating reactor using this type of catalyst must probably take into account particular catalyst pore structure connected with the treated feed.

Kumar et al. (1) conducted pilot scale HDT experiments on straight run diesel using commercially available $CoMo/Al_2O_3$ catalyst. The kinetics of HDS and HDN were studied using plug flow model together with the external holdup and apparent diffusivity models reported by Iannibello et al. (30), which considered the physical and chemical complexities in the kinetic analysis of hydrotreating reactions in the three phase system. The chemical complexity of the HDS and HDN reactions were taken into account by assuming nth-order kinetics ($n > 1$), hydrodynamics and other physical effects were incorporated through the apparent kinetic rate constant, and because the authors considered the total reaction pressure effects in the reaction system, the rate of reaction was expressed as:

$$-r_S = k_{app} P^m \left(C_S^L\right)^n. \tag{18}$$

Therefore, the hydrodynamic model resulted in:

$$\frac{1}{n-1}\left[\frac{1}{\left(C_S^L\right)_f^{n-1}} - \frac{1}{\left(C_S^L\right)_0^{n-1}}\right] = \frac{k_{app} P^m}{LHSV}. \tag{19}$$

The pilot plant reactor has deviations from plug flow and they can be effectively accounted for by incorporating external holdup and catalyst wetting in the evaluation of the apparent kinetic parameters. Therefore, for the EH:

$$k_{app} = (k)_{EH} \varepsilon_L. \tag{20}$$

The AD model on the other hand uses the following representation:

$$k_{app} = (k)_{AD} \eta_{CE}. \tag{21}$$

where $(k)_{EH}$ and $(k)_{AD}$ are pseudokinetic rate constants that should be independent of hydrodynamics when appropriate n value is used. It was observed that EH model gave the best data fit among the three models employed.

1.2.3. Models based on axial dispersion

Perfect piston flow (i.e., ideal plug flow pattern) will never occur with Newtonian fluids as there will be always some axial mixing, due to viscous effect and molecular or eddy-diffusion. The deviations from piston flow behavior caused by restricted axial mixing have been traditionally characterized by means of residence time distribution curves. A number of researchers

have proposed that deviation from plug flow of trickle-bed reactors is caused by axial dispersion and have recommended that the hydrodynamic effect must be properly taken into consideration in trickle-bed reactors through axial mixing (66, 67).

Mears (57) established that axial eddy dispersion or backmixing (deviations from plug flow) appears to be responsible for adverse mass velocity effects observed in isothermal laboratory, bench and pilot scale TBRs for petroleum processing.

In order to examine the possibility that axial dispersion might be responsible for decreased reactor efficiency at low mass velocities, backmixing in the liquid phase was described by a 1D plug-flow model with superimposed longitudinal dispersion. Possible channeling or holdup effects in the reactor were neglected by assuming the superficial liquid velocity along catalyst bed to be constant and the catalyst effectiveness factor to be independent of temperature. Thus, the differential equation describing the steady-state concentration profile in an isothermal reactor was given by:

$$D_a^L \frac{d^2 C_i^L}{dz^2} - u_L \frac{dC_i^L}{dz} - r_i = 0. \tag{22}$$

Using perturbation solutions of Eq. (22) obtained by Burghardt and Zaleski (68) for appropriate boundary conditions, considering small deviations from plug flow (large Peclet number) and first order reaction, and substituting the Pe_d number by an empirical correlation proposed by Hochman and Effron (69) and Sater and Levenspiel (70), Eq. (29) is obtained (Table 1).

Schwartz and Roberts (71) presented the application of liquid residence-time distribution (**RTD**) studies for determining the performance of a downflow two-phase fixed-bed reactor (contacting efficiency and reaction rate constant). The RTD of the liquid external to the catalyst pores is the desired information, however sometimes the use of a tracer may include some contribution from the internal holdup as well (6). From these studies it was concluded that any difference in conversion at the same operating conditions between pilot and commercial units must be attributed to differences in liquid-solid contacting between the two units, and that liquid phase deviation from plug flow has insignificant effect on conversion in commercial scale TBRs (56).

With an appropriate redefinition of parameters, it was found that the cross-flow model is mathematically equivalent not only to the modified mixing cell model of Deans (72) but also to a probabilistic time delay model developed by Buffham et al. (73). Results over a range of typical trickle-bed conditions showed that predictions based on the simpler dispersion model slightly differ from those obtained with the more complex cross-flow model. Important differences between these models occur only at high degree of backmixing (short reactors) and at high reactant conversion, therefore, the assumption of

plug flow of liquid represents the TBR behavior quite well and when it is required to account for liquid backmixing, the dispersion model [Eq. (27)] can be selected as an adequate representation, which may be also the more conservative in general. The dispersion model is in addition appropriate for making initial estimates, i.e., whether or not deviation from plug flow will be significant in any specific case (6).

Montagna and Shah (35) investigated both experimentally and theoretically, the backmixing effect on the performance of a pilot-plant HDS reactor with atmospheric residue as feedstock when both gas and liquid are passed cocurrently and upward through the reactor. For upflow operation, an increase in gas and liquid flow rates (at constant temperature and pressure) decreases HDS, HDM and hydrodeasphaltenization (**HDAsph**) reaction rate due to backmixing in the reactor. For very shallow catalyst bed it was also found that upflow operation yields better conversions for all reactions than typical downflow operation under the same reaction conditions. The performance of a cocurrent upflow (both gas and liquid) was compared with that of a cocurrent downflow HDT reactor by using experimental data and the backmixing (or axial dispersion) model reported by Paraskos et al. (5). By assuming that $Pe_d = \kappa(G_{mL})^{\beta}$, the dispersion model [Eq. (27)] becomes:

$$\ln\left[\frac{\left(C_S^L\right)_f}{\left(C_S^L\right)_{f,\,P}}\right] = \frac{\kappa k_{in}{}^2 \eta^2 (G_{mL})^{\beta}}{(LHSV)^2}. \tag{23}$$

The effect of catalyst bed length at constant LHSV or of liquid flow rate on the performance of a TBR in HDS of atmospheric residue was also studied by Montagna and Shah (54). The experimental data were evaluated on the basis of the axial dispersion model of Mears (57), the holdup model of Henry and Gilbert (44), and the effective catalyst wetting model of Mears (59) in order to validate their applicabilities when explaining the catalyst bed length (or superficial liquid velocity) effects on removals of nitrogen, sulfur, metals and asphaltenes from atmospheric residue.

For axial dispersion model [Eq. (27)] it was first necessary to determine kinetic constants and effectiveness factors for the various reactions. Peclet number was expressed according to Hochman and Efrron (69) as $Pe_d = \kappa L_B{}^{\alpha}$ with $1 > \alpha \geqslant 0.5$, and the following equation was derived:

$$\ln\left[\frac{\left(C_S^L\right)_f}{\left(C_S^L\right)_{f,\,P}}\right] = \frac{\kappa k_{in}{}^2 \eta^2 d_{pe} (L_B)^{-(1+\alpha)}}{(LHSV)^2}. \tag{24}$$

It was found that Mears' (57) criterion predicts significantly larger values of $L_{B,min}$ than the ones obtained experimentally. From experimental data it was concluded that backmixing, liquid holdup and effective catalyst wetting

all appear to be strongly dependent on the catalyst particles size or the viscosity of the feedstock.

Shah and Paraskos (74) outlined an approximate solution to the governing differential equations for an adiabatic hydroprocessing TBR operating in presence of axial dispersion effects. With this approximation the following criteria for significant axial dispersion effect was obtained: (1) at high conversion adiabatic operation produces larger axial dispersion effect than isothermal operation, and (2) at low conversion, the opposite results are obtained.

Since axial dispersion effects tend to reduce conversion, it is important to design and operate pilot plant reactors under conditions where this effect is minimal. Under that premise, Mears' criterion was extended by Shah and Paraskos (74) to the case of pilot scale adiabatic trickle bed hydroprocessing reactors using the mass balance given by Eq. (24), for a reactant undergoing an nth order irreversible reaction in the slower moving liquid phase. The criteria derived by Mears (57) and Gierman (39), among others, are used to evaluate the order of magnitude of Peclet number required to avoid axial dispersion effect in pilot scale adiabatic reactors for (a) residual HDS, (b) HCR of gas oils, and (c) hydrodenitrogenation of shale oils. The results indicate that axial dispersion effect is of less importance in case (c) than in cases (a) and (b).

1.3. Empirical Correlations

Due to the existence of different phases is neglected in pseudohomogeneous models and catalytic reaction rates can be described only with concentrations in the liquid bulk, the following empirical approaches can fit in the simple pseudohomogeneous models classification as they do not need to recognize variations of mass and heat between phases.

Nowadays many desulfurized middle distillates although relatively low in total sulfur, contain high concentration of β-DBTs (dibenzothiophenes (**DBT**) with sulfur atoms in 4 and 6 positions). This means that the typical HDS technology may be viewed as a pretreater of raw middle distillates. The challenge then is to effectively reduce the sulfur from these prehydrotreated distillates to less than 10–15 ppmw. The solution may be the concept of two-stage process, where the liquid effluent from the first stage is fed to a second hydrotreater aimed to desulfurize residual β-DBTs.

For refiners the most important consideration in ultra-deep HDS is feedstock quality since they constantly face the question of which feedstocks from widely different origins and pre-processing histories are most attractive. Therefore, the development of phenomenological property-reactivity correlations in terms of readily measurable properties can guide the feedstock selection and blending. These correlations can also be useful for designing

model compound experiments, kinetic data interpretation, process modeling, and economics/planning studies.

There may be various correlations in the literature, which try to "predict" product properties (mainly sulfur content) as function of feed properties and composition, reaction conditions, etc. However, they are highly empirical in nature and not many attempts have been made to develop suitable and well-supported correlations. Here, the most significative efforts for representing the effect of feed properties on HDS reaction rate are briefly described.

Some of such correlations were developed by Tsamatsoulis et al. (75), which were obtained from results in bench scale TBR using atmospheric heavy residue as feed and commercial $CoMo/Al_2O_3$ catalyst. The empiric correlations shown in this work are called design equations, which interrelate the chemical reactions considered (HDS, HCR, hydrogen consumption rate (**HCON**), asphaltenic fraction desulfurization, and non-asphaltenic fraction desulfurization) and relate the characteristic properties of the products (density, viscosity, Ramsbottom carbon residue, API gravity, and Conradson carbon residue) with the severity level of the HDS and HCR reactions. One important finding of this work is that in the range of temperature used in the experiments (350–465°C), the relation between HCR and HDS was not affected by reaction temperature and residence time.

The relationships between percentages of sulfur removal and metal removal during HDT process were investigated by Callejas and Martinez (76) employing a residue coming from Maya crude. Typical conditions, pressure of 10–15 MPa and temperatures ranging from 375–415°C, were employed. At the lowest temperature studied, 375°C, high dependency of hydrodemetallization of nickel (**HDNi**) and vanadium (**HDV**) on HDS conversion was observed. Finally, empirical linear equations showing the dependence with HDS conversion were obtained at 375 and 400°C for demetallization reaction. It was observed that pressure only affects HDS rate constant along the range of pressures studied, but it is necessary to keep in mind the possible effect of pressure over HDN and HDM reactions for values of this variable out of the reported range.

Ho (77) developed a correlation for the single stage HDS of raw distillates at low H_2 pressures over a sulfided $CoMo/Al_2O_3$ catalyst which has the following general form:

$$k_{HDS} \propto (API)^{\alpha} \left(C_{DBTs}^{L}\right)^{\beta} \left(C_{N}^{L}\right)^{\gamma}. \tag{30}$$

This correlation may not be applicable to prehydrotreated distillates that are more likely to be desulfurized at relatively high H_2 pressures over sulfided NiMo or NiW catalyst because of their higher hydrogenation functionality compared with sulfided CoMo catalysts. The property–reactivity correlation

for prehydrotreated distillates was obtained from a simple competitive adsorption model based on the Langmuir isotherm:

$$k_{HDS} \approx k_{app}\left(1 - \lambda K_N \left(C_N^L\right)_0\right), \tag{31}$$

where k_{app} is a phenomenological rate constant for HDS; λ the extent of HDN reaction; K_N is an inhibition constant; and $\left(C_N^L\right)_0$ is the feed nitrogen content. The latter expression indicates that the feed nitrogen content should be used as an approximate overall indicator of the feed reactivity, measured by means of the overall rate constant k_{HDS}.

Ho and Markley (78) also proposed a property–reactivity correlation for hydrodesulfurization of prehydrotreated distillates as diesel fuels. It was found that HDS reactivity of such prehydrotreated distillates decreases primarily by the feed nitrogen content in a linear fashion.

In order to optimize process conditions employing the minimum of experiments, Ferdous et al. (79) has performed an statistical design which involves the effect of intensive parameters namely LHSV, pressure and temperature which have significant effects over HDS and HDN of a heavy gas oil derived from Athabasca Bitumen employing a NiMo/Alumina catalyst modified with boron. Typical operating conditions for HDT were studied: 340–420°C, 6.1–10.2 MPa, and 0.5–2.0 h^{-1} in a micro TBR. The expressions obtained for HDN and HDS were second order polynomial models, i.e. they showed no straightway dependence of conversion on the optimization parameters. The kinetic studies were also performed in order to have an available tool for prediction of the effect of catalyst activity over process variables. Two types of expressions were employed: power law and Langmuir-Hinshelwood models, obtaining good agreement between predictions and experimental data. These authors (79) also have reported that pressure does not have any effect on sulfur conversion during HDT of heavy gas oil using $NiMo/Al_2O_3$ catalyst containing boron. This result contradicts that reported by Jiménez et al. (80) where there is an appreciable positive effect of high pressure for HDS and HDN reactions during HDT of heaviest fractions of vacuum gas oils (**VGOs**). However, according to other researchers (81, 82) that observation, where no appreciable effect on HDS reactions was found, could be right only in narrow ranges of pressure. Shokri et al. (81) pointed out that the viscosity of liquid tends to increase as the pressure does, resulting in lower diffusivity and hence mass transfer. Therefore, all these reports encourage for planning experiments in order to highlight the effects of higher pressure conditions on sulfur conversion.

1.4. Concluding Remarks

Even if dispersed plug-flow models can properly fit experimental data, the existence of backmixing effects is questionable in commercial units as well as

in laboratory – diluted bed – reactors (5, 74). Models based on hydrodynamics can be enhanced if reactant compounds are lumped in more than one chemical species, e.g., the refractory and the non-refractory molecules.

The models based on hydrodynamics are sometimes proposed to be adequate for scale-up purposes. However, due to the different approaches followed, namely holdup, partial wetting and axial dispersion, these phenomena may simultaneously occur and, if they are not modeled separately, misinterpretation of results could be obtained and parameters could be masked in a single parameter.

The evaluation of Mears' criterion requires reliable correlation of Peclet number, which could be not available *a priori*. It has been observed that Mears' criterion can predict very large length of reactors for deep desulfurization, but experimentally shorter length than predicted are observed. Some modifications have been proposed and further investigations must be performed to establish the limits of applications of such a criterion.

2. *Continuous Pseudohomogeneous Models*

2.1. Steady-State Continuous Pseudohomogeneous Models

Among different approaches, steady-state continuous pseudohomogeneous models have been widely reported in the literature. This is due to their reliability and simplicity. A pseudohomogeneous model generally assumes power law kinetic type, although sometimes Langmuir-Hinshelwood expression has been employed. The use of power law for kinetics has been questioned due to its meaningless, i.e., it does not permit following the phenomena occurring intrinsically, such as reaction mechanism and inhibitory effects, however, for certain range of temperature and composition, power law kinetic model has been successfully employed for preliminary designs and to explore related phenomena such as hydrogen consumption, catalytic deactivation, quench studies and dynamic behaviors, among others.

The reactor is modeled considering no gradients of mass or temperature between two adjacent phases. Generally 1D analysis and few reports of 2D modeling reactors for HDT have appeared in the literature. the main contribution in modeling TBR systems applied to HDT process by pseudohomogeneous models are briefly described below.

Shah et al. (83) discussed the proper location for a quench in an exothermic, time-dependent catalyst activity system. The system chosen for study was a trickle bed reactor and the feedstock was residue oil. Empirical catalyst activity functions for HDS and HDM were developed from pilot plant data. Differential mass balances for irreversible first order reactions of HDS and HDM were written considering ideal plug flow conditions, whereas the energy balance was formulated under adiabatic conditions. They concluded

that the value of the maximum cycle life and the quench position depend significantly on the reaction variables such as feed temperature, feed concentrations of sulfur and metals, activation energies of sulfur and metals removal reactions, residence time, and sulfur conversion level. This model seems to be the first attempt to predict, although empirically, the deactivation in a TBR system sustaining HDT reactions. Although this report is interesting by itself, almost all the studies performed with quench systems take the maximum allowable temperature as criterion for localization of quench, that is, the temperature at which the quality of products may become undesirable and they relegate the quench location dependent of maximum catalyst life.

Kodama et al. (84) developed a simulation model of residue HDS reaction based on a catalyst deactivation model. To represent the fouling process, an improved model which included both the interaction of coking reaction and vanadium removal of the pore plugging was proposed. Both rate equations of desulfurization and vanadium removal were expressed by second order reactions, and they were assumed to be proportional to the hydrogen concentration in the liquid phase. The material balances of sulfur and metals in a plug flow reactor were performed and the energy balance was developed considering an adiabatic reactor and heat of reaction was attributed only to HDS reaction. Mass transfer in the porous catalyst was taken into account through the effectiveness factor. The model allows for prediction of the actual operations of bench scale fixed bed and moving bed reactors. This model was validated with enough data and thus its predictions can be expected to be reliable.

By using plug flow reactor model and power law kinetics, Akgerman et al. (85) showed the effect of liquid volatility on the conversion, arriving to the conclusion that the difference between predictions of models, assuming either volatile or nonvolatile liquid phases, is significant. For the first order case differences range from 24–38%. At high conversions, the difference between the models, volatile and nonvolatile, diminishes due to the depletion of the limiting reactant. This can be attributed to change in concentration in the liquid phase. In another work of Akgerman et al. (86) comparison of several equations of state for prediction of partial vaporization of feed in reactor performance was performed. Although VLE has to be performed in each step of integration through the length of reactor, these authors by-passed this feature supposing linear variation of equilibrium constant between the inlet and outlet conditions. They assumed almost complete wetting and no appreciable influence of vaporization effects were observed in the conversion. Further studies in this direction have confirmed the importance of taking into consideration the volatility of the light feedstock in HDT reactions, because it can cause incomplete wetting and thus poor performance of catalytic bed,

increase of conversion of refractory species and depletions on conversion of reactive species and other related phenomena.

Döhler and Rupp (87) performed laboratory-scale experiments with the same feed and catalyst as those in an industrial VGO hydrotreating unit in order to simulate the adiabatic behavior of the industrial reactor using a plug-flow pseudohomogeneous 1D reactor model. The model was validated only with HDS, HDN, and hydrodearomatization (**HDA**) reaction data. They pointed out that the calculation of Weight Average Bed Temperature (**WABT**) in an adiabatic reactor having delta T of 55°C or higher does not agree well with the isothermal temperature of experimental reactors because there is a nonlinear relationship between temperature and rate of reaction.

Used oil hydrotreating in a pilot TBR was simulated by Skala et al. (88) employing a pseudohomogeneous model with a power term for LHSV, where HDS, hydrodeoxygenation (**HDO**), and HDM reactions were used for validation. Those reactions were described by first-order power-law kinetic models which were then used for the simulation of an industrial TBR. Catalyst deactivation by coke and metals was also simulated according to the model of Shah (83) and similar model was used to predict the pressure drop dependence on decrease of the bed porosity. Good agreement between the model and industrial data of pressure drop was reported. The model for pressure drop dependent on catalyst activity could be useful for industrial analysis of reactor performance affected by continuous plugging of catalyst bed.

Tsamatsoulis and Papayannakos (89) employed real feeds and operating conditions as those encountered in hydroprocessing of heavy VGO and a set of four non-porous catalysts to derive a correlation for predicting the Bodenstein number (Bo) as function of bed characteristic and Reynolds number. Two thirds of their data fell within the Bo range given by Gierman (39). In another work of the same authors the effects of liquid dispersion in a bench scale HDT on the determination of the intrinsic desulfurization kinetics and on reactor performance for three porous catalysts with different activity was studied. Porous catalysts were used. Only two reactions, hydrodesulfurization and hydrogen consumption were considered. Activation energies for HDS and HCON were almost the same for each catalyst, but higher values were estimated when axial dispersion model was used instead of plug flow although the difference was negligible. Some observations given by these authors were: the plug flow model can be applied successfully for HDS and hydrogen consumption predictions when the conversion is kept low, but for higher values, such as deep desulfurization ($> 95\%$), deviation of up to 40% can be estimated when axial dispersion effects are incorporated in the plug flow model. Therefore, the influence of dispersion effects on reaction kinetics must be taken into account when using data at high conversions.

A commercial kero-HDS reactor was simulated successfully by Sau et al. (90) by means of a pseudohomogeneous plug flow model. The novel continuum theory of lumping was employed for kinetics, and very good predictions were observed. This work is a good example of how, with a simple reactor model but following the chemistry closely, it is possible to achieve reliable predictions with an important reduction in the total number of model parameters.

The HDS, HDN, and olefins hydrogenation (**HGO**) reactions were simulated in a commercial diesel HDT reactor by Cotta and Filho (91) employing a 1D pseudohomogeneous model. Each reaction was described by a power-law kinetic model because they found the Langmuir-Hinshelwood model to be inconsistent with their results. They observed higher experimental values than calculated for HDS while the opposite effect was found for HDN. This behavior could be attributed to the fact that the model does not take into account the inhibiting effect of H_2S.

A deterministic quasi-steady state model of the reaction section of the atmospheric residue desulfurization unit was developed by Lababidi et al. (92) to simulate the long-term behavior of the catalyst bed. A single fixed bed experimental reactor was first considered, followed by an industrial scale reactor. An appropriate correlation to determine the dissolved hydrogen concentration in the oil was used. Simulation results of the single bed reactor showed perfect match with Kodama's work (84), which validate the main assumptions of the proposed model. After validation, a series of four industrial scale reactors were simulated. Their conclusions were that actual industrial profiles of concentration and temperature with respect to time were very similar to the predicted ones. Deviations were observed at the start-of-run (**SOR**) and at end-of-run (**EOR**), whereas the model was capable to predict perfectly the middle-of-run (**MOR**). According to the authors, the simulation program developed might be useful for predicting the life of the catalyst if the product temperature is considered as an acceptable measure.

In order to select the best rate expression to predict the industrial reactor behavior, an adiabatic diesel hydrotreating trickle-bed reactor packed with commercial NiMo catalyst was simulated by Cotta et al. (93). The HDS, HDN and HGO reactions were considered. Power law kinetics was employed in this system and parameters for HDN and HDS were obtained from experimental isothermal downflow pilot plant fixed bed reactor, while for HGO, kinetic parameters were obtained from the literature. One-dimensional pseudohomogeneous model was employed in this work. The authors identified on basis of their results that it is necessary to use the most severe processing conditions (pressure of about 95 atm and temperature of 390°C) to increase HDN conversion, and the best model to represent HDN and HDS process is a power law kinetic instead of a Langmuir-Hinshelwood type under typical conditions. Due to the complex composition of different feedstocks, the intrinsic kinetics

assumed for estimating HGO conversion could be not adequate and results obtained from the model could be not reliable.

Mejdell et al. (94) modeled an experimental plug flow TBR reactor for HDS of oil products based on a discretization of the entire spectrum of sulfur components into small pseudocomponents of only 1°C boiling point range (132 pseudocomponents), and identifiable components with low reactivity like 4-Me-DBT and 4,6-DMe-DBT (6 real components) were modeled separately. A Langmuir-Hinshelwood kinetic type expression was used. Experimental data to estimate the 277 kinetic parameters were obtained on a reactor operated in up-flow mode employing light gas oil (**LGO**) as feed. Predictions of conversion were carried out and results were compared with experimental ones, showing good agreement. An observation derived from this work was its utility for simulating HDS process at high conversions because it permits the prediction of conversion of pseudocomponents with high reactivity and also conversion of refractory components which suffer from large deviations from TBP-reactivity tendency. This approach also may have certain generality for other feedstocks if one assumes that the reactivity for the lumps is the same for other oils. Although the authors have reported the implementation of this model in an industrial TBR and they claimed very well predictions in conversion, they did not give any evidence of such a study.

Bellos and Papayannakos (95) studied the HDS and hydrogen consumption kinetics of a straight run heavy gas oil in a microreactor loaded with a diluted bed of commercial catalyst which was simulated by means of two models, one of them was a plug flow pseudohomogeneous model assuming no liquid evaporation and the other one was an improved model that took into account feed evaporation and gas-liquid phase equilibrium along the reactor axis. The former was developed only to derive the initial values for the kinetic parameters of the improved model. Predictions of gas-liquid phase equilibrium were carried out at each step of integration over the entire length of reactor. Miscalculation in the mass balance of the improved model was observed when catalyst mass was taken as constant value, since the mass of catalyst was also a function of the bed length.

Melis et al. (96) employed a pseudohomogeneous axial dispersion reactor model for the interpretation of the HDA reaction during gas oil HDT. This model only considers the HDA reaction by means of a lumped scheme for aromatics composition in gas oil and assumes that hydrogenation/dehydrogenation reactions occur according to the Langmuir-Hinshelwood mechanism. The developed model was capable to predict experimental results with different types of feed containing different concentrations of aromatics.

A process for LGO HDS via catalytic distillation was proposed by Vargas-Villamil et al. (97). It was compared with an optimized conventional HDS process using similar flow conditions which represented an industrial plant. A

compromise was established among the production of diesel and naphtha and the operating costs in order to optimize the conventional HDS process. The kinetics of HDS employed was represented by a Langmuir-Hinshelwood equation, using DBT as representative of all sulfur compounds to HDS via two parallel pathways, hydrogenolysis, and hydrogenation. A pseudohomogeneous plug-flow model of an industrial TBR was developed and incorporated to an HDS unit which was modeled using commercial software. The energy balances and the distribution of the components between the phases were defined by isoenthalpic equilibrium. An effectiveness factor was also included to describe industrial-size catalyst which accounts for the intraparticle transport phenomena. Some remarks were given with respect to the use of catalytic distillation such as the possibility of improving the quality of products even higher than conventional process keeping lower fixed and operational costs. This technology is very prominent to meet future requirements in specifications of low sulfur contents in diesel fuel.

A simple 1D pseudohomogeneous plug-flow reactor model for a multicatalyst system was developed by Kam et al. (98) to study the deactivation mechanisms of hydroprocessing catalysts in atmospheric residue desulfurization (**ARDS**) units due to coking and metal deposition. Three different stages of deactivation are considered: SOR, MOR, and EOR. The reactions considered were HDS, HDM (both removal of vanadium and nickel were considered separately), and HDAsph, the latter accounts for catalyst deactivation. The equations for the mass and heat balances are under pseudo-steady-state because of catalyst deactivation. The model was further applied to a parametric study that examines the effects of LHSV, temperature, and maximum capacity on the performance catalyst systems.

A steady-state pseudohomogeneous plug flow model to predict HDS conversions in an experimental TBR was developed by Sertić-Bionda et al. (99). The simple reactor and kinetic models proposed in this work were used in order to investigate the influence of some reaction parameters (H_2/Oil ratio, pressure, and LHSV) on HDS, using atmospheric gas oil and LCO from FCC as feeds.

Toulhoat et al. (100) have presented a plug-flow pseudohomogeneous model to predict the performance and cycle length of fixed-bed residue hydroprocessing units. The model simulates catalyst activity in pseudo steady-state regime and resistance to deactivation by metals and coke deposition. Both HDS and HDAsph reactions which were described by pseudo Langmuir-Hinshelwood kinetics were considered,, while coke deposition was assumed to be first-order with respect to a driving force equal to the difference between actual and equilibrium coke concentrations in solid phase.

By taken the same model developed by Kam et al. (98) and adding hydrothermal treating consideration as a term which was modeled as power

law, Juraidan et al. (101) simulated the long term behavior of a catalyst and reactor considering the same reactions previously studied by Kam et al. (98) and also carried out the same parametric study. The additional term (coefficient and exponent) was obtained from results of blank experiments in laboratory scale reactor, i.e., experiments carried out with only inert materials without catalyst. Other conditions were the same that those employed by Kam et al. (98). Kinetic parameters for HDM (HDV and HDNi) and HDAsph reactions using Boscan crude were estimated. The model was utilized to predict the complete accelerated test run of experimental results obtained from pilot plant after verification. Simulated results from this model matched quite well with those of pilot plant. A marked improvement over the original model of Kam et al. (98) was achieved.

A two-stage micro TBR for HDT of heavy gas oil derived from Athabasca bitumen was simulated by Botchwey et al. (102). A 1D pseudohomogeneous mass transfer model and a two dimensional heat transfer model were developed. Kinetic models for HDS and HDN reactions used in simulations were based on the Langmuir-Hinshelwood approach. This paper represents an earlier work on the modeling of a two-stage micro TBR for HDT with inter-stage H_2S removal. It was observed that removing H_2S improved the levels of HDN and HDS.

Galiasso (103) developed a simplified pseudohomogeneous plug flow model for isothermal TBR and gas- and liquid-phase reactors in order to optimize a scheme of reactors and to minimize investment. The effect of adding reactor volume to existing units to produce a low-emission diesel fuel was compared by using the new scheme of reactors and the conventional TBR. The model reproduced HDS, HDA, and HDN reactions. It was shown that using the new gas- and liquid-phase reactor, the aromatic hydrogenation and hydrogenolysis reactions can be enhanced. Simplified kinetic rate models (Langmuir-Hinshelwood type) in gas- and liquid-phases for simple lumps of HDA reactions were used in the simulations and kinetics and fluid-dynamic related parameters were previously calculated through an optimization algorithm.

2.2. Dynamic Continuous Pseudohomogeneous Models

Since perturbations can occur in the different HDT process due to changes in composition of reactants, flows, inlet temperatures, etc., it is highly desirable to account for a robust model capable of predicting the performance of the reactor system under such suddenly changes. In this direction some works have been reported in the literature, which main contributions are summarized in the next paragraphs.

Chao and Chang (104) showed a 1D pseudohomogeneous model incorporating the effects of mass and heat dispersion, mass and heat transfer

resistance inside catalyst particle, and catalyst deactivation in order to investigate the dynamic behavior of an adiabatic residue HDS trickle-bed pilot reactor system. The reactions taking into account were HDS, HDV, and coking deposition rate on catalyst. This dynamic model was validated using the experimental data of Kodama (84) and producing step-changes on feed composition, feed rate, and inlet temperature. This rigorous model could be used only for off-line studies because it involves a large number of equations and as a consequence its solution requires huge amount of time.

Oh and Jang (105) presented a rigorous modeling and simulation of commercial naphtha HDS reactor in dynamic regime. The mathematical model is 2D pseudohomogeneous and it uses a kinetic model of Langmuir-Hinshelwood type in order to describe HDS reaction. They also have studied the influence of changing hydrogen flowrate by 10% showing how it influences conversion and temperature. The agreement between predictions and design data can be attributed to well-establish correlations for gas-solid systems.

Chen et al. (106) proposed a pseudohomogeneous 2D-reactor model to describe the dynamic and steady-state of a fixed-bed pilot-plant hydrotreater used for the hydrotreatment of partial stabilized light-coker naphtha, therefore, the reaction system was gas-solid. The rate reaction parameters were obtained in an experimental pilot plant reactor and kinetics was assumed as power *n*th order. Dynamic behavior was induced by changes in hydrogen volumetric flowrate. As main conclusion, it was reported that thermowell can provoke heat conduction within the reactor, thus temperature measurements in the thermowell could differ from those of the bed and due to that special care must be taken when interpreting pilot plant data.

3. Heterogeneous Models

3.1. Steady-State Heterogeneous Models

3.1.1. Continuous models

The main reason for developing heterogeneous models, i.e., models which distinguish the phases in a trickle bed reactor is accounting for inhibitory effects. In the literature, the majority of reports have supposed no significant resistance to mass transfer from gas phase to gas-liquid interface. On the other hand, several researchers have modeled heterogeneous adiabatic systems considering isothermal bed catalyst, due to the lack of properly correlations accounting for this feature. Generally, the energy balance is carried out by supposing pseudohomogeneous behavior even though material balances are considered heterogeneous. Different features remain for discussion such as the influence of axial dispersion in countercurrent operation, the level of vaporization during HDT reactions, the degree of saturation of liquid phase and phase equilibria, among other relevant aspects. Some important

contributions considering different aspects of this type of model applied to HDT processes are reviewed below.

Van Parijs and Froment (107) simulated an adiabatic reactor for hydrodesulfurization of naphtha, using 1D heterogeneous reactor model, Hougen-Watson type kinetic expressions, considering internal concentration gradients. The thiophene was chosen as model sulfur compound for HDS reaction.

A review of equations accounting for interfacial and intraparticle gradients was presented by Froment (32) who also recommended Hougen-Watson approach for expressing rates of catalytic reactions, since power law equations insufficiently account for the interaction of the reacting species with the catalyst. It was also pointed out that kinetics and transport phenomena have to be separately treated in order to successfully simulate and design the reactor. These models seem to be the first rigorous heterogeneous models presented in the literature for HDT process.

Trambouze (108) carried out comparative simulations of concurrent and countercurrent fixed-bed heterogeneous reactors. The criterion selected to make the comparison was the conversion of one of the reactants, while the quantity of catalyst employed was taken as reference. It was remarked that countercurrent reactor requires smaller amount of catalyst than the cocurrent reactor to obtain the same conversion in irreversible reactions, equilibrium reactions or those inhibited by one of reaction products that are typical cases of hydrogenation of aromatics and hydrotreating of petroleum fractions. It is known that axial dispersion is more important when operating in countercurrent mode compared with cocurrent downflow mode, however this author neglected this feature, probably because the objective of his work was only to show the potential of countercurrent operation although some miscalculation can affect quantitatively the results by taking into account or overlooking axial dispersion in a real system.

A 1D heterogeneous model was also employed by Froment et al. (10) to simulate diesel HDS using a kinetic model for HDS of DBT and alkyl-substituted dibenzothiophenes based upon structural contribution. This kinetic approach, that retains the details of the complex reaction network of every feed component, allowed reducing significantly the number of parameters with respect to molecular approach and satisfactory represented experimental data of HDS. It was proposed that the kinetic approach can also be applied to nitrogen-containing compounds. This approach gives good results, but the model is complex and involves extended analytical work to identify the components (94).

A set of differential first order equations was solved by Korsten and Hoffmann (109) in order to simulate the performance of a pilot trickle-bed reactor. The main reaction was the desulfurization of VGO, which was

assumed to be saturated with hydrogen at the inlet of reactor bed. Mass transfer coefficients, pressure drop and physical properties were estimated with correlations reported in the literature and kinetic parameters of Langmuir-Hinshelwood type were obtained from pilot plant experiments. Although correlations employed were developed for non-reacting systems and ambient pressure and temperature, the mathematical formulation showed reasonably good agreement with experimental results. These authors pointed out on basis on their observations that scale-up of pilot plant data to an industrial trickle-bed reactor can yield some miscalculation due to differences in mass-superficial velocity which strongly affect the contact effectiveness between the fluid phase and the catalyst. It seems that the correlation used for the solubility of H_2S in oil is not applicable at other conditions because it neglects the influence of pressure.

An attempt to address the main requirements by relaxing many of the assumptions used in previous models was proposed by Khadilkar (110), who also reported three models. The first one was at pellet-scale level, assuming power law kinetics and the second one was at reactor-scale level, which considers dry and wet zones, but without distinction between external and internal wetting of catalyst pellets. The last model was a combination of both levels: rigorous multicomponent mass and energy balances at reactor-scale and its extension to pellet-scale. The model was formulated by a set of steady-state 1D differential equations and tested with data available for cyclohexene hydrogenation, showing to give accurate predictions of conversion and temperature profiles at reactor-scale. Additional features such as capillary effects, incomplete catalyst filling and evaporation were incorporated in the third level model. They recommended their rigorous approach, level three, for future models with complex reaction systems and volatiles. This model could be implemented for HDS of diesel when considerable volatilization occurs.

Van Hasselt et al. (111) developed a novel model for the countercurrent three-levels-of-porosity reactor and for the internally finned monolith reactor and compared them with traditional cocurrent reactor model in the hydrodesulfurization of VGO. In order to develop the simulation, combination of continuous approach and discrete cells were employed; the former approximation was used to simulate the reactions occurring in a cell-package and the latter to simulate gas-liquid contacting through channels existing through packed bed conceived as quench, hence modeling of reactor can be visualized as a combination of continuous and discrete models. For comparison, the TBR model was simulated with one dimensional heterogeneous model and equations were written for mass and energy balances. Deep conversion was chosen as 98%. It was observed that the required catalyst volume for countercurrent flow is lower than that for cocurrent flow, but the main disadvantage of countercurrent flow was observed to be cooling because

it is less effective since hydrogen flows from high-to-low temperature areas. Due to high degree of freedom for developing this new model, packing could be adapted in order to satisfy demands imposed by mass transfer mechanisms.

A one dimensional heterogeneous model for simulation of commercial trickle-bed reactor was presented by Lopez and Dassori (112). The fluid pattern in gas and liquid phases were approximated by plug flow. Kinetics was of Langmuir-Hinshelwood type for the main reactions considered: hydrodesulfurization and hydrodenitrogenation. The model incorporated catalyst deactivation caused by metal deposition, coking and decrease of effective diffusivity. Parameters of the model were obtained from the literature as well as information compiled from runs in VGO hydrotreater units for HDN and frequency factor, activation energies, absorption equilibrium constant and catalyst deactivation coefficient. Also, they have reported ammonia profile within the reactor but did not report the correlation employed for this prediction.

Bhaskar et al. (9) used a three-phase heterogeneous model to analyze the performance of pilot plant trickle-bed reactor employed for hydrodesulfurization of atmospheric gas oil fraction and to show the influence of intrinsic kinetics and hydrodynamic. Effects of pressure, temperature, space-velocity and hydrogen-to-oil ratio were discussed on model results basis. The simulation showed good agreement with the experiments carried out in a wide range of operating conditions.

A 1D heterogeneous model was employed by Vanrysselberghe and Froment (113) in order to illustrate the performance of industrial hydrotreatment reactor. The continuity, energy and momentum equations were formulated and appropriate correlations were employed to determine physical properties. A synthetic diesel mixture was chosen and detailed Hougen-Watson kinetics based on structural contributions was used. Predictions on evolution of the content of a number of sulfur components and also the molar flux of hydrogen in the liquid phase were showed.

A heterogeneous adiabatic plug flow model reactor for trickle-bed reactor based on previous works (109, 113) was applied by Marroquín et al. (40) to represent diesel hydrodesulfurization and hydrogen consumption. Model compounds were chosen and kinetic parameters were taken from the literature, although finally some changes were necessary to fit monoaromatics in the bench scale data and sulfur content in the industrial diesel product.

Avraam et al. (114) employed a steady-state model for trickle-bed reactor to simulate the hydroprocessing of light oil feedstocks. Plug flow conditions and uniform pellet conditions were assumed. Four general chemical processes were modeled: HDS, HDN, HGO, and hydrogenation of mono-, di-, and triaromatics, taking into account equilibrium aromatic and inhibition by hydrogen sulfide, ammonia and aromatics. This is an important contribution

and seems to be the first one to consider changes in liquid and gas hold up along an HDT reactor due to volatility of light oil compounds. Excellent agreement was found between predicted and pilot plant results.

Chowdhury et al. (2) investigated the desulfurization and dearomatization of diesel oil in an experimental isothermal trickle-bed reactor. A 1D reactor model based on Korsten's model was developed for a two-phase flow reactor considering both mass transfer and chemical reaction, and kinetics for HDS and hydrogenation of three types of aromatics were established. Nonactive zones packed with inert particles, which are located before and after the catalytic bed (the active zone), were also modeled in order to simulate the hydrogen mass transfer from gas to liquid. The correlation between experimental data and predicted ones was higher than 0.9.

Pedernera et al. (115) studied the influence of oil fraction composition on conversion of sulfur compounds in laboratory scale TBR. The reactor model was used to evaluate various configurations of desulfurization process with straight-run gas oil as feed as no advantage was found when separated treatments of individual oil fractions were used. Hydrogen consumption was ascribed to the conversion of sulfur and nitrogen, hydrogenation of aromatics and hydrocracking. Additionally, liquid distribution and wetting efficiency were determined by using magnetic resonance imaging technique. The model used by these authors was an extension of that presented by Chowdhury et al. (2), which also includes modeling of the heat balance in an adiabatic industrial reactor. This paper illustrated the use of new techniques for flow pattern characterization which highlight the trends for hydrodynamic studies in the future.

Bhaskar et al. (116) developed a 1D heterogeneous reactor model to simulate the performance of pilot-plant and industrial TBRs applied to HDS of diesel fractions. It employed a three-phase heterogeneous model based on the two-film theory. The major HDT reactions were modeled: HDS, HDN, HDA, HGO, and HCR. The kinetic parameters were obtained from pilot-plant experiments. The authors reported that the model was capable to successfully reproduce industrial profiles of temperature and concentration of impurities. This work is one of the first that simulate most of the HDT reactions.

Cheng et al. (117) investigated the performance of fixed-bed reactor in cocurrent and countercurrent flows to remove sulfur and aromatics in diesel fuel. The model presented by this group is 1D heterogeneous and accounts for HDS and HDA reactions to simulate the concentration profiles of the reactants and products in the gas, liquid, and solid phases. Superior performance for removing sulfur was observed when experimental reactor was operated in countercurrent mode with respect to cocurrent mode. These authors have expressed adequately HDA reaction rates in comparison with Chowdhury et al. (2) and Bhaskar et al. (116).

Froment (118) illustrated a fundamental approach for kinetic modeling of HDS accounting to a maximum extent for the information provided by the physical-chemical characterization. This structural contribution approach considers detailed feedstock compositions but also transfer limitations inside the catalyst. To validate this approach, an adiabatic commercial reactor for HDS of synthetic diesel mixture was simulated using a heterogeneous plug flow model. The rate equations were considered for the conversion of thiophene, (substituted) benzothiophene, and (substituted) DBT. The results of simulations showed an improvement in the removal of the majority of refractory sulfur components by intermediate flashing of H_2S.

The effect of different catalyst particle shapes on HDS reaction was studied by Macías and Ancheyta (119). They employed an isothermal heterogeneous reactor model, which was validated with experimental information obtained from a small HDS reactor using straight-run gas oil as feed. This study provides a series of formulae for calculating characteristic factors of the catalytic bed involved in the development of the reactor model.

Rodríguez and Ancheyta (120) have extended the model of Korsten and Hoffmann (109) to include mathematical expressions for the rate of HDS, HDN, and HDA reactions. The HDS reaction was described by kinetic equations of the Langmuir-Hinshelwood type; HDN was modeled as a consecutive reaction scheme in which nonbasic compounds are hydrogenated first to basic nitrogen compounds ($\mathbf{HDN_{NB}}$), which undergo further reactions to eliminate the nitrogen atom from the molecule ($\mathbf{HDN_B}$); and HDA was represented by a first-order reversible reaction. The model was validated with experimental information obtained during HDT of VGO in a pilot-plant reactor operated under isothermal conditions. The commercial reactor was simulated and temperature and concentration profiles were obtained.

Yamada and Goto (121) also used the model proposed by Korsten and Hoffmann (109) to simulate and compare the HDS of VGO in a TBR for both modes of operation, cocurrent and countercurrent. Simulations were performed for pilot- and industrial-scale with both modes of operation. The hydrogen velocity was also varied in both reactor scales in order to observe its effect on the outlet sulfur concentration. They assumed almost no resistance between gas and liquid phases. It was recognized that more research is necessary for the correct simulation of countercurrent mode of operation because it could involve significant axial dispersion.

To optimize a cost function representing the essential economical parameter of HDT process Al-Adwani et al. (122) employed a reactor model described by Lababidi et al. (92) including deactivation model. The model was time dependent, which means that all operating variables were time variant. However, since catalyst deactivation is a slow process, the mathematical model was considered as a quasi-steady state model. Heavy residuum was

used as feedstock. This study was focused on conversion, throughput and catalyst life. An industrial scale atmospheric residue HDS process was selected as typical HDT unit to demonstrate the capabilities of the optimization model. This study showed that the optimum cost is highly affected by catalyst cost and the monetary benefit of lower sulfur products.

Jiménez et al. (80, 123, 124, 125) illustrated the use of a steady-state 1D heterogeneous TBR model with both gas and liquid phases in plug and up flow, based on data obtained at pilot-plant scale to predict the quality of products during HDT of VGO and Demetalized Oil (**DMO**) over commercial CoMo/γ-Al_2O_3 (123) and NiMo/Al_2O_3 (80) catalysts. The model involved HDS, HDN, and HDA (mono-, di-, and tri-aromatic) reactions, and combined Froment et al. (10) and Korsten-Hoffmann (109) models. The HDS reaction was described by the kinetic model of Broderick and Gates (126) for DBT, while HDN and HDA reactions used the kinetic models proposed by Avraam et al. (114). Two types of sequential design of experiments were used: for optimal model discrimination and for optimal parameters estimation during kinetic investigation. In most recent papers (80, 125) HDS process was simulated using the mathematical model developed in previous works (123, 124) and several kinetic models reported in the literature. The selection of the best kinetic model and its optimal parameters estimation was done by means of sequential design of experiments (**SDE**). They also reported that water markedly enhanced the capacity to remove sulfur and nitrogen compounds during HDT of heaviest fractions of VGOs (80).

Mostoufi et al. (127) developed a 1D plug flow heterogeneous model in order to simulate the two-stage pyrolysis gasoline hydrogenation process to obtain a C_6-C_8 cut suitable for extraction of aromatics. The first hydrogenation stage was performed in the liquid phase in an adiabatic TBR over Pd/Al_2O_3 catalyst in which hydrogenation of di-olefins was the main reaction. The second hydrogenation stage took place in a two compartment adiabatic fixed-bed reactor in series loaded with NiMo/Al_2O_3 and CoMo/Al_2O_3 catalysts, and operating in vapor phase. Hydrogenation of mono-olefins took place in the first compartment while sulfur was removed in the second compartment. Simulations for HGO and HDS reactions in the second stage reactor were carried out considering model compounds such as cyclohexene and thiophene, respectively. The proposed model considered hydrodynamic parameters i.e. pressure drop, liquid holdup and catalyst wetting efficiency.

Stefanidis et al. (128) presented a study on the improvement of representative operating temperature from temperature profiles of an industrial adiabatic reactor, which is used to simulate reactor performance by laboratory-scale isothermal reactors. To validate the estimated temperature, a steady-state pseudohomogeneous plug flow model with no resistance to mass and heat transfer was developed to describe mass balances of sulfur,

hydrogen sulfide, hydrogen consumption, and hydrogen, as well as heat balance in the adiabatic HDT reactor with feeds ranging from heavy gas oil to diesel. The main disadvantage of this technique is the need of three experimental points: inlet, middle and outlet, while the main advantage is its reliable predictions when deep desulfurization is performed.

Nguyen et al. (129) developed 1D heterogeneous model at steady-state regime with axial dispersion to analyze the influence of fluid dynamic nonidealities on the HDS performance of gas oils in isothermal bench-scale reactors. Langmuir-Hinshelwood type rate model was used to represent HDS rate of reaction.

Recently, Shokri and Zarrinpashne (130) developed a two-phase (liquid-solid) heterogeneous model for the effectiveness factor of HDS reaction with DBT as representative of sulfur compounds in gas oil. The mathematical model is at particle scale conditions because it was based only on the mass balance equations inside catalyst particle. However, in a lately work (81) the authors reported a hybrid model, the previous one with a plug-flow 1D heterogeneous model which was validated with gas oil HDS pilot data. The model was implemented in HYSYS commercial software through FORTRAN codes. The rate of chemical reactions was described by kinetics of Langmuir-Hinshelwood-Hougen-Watson type with DBT representing all the sulfur compounds in the feedstock.

Murali et al. (131) developed a one dimensional heterogeneous model in order to simulate the performance of bench- and commercial-scale HDT reactors. The HDS, HDA and HGO reactions were taken into account in the model. The HDS reaction kinetics was described by a single lumped model for total sulfur similar to Langmuir-Hinshelwood type rate equation used by Korsten and Hoffmann (109), whereas kinetic model for HDA reactions was taken from Chowdhury et al. (2). In the simulations significant amount of feed vaporization (20–50%) was found under normal operating conditions of HDT, which suggested that partial-feed vaporization during simulations needs to be considered. The model was validated with pilot-plant data obtained from up-flow operating mode, near ULS levels to properly account for feed vaporization in heat balance equations. It was mentioned that diesel vaporization is very important in heat balance equations for adiabatic plant simulation because it consumes significant amount of energy, but it is normally neglected in models reported in the literature. Therefore, the most important contributions of this work in the simulation of HDT reactors were the consideration of diesel vaporization and temperature-H_2/oil ratio to be dependent on liquid specific heat capacity.

A 1D heterogeneous plug flow model, which accounts for intraparticle transport of the compounds by Fickian diffusion inside the catalyst pellets, was developed by Verstraete et al. (132) to predict the performance of fixed-bed

hydrotreating units. The feedstock of this study was vacuum residue and experimental data were obtained from isothermal fixed-bed reactor unit. The model predicts the evolution of concentration profiles of gas, saturates, aromatics, resins and asphaltenes, their atomic composition in terms of C, H, S, N, O, Ni, V, and the hydrotreating performances throughout the reactor. It was remarked that it is necessary to take into account the intraparticle diffusion when modeling residue hydrotreating processes.

Different alternatives of quenching a trickle bed reactor were analyzed by Alvarez et al. (34) by employing a 1D heterogeneous model and correlations reported in the literature. The HDS, HDN, and HDA were modeled and energy balance was performed in order to predict profiles of temperature along the reactor bed when quenching was employed.

Liu et al. (133) proposed a novel methodology to understand the dynamic behavior of HDT process. The new methodology is known as the system dynamics (**SD**) model which can predict the influence of operating conditions on the conversion efficiencies of HDS, HDN, HDA, and consumption of H_2. In this work, the SD methodology was applied for the first time in the HDT process modeling with the intention of simulate individual sulfur, nitrogen, and aromatics compounds separately and achieve successful simulation. The methodology was validated with experimental LCO HDT data. The methodology consists of two steps, in the first one it is necessary to develop the dynamic loop diagram showing how a change in one variable modifies other variables, which in turn affects the original variable, and so on. The second step consists of developing a mathematical model usually shown as a stock-flow diagram that captures the model structure and the interrelationships between the variables. This last diagram is translated to a system of ordinary differential equations (**ODEs**), which in this case represented a steady-state 1D heterogeneous model. The same authors (134) have reported another similar study using the SD methodology in order to simulate HDS process of LCO including the nitrogen and aromatic compounds inhibition effects on HDS activity.

3.1.2. Computational fluid dynamics models

Although great effort has been made to incorporate hydrodynamics in modeling trickle-bed reactors through correlations derived from empiricism, more fundamental approximations must be done in order to account for suitable predictive models. The fundamental approximation in modeling, from rigorous point of view, must be performed by solving the conservation equations called the Navier-Stokes equations, a set of nonlinear partial differential equations (**PDEs**), whose solution is possible only for a few simple flows in simple geometries; however the analysis of fluid dynamics is

mathematically complex for actual packed beds. Additionally, constitutive relations that govern material's internal response to external effects must be introduced into the conservation laws. Constitutive relations are derived from correlations; therefore, appropriate selection and validation of those relations are extremely important. Since constitutive equations are established by experimental data, experiments are fundamental in the study of fluid mechanics.

Realistic problems in fluid mechanics can be solved quite effectively by using both computational methods, called CFD, which solves conservation equations, and experimental information. Some assumptions must be done in order to reduce the complexity of conservation equations such as the consideration of lack of effect of viscosity.

The CFD models can be employed as competitor and natural complement to experimentation. For many problems, computational fluids dynamics provides a cost-effective alternative to experimental fluid mechanics. Various physical effects can be turned off, thus providing the opportunity of partially study the phenomena. Simulation of fluid dynamics can help to understand the hydrodynamics of trickle bed reactors and hence performing the scale-up and scale-down properly.

Dudukovic et al. (135) have reported the use of CFD models for hydrodynamics. It was highlighted the common two approaches employed: Euler-Euler formulation and Euler-Lagrange approach. Although the second one seems to be more fundamental, it contains tuning of parameters which in turn must be validated with experimental information. Moreover, no clear advantages of one over the other formulation have been documented.

An application of CFD was given by Gunjal et al. (136) who simulated fluid dynamics of trickle-bed reactors in order to understand its interaction with chemical reactions in laboratory scale and commercial scale reactors. The model was employed to understand the influence of porosity distribution, particle characteristics and scale on the overall reactor performance. The CFD model for TBR was comprised of two main parts: implementation of porosity distribution in the bed and flow equations for each phase (mass and momentum equations), which are based on Eulerian-Eulerian multi-fluids models. The model was applied to HDS and HDA of diesel oil and configuration and operating conditions were similar to that reported by Chowdhury et al. (2). It was pointed out that CFD based models with appropriate validation can be helpful in reducing the gap that exists on prediction between laboratory scales and commercial reactor. It was also reported that CFD model overpredicted conversions because it uses apparent kinetic parameters reported in the literature which have previously lumped hydrodynamics and intrinsic kinetic parameters. Therefore, when those apparent kinetics parameters are used again in the CFD model, which takes

into account the prediction of hydrodynamic parameters, the hydrodynamic effects are being estimated twice (i.e., liquid holdup effects). However, the authors mentioned that the CFD model was used only to understand the influence of reactor scales on its performance. The CFD simulations indicated that porosity distribution is an important parameter when estimating hydrodynamic variables (i.e., pressure drop, liquid holdup, wetting efficiency, etc.), which needs to be taken into account for proper prediction of reactor performance (135, 136). The authors also recognized that H_2S solubility in oil fractions is not correctly predicted by empiric correlation at different operating conditions; hence it is advisable to use an equation of state (**EoS**) in order to improve the estimation. The use of an EoS makes possible to include the effects of both, temperature and pressure; however, suitable interaction parameters could be the limiting face.

3.1.3. Discrete models

Instead of employing the continuum theory, i.e., modeling a TBR with a set of differential equations, some relaxations have been proposed such as the supposition that the system can be treated as a number of connected cells. This assumption allows for simplifying the problem of complex reactor systems modeling and also favors the use of commercial simulators which accurately predict the results of light petroleum fractions.

3.1.3.1 Cell models. A trickle-bed reactor was modeled by Sánchez et al. (137) as a group of consecutive cells, consisting in a CSTR reactor coupled with a separator, in order to take into account vapor liquid equilibrium existing in the reactor. The flash calculations were performed using a commercial simulator, while proper correlations were taken from the literature for simulating pressure drop and catalyst wetting fraction. The pseudocomponent evaluations were calculated by lumping a set of 500 different molecules into three compound types: paraffins, naphthenes and aromatics. The reactions of hydrogenation and hydrocracking were selected and low conversion was maintained. First order irreversible reactions were assumed. The plug flow model was reached by using 25 cells. It was observed that increasing the number of cells had minor effects on product-distribution simulations. The main conclusion was that using proper thermodynamic properties and compound class lumping can be an effective way for trickle-bed reactor modeling and kinetic parameter estimation of complex reaction network. This work shows how available tools such as commercial simulators (Aspen, PRO/II, Hysys, etc.) can be used to save time and effort when simulating multiphase catalytic reactors.

Guo et al. (138) developed 1D and 2D mixing-cell reaction network models to simulate the steady-state behavior of TBRs using the highly exothermic benzene HDT reaction to validate the model. The model was based on a network of CSTRs. Each cell was designed to consider the contribution of interphase mass transfer, reaction kinetics, heat transfer and vaporization effects. This model was developed with the intention of handling multiphase flow and reaction rates, as well as external wetting efficiency, liquid holdup and temperature change due to both phase transition and flow maldistribution for a TBR. The model showed to be suitable and efficient to predict temperature runaway in catalyst bed, and it could be also applied in the scale up of FBRs.

3.1.3.2 Stage models. Jakobsson et al. (139) modeled the cocurrent and countercurrent operations of an HDS reactor using a mixture consisting of DBT, 4,6-dimethyldibenzothiophene (**4,6-DMDBT**), H_2, H_2S, and n-eicosane as solvent. Previous models were used for simulation of cocurrent (140) and countercurrent mode (141) of operation. The countercurrent operation was studied to demonstrate the separation of H_2S during HDS process. Since H_2S inhibits HDS reaction, the countercurrent operation was proposed to be used to protect high performance catalysts. The modeling of countercurrent operation used the so-called rate-based stage model, where the reactor is modeled as a series of rate-based segments (or stages) and each rate-based segment can be indentified as a segment of a packed bed, which directly considers diffusion, heat transfer and multicomponent interaction effects on the calculated segment. These segments are connected by means of mass and heat balance equations to form the reactor model.

To demonstrate the benefits of countercurrent contacting of gas oil with H_2 over conventional cocurrent contacting in a TBR for HDS, Ojeda and Krishna (142) used the equilibrium stage (**EQ**) model of Taylor and Krishna (143), in HDS reactions in the liquid phase. DBT was selected to represent the most refractory sulfur compounds in a liquid feed of n-hexadecane which represented a diesel fraction. The reaction rate for DBT was described as a Langmuir-Hinshelwood type, and it was assumed a plug-flow pattern for both gas and liquid phases flow. It was observed that increasing BT concentration in the feed leads to a lower sulfur concentration in the reactor effluent. That finding was attributed to higher heat of reaction liberated, which provoked higher temperatures and hence conversions were higher. Therefore, and in addition to the fact that countercurrent gas phase cools down the liquid phase, accurate modeling of thermal effects in the reactor during HDS process must be performed. However, it was observed that profiles of sulfur content in liquid phase along the reactor do not match those from continuous models.

3.1.4. Concluding remarks

Given that one pure compound of high molecular weight cannot totally mimic all thermophysical properties of real feedstocks, it maybe inaccurate to consider it as representative of the petroleum fraction (as it is assumed by various authors (144)); therefore, it is advisable in any case to characterize real feeds in various pseudocomponents, for instance, by using distillation curve, SARA analysis (saturates, aromatics, resins, asphaltenes). It is also desirable to account for changes in composition as the mixture reacts. Continuous kinetic models are preferable for such a purpose. The number of pseudocomponents employed to simulate the feedstock will then depend on the desired accuracy to match real properties (114).

Commercially available models, typically based on semiempirical approaches, despite their capability to correctly predict the main characteristics of hydroprocessed gasoil, are not enough detailed to interpret the HDA behavior and can hardly be used for the evaluation of polyaromatics content.

Carruthers and Dicamillo (145) described the influence of catalyst moisture content effects on HDS and HDN of several commercial catalysts, and found that activities generally decreased with increasing moisture content of the catalyst. However, this finding contradicts other reports (80, 131), since it was observed that water markedly enhanced the capacity to remove sulfur and nitrogen compounds during HDT of the heaviest fractions of VGOs. The enhancing behavior may be explained since water facilitates the solubility of pure molecules added in a VGO severely hydrotreated, which was used as a matrix feed (80). According to Furimsky and Massoth (146), water content gives both enhancing and inhibiting effects by modification of catalyst structure. The effect of water on HDS and HDN reactions gains on importance with increasing concentration in the feed, and after certain level is exceeded the poisoning effect of water may be quite significant.

The diesel vaporization is very important when simulating heat balance equations for non-isothermal plant, however, it is generally neglected. Since diesel vaporization consumes significant amount of energy, and considerable vaporization takes place at typical HDT operating conditions, it is important to properly account for it to simulate catalyst bed temperature rise in an accurate manner (131). Only very few models (2, 47, 48, 131), among others, have taken into consideration partial vaporization of liquid feed in the simulation of HDT reactors. Other authors (114) have also supposed gas-liquid equilibrium along the reactor.

Murali et al. (131) highlighted the need for using more detailed feed characterization considering different types of sulfur compounds when explaining desulfurization rates in commercial plants. An expression of the liquid specific heat capacity that must be function of both temperature and H_2/oil ratio was also suggested in order to account for enthalpy change due to feed

vaporization, and adequately simulate catalyst bed temperature profiles, product quality and chemical H_2 consumption in commercial reactors.

The novel SD model seems to be a promising methodology to dynamically simulate commercial HDT process, namely, to relate the changes that the variables undergo in a reactor model, which in turn are inter-related (133, 134). Since the SD model can easily address the relationships between the variables, it has successfully predicted how the operating conditions influence the conversion efficiency of the main HDT reactions, the impact factors for inhibition effects, the increment of temperature at the outlet, and the consumption of H_2 in the reactor. It is important to point out that this method may use both steady-state or dynamic mass and heat balance equations in its step of mathematic formulation.

The simulation of HDS is complicated as many parameters have to be determined for different feeds, catalysts and operating conditions. This complexity is a great challenge for the deterministic models (134). SD model has been reported to be able to predict casual relationships between variables, although they must be first validated to remove structure flaws. The use of SD model for analysis of various scenarios could be of interesting application due to its ability to optimize the various parameters involved in a TBR, because it has been reported to be easier than other simulation methods.

The cell network approach seems to be suitable for systems with large amount of heat released by chemical reactions, thus the use of models that consist of a set of ODEs is not promising since the numerical solution of it becomes difficult due to the stiffness of the equations (138).

3.2. Dynamic Heterogeneous Models

Reliable three-phase reactor modeling and simulation should be based on true dynamic heterogeneous models, which can be used not only for scale-up, start-up, shut-down, and operability studies, but also to obtain a meaningful continuity path to the steady state of the reactor and to investigate the existence of exotic phenomena such as oscillations and steady state multiplicity, since dynamic models provide a realistic description of the transient states of three-phase reactors. The study of the dynamic behavior of the three-phase reactor also allows for designing the best system control in order to obtain a safe, efficient and profitable operation. The dynamic models, although more complicated to formulate and to solve, should be preferred over steady-state models because the numerical solution strategy of dynamic models is more robust than the solution of steady-state models (147, 148). Some important reports using such models are described in the following sections.

3.2.1. Continuous models

The hydrogenation reaction of toluene to methylcyclohexane, which occurs in a three-phase trickle-bed reactor with countercurrent and cocurrent gas and liquid flow, was simulated by Wärnå and Salmi (147) by means of a dynamic three-phase reactor model. The model equations for the gas, liquid and catalytic phases consisted of ODEs and parabolic PDEs, which were solved by using numerical methods. The reactor was assumed to operate adiabatically and non-isothermally. The reaction rate for toluene hydrogenation was of first order and kinetic parameters were obtained in an isothermal laboratory scale cocurrent trickle bed reactor at total pressure of 4 MPa and temperature ranging from 65–125°C. It was observed that countercurrent operation gave slightly higher toluene conversion than cocurrent operation. This work showed that the dynamic approach provides a meaningful path to steady sate of the reactor and gives valuable information of reaction dynamics. Because no mass transfer resistances inside the catalyst were considered, the model is only applicable for non-porous particles.

The dynamic modeling principles for fixed (trickle) beds were described by Salmi et al. (148). An axial dynamic heterogeneous model was applied for the hydrogenation of aromatics simulation. The kinetics was conveniently measured in laboratory-scale autoclave. It was proposed that dynamic models should be preferred instead of steady-state models, since the former provide a realistic description of transient states of three-phase reactors and the numerical solution of dynamic models are more robust, and so the solution of steady-state models. The case studies revealed the importance of internal mass transfer resistance in catalyst particles as well as the dynamics of different phases in three-phase reactors. This study confirmed the disadvantage of the Wärnå and Salmi (147) previous model where intraparticle mass transfer resistances were not considered.

A 2D model for temperature and concentration was applied by Hastaoglu et al. (149) to simulate gas-solid reactions in a desulfurization fixed bed reactor. Three levels of process space were used: bed, pellet, and grain. Steady-state experimental naphtha HDS data of a fixed bed reactor were used to validate the bed model for concentration whereas thermal behavior was validated transiently. The model was tested by generating the transient concentration of each component, and profiles of system parameters were obtained, giving good insight into the behavior of the system variables. However, since the model was developed for a gas-solid system, it does not include all the mass and energy transfer terms that should be present in a three-phase reactor model to simulate a TBR.

Vogelaar et al. (150) derived a plug flow model to describe coke formation and metal deposition profiles in catalyst pellets found in hydroprocessing as a function of position in the isothermal reactor, and to predict catalyst

deactivation behavior due to pore blocking at reactor level. A lab scale HDM experiment was simulated as case study. The model is based on three levels of scale: the reactor level, the catalyst particle level and its active phase. The modeling of this process provides a better insight in the deactivation mechanism of hydroprocessing catalysts, and can be used to predict their deactivation behavior in industrial reactors. At particle level, the effective Fickian diffusivity $\left(D_{ei}^{f}\right)$ of a molecule inside porous structure was estimated considering friction between the solute and pore walls by a restrictive factor due to that friction with the pore wall.

The deposition process of fine particles under chemical reaction conditions in a high pressure/temperature TBR was analyzed theoretically by Iliuta et al. (144) using a dynamic multiphase flow deep-bed filtration model coupled with heat and mass species balances equations in the liquid, gas and solid (catalyst+solid deposit) phases. This deep-bed filtration model incorporated the physical effects of porosity and effective specific surface area changes due to fines deposition/detachment, gas and suspension inertial effects, and coupling effects between the filtration parameters and interfacial momentum exchange force terms. The three-phase heterogeneous model developed in this work to simulate the TBR performance incorporated the intraparticle mass transfer resistance and solid deposits by fine particles that lead to porosity reduction and bed plugging. It was found that fine particles deposition does not influence appreciably TBR performance, the only undesirable consequence of fine particles deposition process was reflected in an almost exclusive hydraulic effect of bed plugging and the increase of the resistance to gas-liquid flow.

Ho et al. (151) developed a four-parameter plug-flow 1D heterogeneous model that gave more quantitative insight of how sulfur, nitrogen, and catalyst surface interact on many widely dissimilar time scales. The theory in which the model is based on is applicable to reaction systems where catalyst poisoning dynamics is driven by nonequilibrium adsorption. Modeling of nitrogen competitive adsorption phenomenon effects in HDS of oil fractions at the catalyst surface level was addressed with special attention to the design of robust catalyst-deactivation-compensation operating strategies in deep HDS of middle oil fractions. The experiments were carried out in a cocurrent fixed-bed reactor operated isothermally in upflow mode. The model was capable of reproducing the observed inhibiting effect of nitrogen species on HDS of hindered heterocyclic sulfur compounds.

Mederos et al. (152) developed a dynamic heterogeneous 1D model to simulate the behavior of TBRs used for catalytic HDT of oil fractions in pilot and commercial scales. It considered the main reactions present in HDT process of oil fractions: HDS, HDN and HDA (total aromatics). The model was validated with experimental data obtained in an isothermal pilot reactor

during HDT of VGO over a commercial NiMo catalyst. After validation of dynamic model with pilot-plant data, it was applied to predict the dynamic behavior of a commercial HDT reactor. The start-run simulation of the commercial HDT reactor showed the "wrong-way" behavior in the temperature axial profiles before steady-state was reached, a phenomenon already reported in other previous papers. The combining of heterogeneous mass balance and pseudohomogeneous heat mass balance, as reported by Rodríguez and Ancheyta (120), seems to be inconvenient; however Mederos et al. (152) demonstrated that this assumption is correct if only predictions of concentration and temperature profiles at steady-state are necessary. In other contribution of the same authors (3), the effect of cocurrent down flow and countercurrent flow operation modes on HDS, HDN and HDA was analyzed by employing the same model (152). An important finding was that higher HDT conversion in countercurrent mode of operation is obtained with respect to cocurrent flow mode, which justifies the development of new reactor internals to improve the performance of TBR operating in countercurrent mode.

3.2.2. *Cross-flow models*

The cross-flow model seems to be more realistic than others because it considers a stagnant zone and a dynamic zone, which is a reasonable supposition for trickle-bed reactors. Only one work dedicated to HDT process with this consideration is available in the literature.

Tsamatsoulis and Papayannakos (153) employed a cross-flow model to investigate the non-ideal behavior of the liquid flow in dynamic regime in a bench scale TBR under HDT operating conditions. The development consists of two first order PDEs to model the static and dynamic regions, which were solved analytically. This study provides information on how a catalyst bed should be diluted with inert particles so that the plug flow pattern describes the liquid flow in an experimental trickle-flow hydrotreater in order to derive kinetics. The main disadvantage of this model was the use of non porous grains.

3.2.3. *Concluding remarks*

Although the HDT reactor in countercurrent operation has been modeled by several researchers (3, 117, 121, 139, 142), only some of them ((3)) have studied this mode of operation in dynamic regime for HDT reactions. More investigation in this field is necessary in order to properly establish the influence of parameters such as axial dispersion and heat effects on reactor behavior. For instance, only few correlations for calculating such parameters in the case of countercurrent flows are available.

Dynamic heterogeneous models are frequently used to study process control; however the computational time demand could narrow their use to those cases when time is not a limiting factor. Most of the times, when online analysis is desirable, a simplified model (as neural network model) is commonly employed.

4. Learning Models

An Artificial Neural Network (**ANN**) builds an internal model of the governing relationships embedded in the data base used for training. The basic method of neural network refers to implementing in the computer, by software or special hardware of processing nodes – neurons – that are linked to each other by variable-strength connection weights. Causal relations between each model input and output may be calculated from the analysis of the trained ANN structure.

The ANN must learn about the problem under study, and this learning stage is commonly called the training process. Once an ANN is trained, it can be used to properly simulate an HDT unit, the effect of type of evaluated catalysts and feedstocks on unit performance, control the operation, optimization of the unit, etc. Since ANN approach presents user-friendliness and simplicity, suppressing the difficulties and complexities associated with first principle models, it is not necessary to have sufficient mathematical and programming expertise to formulate complex objective functions and constraints.

ANNs was applied by Berger et al. (82) to model hydrodesulfurization of atmospheric gas oil in a mini-pilot plant trickle-bed reactor as a function of temperature, pressure, LHSV, inlet sulfur concentration and staging. The hidden layer contained three neurons. Inputs were normalized in order to give equal importance to each input and to reduce the effect of outliers in the database. The database containing 25 examples was randomly divided into learn and test sets containing 17 and 8 examples respectively. The results calculated by the ANN model were compared with the experimental data and an average relative error of 10% was observed. Causal index (**CI**), which determines the relative effect of each input variable on the model outputs was applied to the five variables tested in the HDS system and the relative significance of LHSV and temperature over HDS was observed. Almost linear dependence was observed for sulfur outlet as function of LHSV, however, this behavior does not correspond to experimental data trends. Probably, it is necessary to input more data to the model in order to do better learning at low spaces velocities.

Lopez et al. (154) proposed different structured and trained models based on process data and laboratory analysis obtained from a commercial VGO

hydrotreater unit. The authors showed the power of a three-layered perceptron ANN used as an analysis tool for the optimization of several existent functions between important process variables controlling the continuous operation of a VGO unit. Those different ANN models were used to predict the following operating conditions: feedstock composition (paraffins, naphthenes, total aromatics, and mono-, di-, tri- and tetra-aromatic compounds), feedstock and liquid product quality properties (sulfur and metals content, API gravity, TBP at 50 vol%, and refractive index), and process operating variables (product flow rate and average reactor temperature). After comparison of results predicted from correlation modeling and ANN, it was observed better data fitting for the last approach. This feature could be attributed to the fact that ANN model globally takes all effects occurring in the reactor while correlations only allow for predicting specific parameters ignoring some effects such as transport problems within the reactor.

Commercial data were used by Bollas et al. (155) to develop predictive models for integration of two units, HDS and FCC, and examine the economical benefits of their optimization. The 350 data series were randomly split into training and validation sets consisting of 225 and 125 data series, respectively. The HDS kinetics derived from pilot plant studies was first simulated by predictive model and then the operation of commercial unit. Vacuum gas oil was considered as feed to HDS and the liquid product obtained from this process was fed to FCC unit. The main product, gasoline fraction, was subject to maximization and restrictions. The neural network was a multi-layer perception (**MLP**) consisting of three layer: an input layer with as many nodes as the input variables, a hidden layer with number of nodes varying from 1–5 and an output layer with as many nodes as output variables. Simulated trends agreed well with the existing experience although the model performance deteriorated for predictions of sulfur in gasoline fractions.

A hybrid neural network model, a deterministic pseudohomogeneous mathematical code coupled with a neural network, was presented by Bellos et al. (156). This model was used to predict catalyst deactivation rate and dependence of catalyst activity with liquid feed quality. The reactions taken into account to validate the industrial HDT reactor model were HDS and HCON. Part of the kinetic parameters was obtained from industrial reactor operation data and also from experiments carried out in a small scale reactor using industrial catalyst size and representative feeds.

Salvatore et al. (157) used a hybrid approach based on **ANNs** together with a post-processing classification algorithm to detect faults in a simulated HDT unit. An HDT model to represent the real unit was also developed. The modeling equations were chosen so the process showed similar dynamic to existing units, by means of concentration and temperature profiles through

the catalytic beds. The model of the reactor was built assuming that the reactor is composed by n CSTR-cells (12 stages) in series with equations describing mass and energy balances in each stage.

Zahedi et al. (158) presented an ANN model for the simulation of an industrial HDT unit based on measured plant data. The proposed model predicts hydrogen demand for HDS, outlet API, and sulfur content as a function of inlet API and sulfur content in weight percent for seven different feedstocks including kerosene, furnace oil, diesel, coker gas oil, cat cycle oil, thermal cycle oil, and virgin gas oil. Eighty three data sets were used for training and then forty data sets were predicted and compared with those collected from operating plants. Optimum architecture of ANN was determined in order to achieve good generalization. The ANN model results were compared with those predicted by a conventional simulator and it was observed that the ANN model accuracy outperforms the traditional simulator.

Recently Lukec et al. (159) developed ANN models to determine sulfur content in the hydrotreatment product of LGO and VGO. The models were trained using the process and laboratory data of routine refinery production. As the models showed to be simple, easy to use, with a good predictability they were used in practice for accurate continuous process monitoring, continuous on-line predictions, process fault detection, estimation of unmeasured states and parameters, pointing out a measurement error to the hardware analyzer, process regulation, adaptive control, real time optimization, and efficient product quality control. This work emphasizes the main advantage of the neural network models because they can estimate the kinetic parameters for different feedstocks, which mainly depends on the amount of data set used during the training process.

E. Advantages and Disadvantages of Models

Some researchers have established that probabilistic models can be fitted more flexibly than deterministic models to the experimental data for TBRs, which suggests that a probabilistic description of TBRs corresponds more closely to reality than a deterministic description (37). However, still further research is required in order to reach a final conclusion, for instance, the usefulness of such complex models. The advantages and disadvantages of the different models reported in the literature to simulate HDT reactors are shown in Tables 2, 3, and 4.

F. Concluding Remarks

A kinetic model based on detailed description can be only described by a large system of deferential and algebraic equations, implying a huge number

Table 2: Advantages and disadvantages of pseudohomogeneous models.

Model	Advantages	Disadvantages
Based on kinetics	1. Currently used for testing and evaluating catalyst in bench-scale reactors (9). 2. When reaction being studied is first-order or pseudo-first-order, residence-time distribution curve can be used to calculate the intrinsic reaction rate constants, which allows determining contacting efficiency (58). 3. Easy and fast application to systems where rate of reaction is limited only by intrinsic reaction kinetics (44).	1. Based on *a priori* assumption of appropriate kinetics and week underlying theory (116). 2. Do not account for the influence of hydrodynamics and related phenomena (i.e. mass transfer) on conversion (9, 111). 3. The use of these models for comparison of different catalysts may suffer from uncertainty, because of superimposition of kinetic and hydrodynamic effects (32). 4. Kinetic models have very restricted application for deep desulfurization calculations (160). 5. Sometimes k_{in}'s obtained with kinetic models do not really come from intrinsic kinetics because these are frequently masked by transport limitations, and for this reason they are also known as ''effective'' rate constants ($k_{e,j}$) (32).

Table 2: Continued.

Model	Advantages	Disadvantages
Based on hydrodynamics	1. Flow regime in which the reaction occurs is taken into account. 2. Contacting effectiveness factor and liquid holdup are incorporated. 3. Results from experimental reactors and industrial plants can be correlated (37). 4. Predictions of these models are superior at low levels of conversion (62).	1. Group various phenomena in few parameters (37). 2. No theoretical justification for assuming that reaction rate is proportional to total liquid holdup has been found (6). 3. Representing deep conversion as in the case of HDS reaction is not possible by using hydrodynamic models. 4. It may not be able to explain the performance of TBRs satisfactorily because of the existence of stagnant zones, particularly in the case of porous catalyst (8, 37). 5. Since the catalyst effectiveness factor and incomplete wetting are strongly coupled phenomena, they cannot necessarily be expressed in the regime of interest by a single product of catalyst effectiveness for a completely wetted pellet and fraction of external area wetted as it was suggested in this type of model (37). 6. Physical reality is very far from these empirical descriptions which cannot account for characteristic phenomena such as channeling or hot spots formation, the latter is formed mainly by poor solid-liquid contacting (28, 61). 7. Parameters could vary substantially depending upon the flowrate region being considered. 8. Assumption of reaction order *a priori*.

Table 2: Continued.

Model	Advantages	Disadvantages
Continuous	1. A unique phase is considered, reducing the number of variables, making easier to reach a solution for the equation balance (40). 2. Useful for simulating industrial scale equipment when volume of reactor is too large compared with an individual pellet (46). 3. Rapid means for obtaining an estimate of the reactor size necessary to achieve any given conversion and examining the influence of several design variables on the reactor's behavior (46). 4. Especially suitable for steady-state analysis (20).	1. The model neglects interfacial resistance, thus it would attribute concentrations different to that actually contacting the catalyst (40). 2. Inhibitory effects provoked by gaseous components such as ammonia and hydrogen sulfide are ignored (109, 112). 3. Hydrogen pressure variation is not considered. 4. Not able to predict effects of volatized fractions (95, 114). 5. One-dimensional homogeneous models do not provide information about the possibility of achieving an excessive temperature at the center of the reactor that can be markedly different from the mean temperature at the same longitudinal position (46).
Empirical correlations	1. Easy to predict quality properties of HDT products from data of feed characteristics and process conditions (75, 77). 2. Polynomial expressions resultant from statistic regression analysis can be employed to perform optimization studies.	1. Correlations are valid only within the range of experimental results that were used for its development; extrapolation can be performed only within a very narrow range beyond extreme values of the experimental framework (75). 2. There is not generality of the equations, even for similar reacting systems (reactor dimensions, size, shape and type of catalyst, feedstock, operating conditions, etc.).

Table 3: Advantages and disadvantages of heterogeneous models.

Model	Advantages	Disadvantages
Continuous	1. Incorporating mass and heat transfer in the three phases, phenomenological effects can be modeled separately and added to the reactor model in order to improve predictions. 2. Adequate for purposes of scale-up and scale-down reactors. 3. Suitable for kinetic studies, and heat and mass parameters estimation. 4. Catalyst incomplete wetting and liquid wall flow are taken into account. 5. Intraparticle diffusion can be considered (10).	1. Validation data using different reactors and reaction systems are scarce (9). 2. There are too many unknown/uncertain parameters involved whose correlations reported in the literature, especially to evaluate mass and energy transfer coefficients, are developed under low pressures and temperatures, which differ from typical conditions employed in HDT process. 3. Data of gas-liquid mass transfer for small trickle bed reactors (low Reynolds number) do not exist in literature (161). 4. The main obstacle when using models which account for evaporation is the difficulty to incorporate it into reactor simulation codes of VLE for the petroleum cut, which include a great number of components (161). 5. Unsuitable representation of radial temperature profiles within the solid phase when a chemical reaction takes place (20). 6. Slow response of the model limits its use as control tool for on-line application in industrial practice (138, 159).

Table 3: Continued.

Model	Advantages	Disadvantages
CFD	1. Can be used to reduce empiricism in scale-up/down and optimization of the TBRs (136). 2. Reduced time of programming and accuracy solutions are provided. 3. Detailed information such as local velocities and local hot spot formations can be obtained since the structure heterogeneity of the packed bed is taking into account (136, 138). 4. It is possible to be used in scale up of packed bed reactors in which the flow distribution is significantly affected by complex reactions, since the non-reactive CFD model can be combined with other reactive models, such as the cell reaction network model (138).	1. User correlations are employed to describe phenomena related to a particular reaction system, hydrodynamics and energy and mass transfer, so that empiricism is still present. 2. CFD models are normally computationally expensive, especially when a huge number of geometrical details or small-scale spatial variations need to be taking into account. 3. Because the general reactive simulation with CFD model is conducted for the macroscopic reactor level and tends to track all catalytic reactions and hydrodynamic phenomena in a simultaneous approach, it is not easy to identify the origin for any numerical difficulty present when kinetics of multiple reactions are highly coupled and non-linear, and/or when reactions are highly exothermic (138).
Cross flow	1. Axial dispersion defined in this model is practically independent of the liquid loading (37). 2. Both stagnant and free flowing zones in a TBR are considered, which is considerably realistic. 3. Experimental responses curves even with strong tail are well reproduced (17).	1. The uncertainties associated with determi nation of third higher moments which are employed to calculate parameters (17).

Table 3: Continued.

Model	Advantages	Disadvantages
Cell	1. Since each cell can be simulated employing an ideal reactor and flash calculations are performed by tools included in commercial simulator, modeling a TBR by this method can lead to save considerable time. 2. Easy way to simulate vaporization in a TBR (137). 3. Chemical composition information of light fractions is retained in the model (137). 4. Suggested for mass transfer analysis since only one steady-state solution is predicted (20). 5. This model type is an option when other models fail to simulate 2D systems with complex kinetics and enormous reaction heat released (138). 6. Due to the sequential approach of the cell models convergence is faster because it is obtained at one geometric position at a time (138).	1. Application of this model to heavy petroleum fractions depends on the accuracy of correlations to calculate parameters employed in the simulator. 2. Excessive computational effort. 3. Fail to reproduce backmixing behavior (20).
Stage	1. Considerable work exists in the literature about equilibrium between phases, which is a supposition in stage-models.	1. Fail to properly account for the influence that chemical equilibrium has on VLE and vice versa (162). 2. No short-cut procedures are available for modeling reactors with the equilibrium stage model (162).

Table 4: Advantages and disadvantages of learning models.

Model	Advantages	Disadvantages
Learning	1. Used when deterministic model cannot describe adequately a system (156). 2. Easily create scenarios for optimizing purposes (155). 3. Ability to analyze non-linear processes (157–159). 4. Successful in process fault detection and diagnosis (157). 5. Noise tolerance (157, 163). 6. On-line adaptability for industrial use (157, 159). 7. Ability to adapt and continue learning (continuous update) to improve performance and extend its applicability (156, 157). 8. High degree of robustness or fault tolerance (157). 9. Comparing the traditional computational time to convergence, ANNs are much faster than traditional modeling (158). 10. Capability of generalizing the answers (158). 11. Acceptable results for unknown samples (158). 12. This kind of models may make use of the heterogeneous models as a complement to accomplish the optimization and on-line control of commercial HDT units (112). 13. Coupled with deterministic models it is possible to predict catalyst deactivation rate in HDT units treating different feeds (156).	1. Require an enormous number of data obtained from experiments or coming from a deterministic simulator for training. 2. The successful of ANN models depends on the quality of process and laboratory data used (159). 3. They cannot be used to extrapolate operating conditions out of the data framework employed for training. 4. There are no reports of using ANNs for scaling HDT purposes. 5. Since the ANNs are empirical models all influences of the HDT complex system cannot be included (159).

of physical and physicochemical parameters. Due to this feature, some simplifications have been proposed.

Among the different approaches in kinetics of petroleum fractions employed during the last two decades, the most common formulation is that based on a single lump by employing a power law or Langmuir-Hinshelwood expression, although it seems that it is most appropriate to divide the reactant mixture into two lumps: the easy-to-convert and the refractory ones. This approach has been employed because of its easy numerical implementation and its dependence on global parameters which in turn can be easily measured. However, single lump is not valid for high conversions because it does not take into account variations in composition of different feedstocks, besides due to future requirements of lower impurities contents in fuels, the power-law model is no longer reliable. Other approaches have been proposed following different criteria. As main contributions, the widely cited structural approach of Froments' work is a novel way of lumping more rationally the huge amount of sulfur species contained in real feedstock although considerable analytical work must be performed for obtaining the involved parameters. Recently Froment et al. (164) have reported the application of this theory for different feedstocks for which the parameters are available by taking almost the same catalyst system and performing few experiments. Thus, data obtained together with the numerical parameters from previous works were employed for reproducing the overall conversion of some compounds. It was highlighted the necessity to establish a catalog of invariant feed elements for different commercial catalyst to apply this approach to routine analysis. Another approach cited by Te et al. (165) is based on computational quantum chemistry, supposing linear relationship between the reaction rate and equilibrium constant. Few reports using this approach in real systems are available; however, with the accelerated development of more efficiently computers and friendly-use quantum chemical software, this approach could be, in the next years, an important trend in exploring the kinetics of real feedstocks.

It seems that although accurate, these approaches are not used for exploratory studies, because they demand considerable analytical work, then they must be hard worked in the future in order to account for more fundamentals and feedstock invariants. The most recent promissory approach employed is the so-called continuum kinetic lumping. This theory assumes the mixture as a continuum where reactants are distributed over the entire mixture and reactivity of agglomerates of molecules decreases monotonically with molecular weight or another index. In this same direction, a novel gamma function distribution has been proposed in order to predict accurately the deep desulfurization of diesel (166). The continuous kinetic approach appears accurate and it involves only few parameters. Moreover, it has been

applied to real feedstocks with closely agreement between predictions and experimental data (90). It seems that continuum kinetic model is enough to describe an industrial process because it is possible to predict accurately the apparent order of reaction and it provides a tool for prediction of physical properties through the length of the reactor, which can be used for prediction of transport and thermodynamic properties. Easy adaptation of power-law or Langmuir-Hinshelwood expression can be incorporated to continuous theory of mixtures. One disadvantage of continuum approach observed by Mejdell et al. (94) was the fact that some components have large deviations from general TBP-reactivity tendency, such as substituted benzothiophenes. Due to that, these authors recommend to model these compounds separately from the rest of spectrum, especially for high conversion kinetics. The same observation although employing discrete lumping has been pointed out by Hu et al. (167), i.e., using multiple lumps based on types of sulfur compounds for explaining desulfurization kinetics at ultra low sulfur levels. This observation is in agreement with Murali et al. (131) who have pointed out that at low LHSV better match could be obtained if sulfur speciation is considered. However, such approaches requires of support of advanced analytical tools to identify the various sulfur compounds present in the feedstock.

The recent trends in the production of heavy crude oils and the need of refining them and their distillates create the necessity of developing suitable reactor models in order to make preliminary calculations in the process design of new refining units. Currently, due to the continuous changes in feedstock composition, only average properties can be obtained and kinetic studies are only carried out by employing the simplest expression, i.e., the power-law or Langmuir-Hinshelwood approach with adjustable parameters and single lump. A better kinetic approach is not usual because of the unavailability of characterization techniques for heavy crude oils and residua. The same happens for the reactor system, since no correlations are available to evaluate all the parameters of a detailed model. For such cases, it has been better and convenient to employ simple kinetic and reactor models. However, these models cannot be used for modeling the complex hydrodynamics existing in an HDT reactor. Recently, Guo et al. (138) have proposed a sequential approach for reducing the gap between CFD simulation and complex reaction system based on the cell network model. Even if one employs a simplistic reactor model, detailed kinetic coupled with such a reactor model is not well suited for on-line analysis or optimization and control. Again, depending on the purpose of the study, one could sacrifice the chemistry in order to study more realistic systems such as those of a simple (lumped) reaction sustained in a reactor in order to analyze the fluid dynamics by means of CFD instead of performing cold flow experiments. Even when powerful computers are available

nowadays, modeling hydrodynamics of complex systems is only able to be performed for simple kinetic models (168).

A deep discussion of kinetic models selection is beyond the scope of this review. More detailed treatment of these kinetic approaches is summarized elsewhere (165). More comprehensive details and limitations of continuum lumping have been revised by Ho (168).

Regarding phase equilibria calculations, two different approaches have been proposed: one involves measurements of bulk properties employing EoS considering the phases as single compound, and the other one is based on continuous thermodynamic, which is rarely used in real systems such as petroleum distillation.

Akgerman et al. (85) reported the influence of feed volatility on conversion in TBRs, arriving to the conclusion that very different level of conversion is predicted if volatility is included with respect to the case when it is not included. Frye and Mosby (47) correlated the level of HDS for light catalytic cycle oil with the liquid vaporization at the entrance of reactor, supposing that appropriate reaction rate constants are provided. The effect of species volatility on deep desulfurization of diesel has been explained by Hoekstra (48), arguing that light compounds are stripped from the liquid and the remaining sulfur compounds increase its concentration favoring reaction rates. Avraam et al. (114) have showed the effect of volatilization through the length of reactor by plotting the variations of liquid and gas holdup as a function of dimensionless position through the reactor and emphasized the importance of volatilization on energy balances. The same conclusion was brought out by Murali et al. (131), who only calculated the vaporization at the entrance of reactor however. These authors have also recognized the need of accurate kinetic model coupled with vaporization effects in order to predict the performance of a reactor for deep desulfurization. Chen et al. (169) conducted a VLE study with LCO in order to investigate the influence of vaporization of feedstock on the operating regime of a pilot plant hydrotreater, although they remark that results observed in this small scale cannot be extrapolated directly to a commercial plant.

More research in this area is necessary particularly for HDT of light fractions of petroleum. It is also necessary to incorporate the continuous thermodynamic approach since it permits the description of realistic systems, such as petroleum fractions, which could be considered as a mixture of infinite number of components (170, 171). As can be inferred, the continuous descriptions together with separately modeling of some identifiable compounds can provide accurate explanation of either kinetics or thermodynamics although a system described by these approaches could be too complex.

It is not strictly necessary to take into account vaporization effects for modeling of hydroteatment of heavy crude oils and residua, because almost all

reactive compounds remain in the liquid phase even at high temperatures employed for these processes as it was observed in a recent study, i.e. less than 1% of mole fraction of VGO in gas phase at typical reaction conditions (34). This simplification can contribute to reduce the complexity of such a model and it favors the exploration of other features such as the chemistry or other related phenomena.

III. GENERALIZED MODEL

When developing a generalized reactor model, nothing should be neglected *a priori*, but all the resistances and others terms must be included in mass and heat balance equations (148). However, such a model can be very complex and difficult to solve, even supposing that all the parameters involved are available, thus some assumptions are still needed. The assumptions, of course, have to be well-supported and preferably validated with experimental data. The mass and heat balance equations in the case of the generalized reactor model for hydroprocessing are detailed in Tables 5 and 6, respectively, which have been developed with the following assumptions: liquid and gas properties (superficial velocities, mass and heat dispersion coefficients, specific heats, holdups, and densities), catalyst properties (porosity, size, activity, effectiveness, etc.), wetting efficiency, and bed void fraction are constant along the whole catalytic bed. Inside the catalyst particle, mass and heat effective diffusivity coefficients may also be assumed constant. Under these considerations, those parameters can be put out of the partial derivatives with respect to axial and radial spatial coordinates. For the case of non isothermal reactor models physicochemical and thermodynamic properties must be evaluated at the temperature of each discretized point in the mathematical model.

Although there are some correlations reported in the literature to predict variation (radial and axial) of bed porosity (129, 172), it is difficult to incorporate them in conventional continuum models. Hence, the effects of porosity distribution and subsequent local velocity variations are also neglected. This assumption could lead to inaccuracies in the predictions of any reactor model as was shown by Gunjal and Ranade (136) using a CFD model. These authors reported that the difference in HDS conversion, considering uniform porosity distribution in the bed, was about 15% higher than in the case where non-uniform bed porosity was considered. The results demonstrated the necessity of coupling the continuous models with rigorous hydrodynamic models to take into account the bed porosity which strongly influences the hydrodynamic performance of PBRs.

Table 5: Generalized mass balance equations (M).

Mass balance \ Term	Accumulation (1)	Convective (2)	Axial dispersion (3)	Radial dispersion (4)	G-L transfer (5)	G-S transfer (6)	L-S transfer (7)	Flowing-Stagnant liquid transfer (8)
(**A**) Gas phase (i = H_2, H_2S, NH_3, LHC)	$\frac{\varepsilon_G}{RT_GZ}\frac{\partial p_i^G}{\partial t} =$	$\pm \frac{u_G}{RT_GZ}\frac{\partial p_i^G}{\partial z} +$	$\frac{\varepsilon_G D_a^G}{RT_GZ}\frac{\partial^2 p_i^G}{\partial z^2} +$	$\frac{\varepsilon_G D_r^G}{RT_GZ}\left(\frac{\partial^2 p_i^G}{\partial r^2}+\frac{1}{r}\frac{\partial p_i^G}{\partial r}\right) -$	$K_{Li}a_L\left(\frac{p_i^G}{H_i}-C_i^L\right)$	$-(1-f_w)k_i^{GS}a_S\left(\frac{p_i^G}{RT_GZ}-C_{SGi}^S\right)$		
(**B**) Liquid phase (i = H_2, H_2S, NH_3, LHC)	$(1-f_{Si})\varepsilon_L\frac{\partial C_i^L}{\partial t} =$	$-u_L\frac{\partial C_i^L}{\partial z} +$	$\varepsilon_L D_a^L\frac{\partial^2 C_i^L}{\partial z^2} +$	$\varepsilon_L D_r^L\left(\frac{\partial^2 C_i^L}{\partial r^2}+\frac{1}{r}\frac{\partial C_i^L}{\partial r}\right) +$	$K_{Li}a_L\left(\frac{p_i^G}{H_i}-C_i^L\right)$		$-f_w k_i^S a_S\left(C_i^L-C_{SLi}^S\right)$	$-k_i^m a_S\left(C_i^L-C_{Si}^L\right)$
(**C**) Liquid phase (i = S, N, A, O, GO, WN, Ni, V)	$(1-f_{Si})\varepsilon_L\frac{\partial C_i^L}{\partial t} =$	$-u_L\frac{\partial C_i^L}{\partial z} +$	$\varepsilon_L D_a^L\frac{\partial^2 C_i^L}{\partial z^2} +$	$\varepsilon_L D_r^L\left(\frac{\partial^2 C_i^L}{\partial r^2}+\frac{1}{r}\frac{\partial C_i^L}{\partial r}\right)$			$-f_w k_i^S a_S\left(C_i^L-C_{SLi}^S\right)$	$-k_i^m a_S\left(C_i^L-C_{Si}^L\right)$
(**D**) Stagnant liquid (i = H_2, H_2S, NH_3, LHC, S, N, A, O, GO, WN, Ni, V)	$f_{Si}\varepsilon_L\frac{\partial C_{Si}^L}{\partial t} =$							$+ k_i^m a_S\left(C_i^L-C_{Si}^L\right)-k_i^S\left(C_{Si}^L-C_{SLi}^S\right)$

Mass balance \ Term	Accumulation (1)	Intraparticle diffusion (9)	G-S transfer (6)	L-S transfer (7)	Generation (10)
(**E**) Solid phase -Wet surface (i = H_2, H_2S, NH_3, LHC, S, N, A, O, GO, WN, Ni, V)	$\varepsilon_{pL}(1-\epsilon_B)\frac{\partial C_{SLi}^S}{\partial t} =$			$+ f_w k_i^S a_S\left(C_i^L-C_{SLi}^S\right)+k_i^S\left(C_{Si}^L-C_{SLi}^S\right)$	$+ \rho_{BS}\sum_{j=1}^{N_{RE}}\upsilon_{ij}^L\eta_j^L r_j^L\left(C_{SLi}^S, T_S^S\right)$
(**F**) Solid phase - Dry surface (i = H_2, H_2S, NH_3, LHC, S, N, A, O, GO, WN, Ni, V)	$\varepsilon_{pG}(1-\epsilon_B)\frac{\partial C_{SGi}^S}{\partial t} =$		$+ (1-f_w)k_i^{GS}a_S\left(\frac{p_i^G}{RT_GZ}-C_{SGi}^S\right)$		$+ \rho_{BS}\sum_{j=1}^{N_{RG}}\upsilon_{ij}^G\eta_j^G r_j^G\left(C_{SGi}^S, T_S^S\right)$
(**G**) Solid phase - Wet inner (i = H_2, H_2S, NH_3, LHC, S, N, A, O, GO, WN, Ni, V)	$\varepsilon_{pL}\frac{\partial C_{Li}^S}{\partial t} =$	$+ \frac{D_{Le}^S}{\xi^2}\frac{\partial}{\partial \xi}\left(\xi^2\frac{\partial C_{Li}^S}{\partial \xi}\right)$			$+ \rho_S\sum_{j=1}^{N_{RL}}\upsilon_{ij}^L r_j^L\left(C_{Li}^S, T_S\right)$
(**H**) Solid phase - Dry inner (i = H_2, H_2S, NH_3, LHC, S, N, A, O, GO, WN, Ni, V)	$\varepsilon_{pG}\frac{\partial C_{Gi}^S}{\partial t} =$	$+ \frac{D_{Ge}^S}{\xi^2}\frac{\partial}{\partial \xi}\left(\xi^2\frac{\partial C_{Gi}^S}{\partial \xi}\right)$			$+ \rho_S\sum_{j=1}^{N_{RG}}\upsilon_{ij}^G r_j^G\left(C_{Gi}^S, T_S\right)$

Table 6: Generalized heat balance equations (H).

Heat balance \ Term	Accumulation (1)	Convective (2)	Axial dispersion (3)	Radial dispersion (4)	f-I transfer (5)	Conductive (6)	f-S transfer (7)	f-W transfer (8)
(A) Gas phase	$\varepsilon_G \rho_G Cp_G \frac{\partial T_G}{\partial t} =$	$\pm u_G \rho_G Cp_G \frac{\partial T_G}{\partial z}$	$+ \varepsilon_G \lambda_a^G \frac{\partial^2 T_G}{\partial z^2}$	$+ \varepsilon_G \lambda_r^G \left(\frac{\partial^2 T_G}{\partial r^2} + \frac{1}{r}\frac{\partial T_G}{\partial r}\right)$	$- h_{GI}a_S(T_G - T_I)$	$+ \sum_{i=1}^{N_{CG}} \left\{ K_{Li} a_L \left(\frac{p_i^G}{H_i} - C_i^L\right) [Cp_{Gi}(T_I - T_G) - \Delta H_{vi}] \right\}$	$- (1-f_w) h_{GS} a_S (T_G - T_S^S)$	$- (1-f_w) h_{GW} \frac{A_W}{V} (T_G - T_W)$
(B) Liquid phase	$\varepsilon_L \rho_L Cp_L \frac{\partial T_L}{\partial t} =$	$\pm u_L \rho_L Cp_L \frac{\partial T_L}{\partial z}$	$+ \varepsilon_L \lambda_a^L \frac{\partial^2 T_L}{\partial z^2}$	$+ \varepsilon_L \lambda_r^L \left(\frac{\partial^2 T_L}{\partial r^2} + \frac{1}{r}\frac{\partial T_L}{\partial r}\right)$	$- h_{LI}a_S(T_I - T_L)$	$+ \sum_{i=1}^{N_{CG}} \left\{ K_{Li} a_L \left(\frac{p_i^G}{H_i} - C_i^L\right) [Cp_{Li}(T_I - T_L) + \Delta H_{vi}] \right\}$	$- f_w h_{LS} a_S (T_L - T_S^S)$	$- f_w h_{LW} \frac{A_W}{V} (T_L - T_W)$

Heat balance \ Term	Accumulation (1)	Axial dispersion (3)	Radial dispersion (4)	G-S transfer (9)	L-S transfer (10)	Generation (11)
(C) Solid phase – Isothermal	$\varepsilon_S \rho_S Cp_S \frac{\partial T_S^S}{\partial t} =$	$+ \varepsilon_S \lambda_a^S \frac{\partial^2 T_S^S}{\partial z^2}$	$+ \varepsilon_S \lambda_r^S \left(\frac{\partial^2 T_S^S}{\partial r^2} + \frac{1}{r}\frac{\partial T_S^S}{\partial r}\right)$	$+ (1-f_w) h_{GS} a_S (T_G - T_S^S)$	$+ f_w h_{LS} a_S (T_L - T_S^S)$	$+ \rho_B \zeta \left[\sum_{j=1}^{N_{RL}} \left(-\Delta H_{Rj}^L\right) \eta_j^L r_j^L (C_{Si}^S, T_S^S) + \sum_{j=1}^{N_{RG}} \left(-\Delta H_{Rj}^G\right) \eta_j^G r_j^G \left(C_{Sgi}^S, T_S^S\right) \right]$
(D) Thermowell	$\rho_W Cp_W \frac{\partial T_{TW}}{\partial t} =$	$+ \lambda_{TW} \frac{\partial^2 T_{TW}}{\partial z^2}$	$+ \lambda_{TW} \left(\frac{\partial^2 T_{TW}}{\partial r^2} + \frac{1}{r}\frac{\partial T_{TW}}{\partial r}\right)$			

Heat balance \ Term	Accumulation (1)	Intraparticle transfer (12)	Generation (11)
(E) Solid phase – Nonisothermal	$\rho_S Cp_S \frac{\partial T_S}{\partial t} =$	$+ \lambda_e^S \left(\frac{\partial^2 T_S}{\partial \zeta^2} + \frac{2}{\zeta}\frac{\partial T_S}{\partial \zeta}\right)$	$+ \rho_S \left[\sum_{j=1}^{N_{RL}} \left(-\Delta H_{Rj}^L\right) r_j^L (C_{Li}^S, T_S) + \sum_{j=1}^{N_{RG}} \left(-\Delta H_{Rj}^G\right) r_j^G (C_{Gi}^S, T_S) \right]$

A. Generalized Mass Balance Equations (M)

In the mass balance equations shown in Table 5, each phase is assumed to be a continuum and represented by an Eulerian-Eulerian framework model (136). Figure 8 shows graphically the interphase (gas-interface, interface-liquid and liquid-solid) and intraphase concentration profiles in a TBR which are represented mathematically by the terms of the generalized mass balance equations. The following sections describe all the terms of these equations and the assumptions under which they were derived.

1. *Gas Phase (MA)*

Mass balance equation in gas phase for non-volatile components is ignored, so that those compounds with negligible vapor pressure, i.e., for i = S, N, A, O, GO, WN, Ni, and V, are excluded from the equation MA, where "M" means mass balance equation given in Table 5 and "A" is row A in the same table (71, 136, 148).

The accumulation term M1 (Table 5, column 1) gives the dynamic (nonsteady-state or transient) behavior of TBR reactor. This term is of great

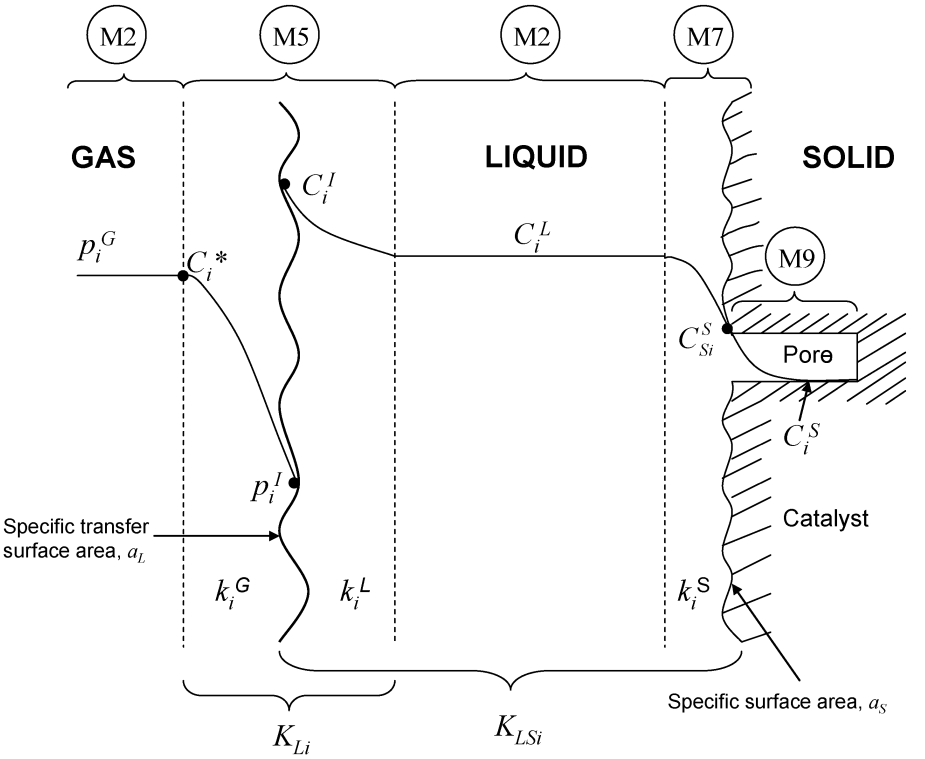

Figure 8: Partial pressure and concentration profiles (for $i = H_2$) in a TBR (37).

interest for modeling and simulation of TBRs for HDT of oil fractions in dynamic conditions, as is reported elsewhere (152).

According to Lopez and Dassori (112), for HDS process a reliable representation of reactor dynamics must be accompanied by a deep study of the reactivity of the different sulfur compounds present in the feed, the kinetic mechanism, and the overall effect of upgraded products over the catalyst performance. Once these tasks have been achieved and the kinetic models of the reacting system have been established, it is possible to propose a reactor model.

The term M2 represents the convective flow, which is considered to be of plug flow type. The use of this term implies that concentration and temperature gradients occur only in the axial direction. The signs "–" and "+" in term MA2 refer to cocurrent flow and countercurrent flow, respectively. Figure 9 shows the axial concentration profiles of reactants and products in cocurrent and countercurrent operation mode of TBRs.

Column M3 deals with the effective transport in axial direction. This term may be neglected during modeling of isothermal TBRs according to the criteria reported by Mears (57) and Gierman (39), and for adiabatic pilot or commercial TBRs as reported by Shah and Paraskos (74). Minimization of fluid flow dispersion in commercial reactors may be also ensured because of the high gas and liquid velocities employed. Mears (57) showed that the axial dispersion effect is much more important in TBRs than in single vapor phase

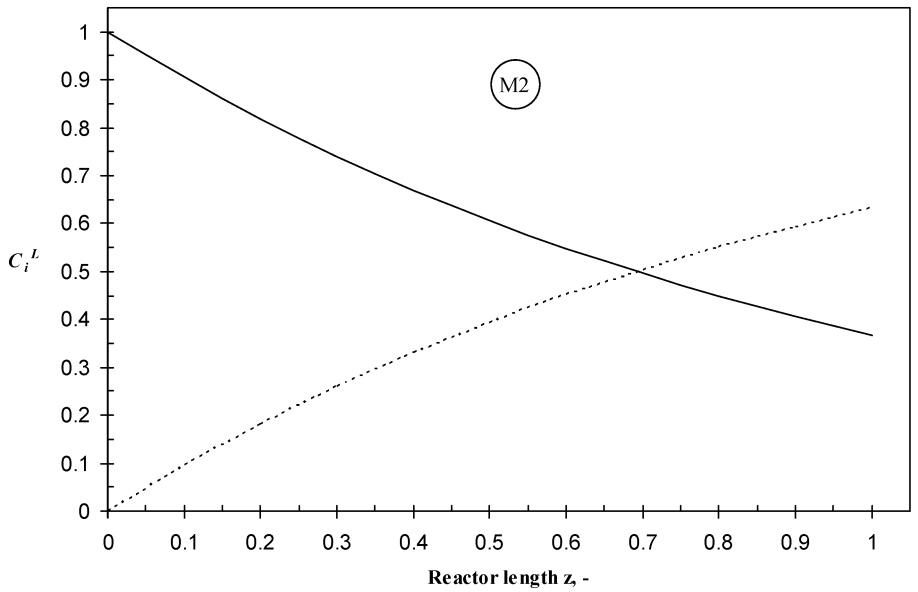

Figure 9: Axial average liquid molar concentration profiles of reactants (–) and products (---) for cocurrent and countercurrent operation mode.

reactors; therefore, for HDS of naphtha for instance, this term may be neglected.

According to Salmi et al. (148), the term MA3 can be neglected since gas phase is closer to plug flow pattern, which implies that its axial dispersion effects can be discarded $\left(D_a^G = 0\right)$.

The term accounting for effective mass radial (or transversal) dispersion is represented in column M4. When this term is used together with the term M2, and in some cases with M3, the model is called 2D; if M4 term is neglected then the model is named 1D. It has been reported that term M4 can be neglected when the d_t/d_{pe} ratio is higher than 25 since radial porosity variation within the reactor is negligible. Figure 10 shows a basic scheme of axial and radial mass dispersion phenomena and the resulting concentration profile inside TBR. The radial mass dispersion term is especially interesting for liquid distributor studies, since it defines the necessary drip point density for adequate liquid distribution, and describes how a bad designed distributor would affect the bed. For commercial TBRs if maldistribution of the liquid is not present, the trickle flow regime is satisfactorily described by plug flow (perfect radial mixing) for both phases (118). In summary, when axial and radial mass dispersions are neglected along the TBR, 1D plug flow has been recommended to be used for both gas and liquid phases (127).

Taking into account the assumptions described above, when a commercial reactor is modeled terms MA3 and MA4 of equation MA are normally neglected because of high L_B/d_{pe} and d_t/d_{pe} ratios. Since the gas temperature (T_G) is also a variable dependent of z coordinate, the resulting MA equation should be written as:

$$\frac{\varepsilon_G}{RZ}\frac{\partial}{\partial t}\left(\frac{p_i^G}{T_G}\right) = \pm\frac{u_G}{RZ}\frac{\partial}{\partial z}\left(\frac{p_i^G}{T_G}\right) - K_{Li}a_L\left(\frac{p_i^G}{H_i} - C_i^L\right) - (1-f_w)k_i^{GS}a_S\left(\frac{p_i^G}{RT_GZ} - C_{SGi}^S\right). \quad (32)$$

Developing the partial derivatives for both sides of Eq. 32, the following expression is obtained:

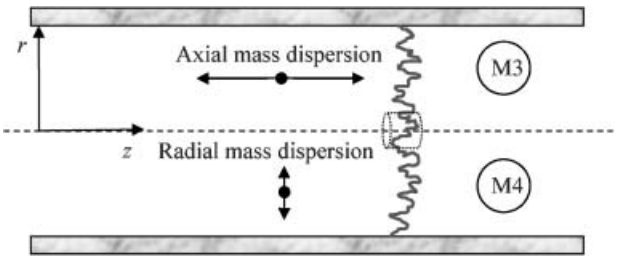

Figure 10: Radial concentration profile resulting from axial and radial mass dispersion phenomena.

$$\frac{\varepsilon_G}{RT_GZ}\frac{\partial p_i^G}{\partial t} - \frac{\varepsilon_G p_i^G}{RT_G^2 Z}\frac{\partial T_G}{\partial t} = \pm \frac{u_G}{RZ}\left[\frac{1}{T_G}\frac{\partial p_i^G}{\partial z} - \frac{p_i^G}{T_G^2}\frac{\partial T_G}{\partial z}\right] - K_{Li}a_L\left(\frac{p_i^G}{H_i} - C_i^L\right) - (1-f_w)k_i^{GS}a_S\left(\frac{p_i^G}{RT_GZ} - C_{SGi}^S\right). \quad (33)$$

However, this expression is very difficult to solve when it is linked with the complete set of PDEs. Hence, this expression is only recommendable for steady-state simulations as it was used by Murali et al. (131).

Column M5 represents the mass transfer from gas phase to liquid phase. The mass transfer resistance is described by the two-film theory (see Section IV.C), in which the interface is assumed to be in thermodynamic equilibrium, and no additional resistance to mass transfer is present. When the overall gas-liquid mass transfer coefficient based on the liquid phase is used (K_{Li}), a fictitious liquid-phase concentration is employed, which for gaseous compounds (H_2, H_2S, NH_3, and light hydrocarbons) is the concentration that would be in equilibrium with the corresponding bulk partial pressure, and is represented by the following relationship:

$$C_i^* = \frac{p_i^G}{H_i}, \quad (34)$$

where H_i (Henry's constant) is an equilibrium relation that represents in some way the solubility of the gaseous compound i in the oil fraction. A higher mass transfer rate for term M5 is only attributed to the enlarged transfer area between the gas and liquid (a_L), and not to a higher degree of turbulence (37).

The gas-solid mass transfer term (column M6) may be neglected when the wetting efficiency is complete ($f_w = 1$) and the molar flow rate of a component i in the gas phase can only change by transfer to or from the liquid phase, since no contact between gas and solid exists (10).

2. *Gaseous Compounds in Liquid Phase (MB)*

The dynamic liquid phase holdup in liquid mass balance equation (row MB in Table 5) strictly varies along the reactor because of partial volatilization of lighter oil fractions. Avraam and Vasalos (114) have reported that there is a decrease of liquid holdup along the bed reactor due to volatilization of lighter oil feedstock, whereas dynamic gas holdup increases.

In the modeling of small TBRs when the catalyst bed is diluted with inert material of smaller size, in order to prevent axial dispersion, the term in column M3 may be neglected if criteria of Mears (57) are fulfilled and/or that

of Gierman (39) using as design parameter the smaller inert particles average diameter. Besides, due to the dilution of the catalyst bed, it is also reasonable to assume no concentration gradients along the reactor radius, leading to the fact that term of radial dispersion in column M4 may also be neglected (102).

The term in column M7 corresponds to the mass transfer at the stationary liquid film of the liquid-solid interface. It has been observed that lower superficial mass velocities normally found in smaller reactors result in incomplete catalyst wetting ($f_w < 1$), which can subestimate contaminants removal than that expected from commercial reactors (116). Because of well designed distributors and high superficial mass velocities, in commercial reactors complete wetting of catalyst particles is normally assumed. Therefore, mass transfer between liquid and solid phases is function of the liquid flow in contact with the external area of the catalytic particles, which originates a gradient between the two phases $\left(C_i^L - C_{SLi}^S\right)$. An increase of this gradient means that the reactant is not being totally transferred to the external area of the particle, which apart from the liquid flow, depends on the shape and size of the particle. Small particles minimize these external concentration gradients as a result of the larger solid surface area and the higher mass transfer coefficients (37, 119).

3. *Nonvolatile Compounds in Liquid Phase (MC)*

For mass balance equation of nonvolatile compounds (row MC), partial vaporization of feedstock is assumed to be negligible under HDT conditions. At these conditions organic sulfur, nitrogen, aromatics, olefins, gas oil, wild naphtha, nickel, and vanadium components can be then considered as nonvolatile (116).

4. *Stagnant Liquid Phase (MD)*

The flowing-stagnant liquid mass balance equation (row MD) assumes that mass can be transferred between the stagnant and flowing portions of liquid in the catalytic bed. As the fraction of stagnant-fluid approaches zero ($f_{St} \to 0$) the TBR flow pattern becomes plug flow (71). The term representing the mass transfer between flowing and stagnant liquid zones is given in column M8. It has been observed that if liquid feed to a TBR is interrupted and the liquid present in the packed bed is allowed to flow off freely, not all of the external liquid holdup (liquid outside of catalyst's pores) drains off freely, but that a definite fraction of the external liquid remains stagnant in the so-called dead zones. Most of these stagnant liquid zones are present in the contact points between particles, mainly at the top of the reactor (37). When the effects of stagnant zones are neglected ($f_{St} \to 0$) the following terms must be

eliminated from the generalized model: MB8, MC8, row MD, and the second term in ME7.

5. Surface of Solid Phase (ME-MF)

The mass balance on the external surface of solid phase considering partial wetting is given in row ME. While, for the external surface of dry catalyst, the mass balance is given in row MF.

In equations given in rows ME and MF, internal mass gradients in the solid phase are evaluated by a catalyst effectiveness factor (see Section IV.B) in the respective generation terms (ME10 and MF10). These gradients inside particles are the product of an effective diffusion, which depends mainly on catalyst porosity and size of the molecules being diffused through the pores. The effectiveness factor $\left(\eta_j^f\right)$ in commercial HDS catalyst (~1/20 – 1/8 in. size) has been reported to be in the range of 0.4–0.6. These low values of η_j^f give $\Phi_j^f > 1$ imply that the HDS reaction may be considered to be within strong internal diffusional limitations in commercial application. Because internal diffusion also depends on external diffusion which in turn depends on flow rates, in order to obtain maximum catalyst effectiveness the reactor should operate with no interphase liquid-solid mass transfer limitations. As in the case of external gradients (gas-liquid and liquid-solid), a reduction of particle size yields an increase in particle effectiveness factor because the path lengths at the interior of the particle are reduced. If the catalyst is to be crushed, the particles are assumed to be isoconcentrational, and the effectiveness factor is considered unity $\left(\eta_j^f = 1\right)$. However, loading commercial reactors with smaller size catalyst will increase delta-P, thus more attention must be given when designing size of catalyst (40, 119).

The results of dynamic simulations when using ME and MF equations may be affected by inaccuracies in the estimation of some model parameters such as bed void fraction since the reader could chose a correlation to calculate the void fraction bed for undiluted bed when the real system under study was diluted. This parameter is needed to estimate the specific solid phase fraction ($\varepsilon_S = 1 - \in_B$) (106).

6. Interior of Solid Phase (MG-MH)

The major fraction of mass transfer resistances exists inside the catalyst particle, mainly when large size of commercially shaped catalysts is used as is shown in Figure 11, where the relative percentage of the various mass-transfer resistances typically found in HDT of oil fractions is reported (119, 173). Thus, to account for internal mass transfer limitations, mass balance equations MG and MH are used since they can affect the kinetics of the

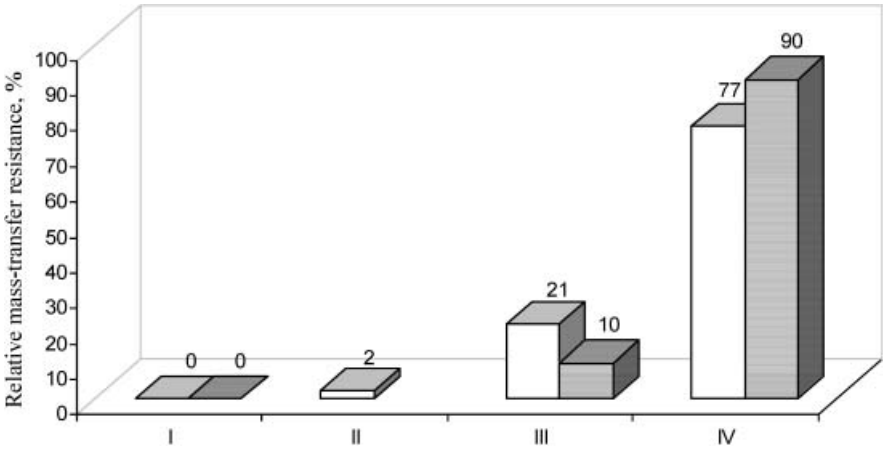

Figure 11: Relative mass-transfer resistances found in a typical oil fraction HDT process. I - From bulk gas to G/L interface, II – From G/L interface to bulk liquid, III – From bulk liquid to external catalyst surface, IV – Intraparticle diffusion and reaction (□ Sie (173); ■ Macías and Ancheyta (119)).

process (37, 102). Figure 12 shows the concentration profile inside a catalyst particle with mass transfer resistance.

The term of intraparticle transport by effective diffusion (column M9) accounts for the concentration gradients inside the catalyst particles because chemical reactions are assumed to take place at the inner surface of the solid catalyst, i.e., inside the pores of the catalyst. Those pores are considered to have uniform properties and to be completely filled with liquid ($\eta_i = 1$) or gas ($\eta_i = 0$) (10, 123, 144).

For the equations inside solid catalyst particles a mass balance over an infinitesimal volume element in a porous catalyst particle was assumed, which

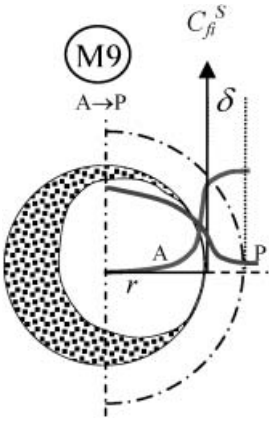

Figure 12: Concentration profile in a spherical catalyst pellet with mass transfer resistance.

can be written as:

$$\varepsilon_{pf}\frac{\partial C_{f\,i}^{S}}{\partial t}=-\xi^{-S}\frac{\partial N_{i}^{f}\xi^{S}}{\partial\xi}+\rho_{S}\sum_{j=1}^{N_{Rf}}\upsilon_{ij}^{f}r_{j}^{\prime f}\left(C_{f\,i}^{S},T_{S}\right), \tag{35}$$

where N_i^f is the molar flux of component i;and s in ξ^s is the shape factor, being ξ the radial spatial coordinate (for slab $s = 0$, for infinitely long cylinder $s = 1$, and for sphere $s = 2$). Non-ideal geometries can be treated with non-integer values. The further development of Eq. (35) depends on which diffusion model is used. Strictly speaking, multicomponent diffusion should be described with Stefan-Maxwell equations, according to which all of the fluxes are related to all concentration gradients (148):

$$N^{f}=-F\frac{dC_{f}^{S}}{d\xi}, \tag{36}$$

where F is a coefficient matrix consisting of binary diffusion coefficients and C_f^s is a concentration vector (174). However, a comparison between different diffusion models has shown that a simpler approach based on the Fick's law is sufficient, provided that the diffusion coefficients are described by an approximated manner, e.g. by using the Tyn-Calus correlation (Table 9) for liquid-phase molecular diffusion coefficient. Thus, by applying Fick's law and assuming the catalyst as a spherical particle Eq. 35 can be rewritten as those reported in rows MG and MH of Table 5 (148).

The generation terms MG10 and MH10 represent the appearance and disappearance of products and reactants by catalytic reactions that take place only at the active sites inside pores of catalyst particles. These terms give the non-linear behavior in HDT reactors, because of the non-linear interactions between mass, thermal, and kinetic processes present in the reacting system (123).

B. Generalized Heat Balance Equations (H)

Commercial HDT reactors operate under nonisothermal adiabatic conditions, and since reactions are mostly exothermic, average reactor temperature would increase always along the catalyst bed (Figure 13) (112, 116). On the other hand, experiments for catalyst screening and process studies are mostly conducted in microreactors, bench- and pilot-plant scales. These systems commonly operate under the same conditions reported in commercial units but keeping the reaction temperature more or less constant (operation in isothermal mode), and hence, the heat balance can be omitted for small reactor modeling. However, since commercial HDT reactors do not operate

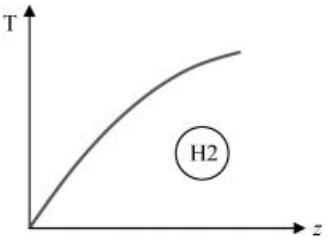

Figure 13: Axial average reactor temperature profile.

isothermally, experimental information generated from small reactors does not represent the commercial operation exactly. Therefore, to predict the real behavior of commercial reactors using experimental data from small reactors it is necessary to add the energy balance in industrial HDT reactor modeling (120).

In the case of HDT of heavy oils, reaction temperature is the most important operating parameter. It is regularly used for adjusting the desired degree of HDS, or compensating for catalyst deactivation, and consequently catalyst life-time. For such processes, it is of vital importance to properly determine the optimum temperature at the entrance of the reactor so that the desired conversion is achieved either for SOR or EOR conditions. This optimum temperature is known as the setpoint temperature which is the main variable to be used in terms on process control (122).

For modeling purposes it is usually sufficient to consider only the liquid and solid phases (rows HB and HC or HE in Table 6), since heat capacity of the gas phase is much lower compared with those of the solid and liquid phases (148).

1. Gas Phase (HA)

Table 6 reports all the terms that need to be included in the energy balance equation. The signs "−" and "+" in term HA2 refer to cocurrent and countercurrent flow, respectively. Commercial HDT reactors are normally considered to operate adiabatically because energy losses from the reactor to its surroundings are usually negligible compared with the energy generated by the reaction (10, 74, 113, 118). Therefore, terms in column H4 can be neglected because a commercial reactor is isothermal only in the radial direction $\left(\lambda_r^G = 0\right)$, and terms in column H8 must be neglected because there is no heat transfer from the fluid phase to the reactor wall (98, 123).

In the case of nonadiabatic operation, the terms in column H3 (except HD3 term) can be neglected due to its insignificance compared with the radial thermal conductivity (102). The basic scheme of radial temperature profile for a nonadiabatic TBR is shown in Figure 14.

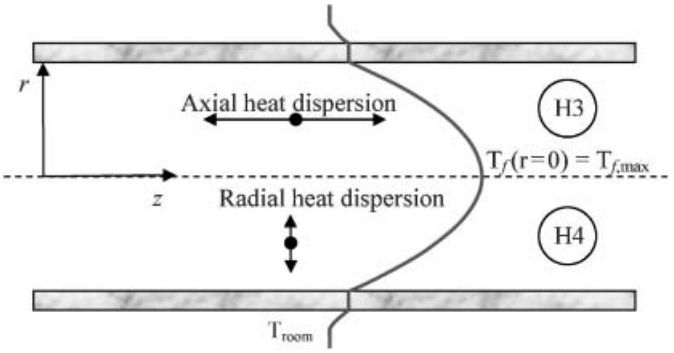

Figure 14: Radial temperature profile in a nonadiabatic TBR.

The terms in column H5 are the fluid phase-interface convective energy transfer, where the driving force is the temperature difference between the bulk gas phase and the interface temperature (T_I) in the case of HA5 term, and the temperature difference between the bulk liquid phase and the interface temperature in HB5 term (10, 40, 113).

The term HA6 corresponds to the conductive heat flux in the gas film side at the gas-liquid interface due to the transport of enthalpy by the interfacial mass transfer. The driving force for the conductive heat flux is also the temperature difference between the gas bulk phase and the interface temperature (10, 40, 113). This term also takes into account the flux of heat by vaporization/condensation between gas and liquid phases, although some author have considered that the heat of vaporization has to be accounted for only in the liquid phase (10, 118). As the partial vaporization of oil fractions is sometimes assumed to be negligible under typical HDT process conditions, the mass transport of nonvolatile components on the gas-liquid interface is neglected as well (116).

Terms in column H7 are: the convective heat flux from gas to solid external surface (HA7 term), and the convective heat transfer from liquid to solid external surface (HB7 term) (10, 113).

2. Liquid Phase (HB)

As in the case of gas phase, if the reactor is considered as adiabatic, terms HB4 and HB8 must be neglected.

The heat of vaporization/condensation is also accounted for in the liquid phase heat balance equation by means of HB6 term. The latent heat (ΔH_{vi}), represents the heat consumed by vaporization only for the reaction products, where the negative sign indicating removing of heat is given by the concentration gradient, since $C_i^L > C_i^*$ for i = H_2S, NH_3, light hydrocarbons (**LHC**). On the other hand, the latent heat represents the heat gained by condensation only for H_2 (113).

The energy balance given by equations HA, HB, and HC in Table 6 considers the heat generation on the solid surface and its transfer to the liquid phase, and finally from the liquid phase to the gas phase by convection and mass transfer. This implies that $T_S^S > T_L > T_I > T_G$.

3. Isothermal Solid Phase (HC)

The catalyst particles may be assumed to be isothermal due to the usually low concentration of the oil fraction in the inlet gas-liquid mixture (99). If the catalyst particles are assumed to be isothermal (internal energy transfer is carried out without resistance), equation HC is used for modeling of TBR, but utilizing concentrations and temperature at solid surface (10, 113).

In the generation term (HC11) the sign of the reaction heat is negative $\left(-\Delta H_{Rj}^f\right)$, since the major HDT reactions are exothermic. However, at temperatures higher than ~420°C thermal cracking reactions are more important, being these reactions endothermic by chemical nature, then the sign of this reaction heat becomes positive $\left(+\Delta H_{Rj}^f\right)$ (106).

4. Thermowell (HD)

According to Chen et al. (106), at the outlet of the catalyst bed the temperature difference between the thermowell and the bed could be as high as 60 K. In this case, the temperature measured in the thermowell cannot represent the temperature in the bed. Therefore, if ignored, it might lead to wrong interpretation of pilot-plant data. The reason for this difference is that the thermowell, a stainless steel tube, has much higher heat conductivity than the catalyst particles of the bed. Hence, heat can be much more easily transferred from the higher temperature zone to the lower temperature zone along the thermowell than along the catalyst bed. That back transfer of heat to the inlet of the reactor along the thermowell and reactor wall enhances heat dispersion in the catalyst bed, leading to a flattened axial temperature profile. This effect is quite pronounced in pilot-plant reactors sustaining highly exothermic reactions because of the relatively small diameter of the catalyst bed and the use of thermowell to measure temperatures inside the bed.

5. Nonisothermal Solid Phase (HE)

The film resistances are very important for heat transfer, while the heat transfer inside the solid catalyst is usually fast. Heat transfer in porous particle may be described with Fourier's law leading to the PDE with respect to temperature for nonisothermal catalyst as shown in row HE of Table 6

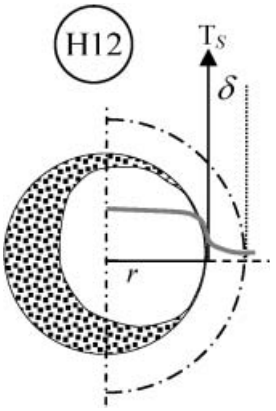

Figure 15: Temperature profile in a spherical catalyst pellet with heat transfer resistance.

(148). Figure 15 presents the temperature profile developed inside catalyst particle and across the external boundary layer of thickness δ.

C. Definition of Boundary Conditions of the Generalized Model

The mass and energy balance equations have boundary conditions which relate the surface properties to the bulk properties of the reacting system. For these balance equations, the so-called Danckwerts' boundary conditions are used usually (66), especially for models with axial dispersion (147), but in the case of numerical difficulties in the proximity of the reactor exit, Salmi and Romanainen (175) have proposed a modified semi-empirical boundary condition. This last suggests that there are a lot of alternative boundary conditions proposed in the literature for the reactor inlet, for the reactor outlet and for the transfer of heat between the catalyst and the reactor wall. Therefore, since the generalized model in Tables 5 and 6 is a system of PDEs, it is necessary to define the initial ($t = 0$) and boundary ($t > 0$) conditions per equation, which are shown in Tables 7 and 8. Hence, in order to fix the boundary conditions at the reactor inlet and outlet, points $z = 0$ and $z = L_B$ on the axial coordinate are assumed to be the entrance and exit of the reactor, respectively (112).

For some authors at the boundary condition $z = 0$ gas and liquid molar flow is normally assumed to be in physical equilibrium at the reactor inlet temperature and pressure (oil fraction is saturated with the gaseous compound), then the following expression is used (109, 115, 176):

$$C_i^f = \left(C_i^f\right)_0 = \frac{\left(p_i^G\right)_0}{H_i}. \tag{37}$$

Others researchers, in order to simulate cocurrent and countercurrent operation of pilot TBRs for HDT of oil fractions, have considered that the oil is

Table 7: Initial conditions ($t = 0$) of generalized mass and heat balance equations.

		Gas Phase	Liquid Phase		Solid Phase		Stagnant Zone
Condition	**Operation Mode**	**(i = H_2, H_2S, NH_3, LHC)**	**(i = H_2, H_2S, NH_3, LHC)**	**(i = S, N, A, O, GO, WN, Ni, V)**	**Surface (i = All compounds)**	**Interior (i = All compounds)**	**(i = All compounds)**
$z = 0$, $0 \leqslant r \leqslant R$	Cocurrent	$p_i^G = (p_i^G)_0$	$C_i^L = (C_i^L)_0$		$C_{Sfi}^S = \left(C_{Sfi}^S\right)_0$	$C_{fi}^S = \left(C_{fi}^S\right)_0$	
	Countercurrent	$p_i^G = 0$	$C_i^L = 0$	$C_i^L = (C_i^L)_0$	$C_{Sfi}^S = \left(C_{Sfi}^S\right)_0$	$C_{fi}^S = \left(C_{fi}^S\right)_0$	
	Cocurrent/ countercurrent	$T_G = (T_G)_0 = T_0$	$T_L = (T_L)_0 = T_0$		$T_S^S = (T_S^S)_0 = T_0$	$T_s = (T_s)_0 = T_0$	$C_{Sti}^S = 0$
$0 < z < L_B$, $0 \leqslant r \leqslant R$	Cocurrent/ countercurrent	$p_i^G = 0$ $T_G = T_0$	$C_i^L = 0$ $T_L = T_0$		$C_{Sfi}^S = 0$ $T_S^S = T_0$	$C_{fi}^S = 0$ $T_S = T_0$	$C_{Sti}^S = 0$
$z = L_B$, $0 \leqslant r \leqslant R$	Cocurrent	$p_i^G = 0$	$C_i^L = 0$		$C_{Sfi}^S = 0$	$C_{fi}^S = 0$	
	Countercurrent	$p_i^G = (p_i^G)_{L_B}$	$C_i^L = 0$		$C_{Sfi}^S = 0$	$C_{fi}^S = 0$	
	Cocurrent/ countercurrent	$T_G = (T_G)_{L_B} = T_0$	$T_L = (T_L)_{L_B} = T_0$		$T_S^S = (T_S^S)_{L_B} = T_0$	$T_S = (T_S)_{L_B} = T_0$	$C_{Sti}^S = 0$
$0 \leqslant \xi < d_{pe}/2$, $0 < z \leqslant L_B$, $0 \leqslant r \leqslant R$	Cocurrent/ countercurrent	–	–		–	$C_{fi}^S = 0$ $T_S = T_0$	–

Table 8: Boundary conditions ($t > 0$) of generalized mass and heat balance equations.

		Gas Phase		Liquid Phase				Solid Phase	
		(i = H_2, H_2S, NH_3, LHC)		(i = H_2, H_2S, NH_3, LHC)		(i = S, N, A, O, GO, WN, Ni, V)			
Condition	**Operation Mode**	**Dispersion**	**No Dispersion**	**Dispersion**	**No Dispersion**	**Dispersion**	**No Dispersion**	**Surface (i = All compounds)**	**Interior (i = All compounds)**
$z = 0$, $0 \leqslant r \leqslant R$	Cocurrent	$p_i^G = (p_i^G)_0$				$C_i^L = (C_i^L)_0$		$C_{Si}^S = \left(C_{Si}^S\right)_0$	—
		$T_\ominus = (T_\ominus)_0$				$T_L = (T_L)_0$		$T_S^S = (T_S^S)_0$	
	Countercurrent	$\frac{\partial p_i^G}{\partial z} = \frac{\partial T_\ominus}{\partial z} = 0$	—	$C_i^L = 0$		$C_i^L = (C_i^L)_0$		$C_{Si}^S = \left(C_{Si}^S\right)_0$	—
						$T_L = (T_L)_0$		$T_S^S = (T_S^S)_0$	
$z = L_B$, $0 \leqslant r \leqslant R$	Cocurrent	$\frac{\partial p_i^G}{\partial z} = \frac{\partial T_\ominus}{\partial z} = 0$	—	$\frac{\partial C_i^L}{\partial z} = \frac{\partial T_L}{\partial z} = 0$	—	$\frac{\partial C_i^L}{\partial z} = \frac{\partial T_L}{\partial z} = 0$	—	$\frac{\partial T_S^S}{\partial z} = 0$	—
	Countercurrent	$p_i^G = (p_i^G)_{Ls}$		$\frac{\partial C_i^L}{\partial z} = \frac{\partial T_L}{\partial z} = 0$	—	$\frac{\partial C_i^L}{\partial z} = \frac{\partial T_L}{\partial z} = 0$	—	$\frac{\partial T_S^S}{\partial z} = 0$	—
		$T_G = (T_G)_{Ls}$							
$r = 0$, $0 < z < L_B$	Cocurrent	$\frac{\partial p_i^G}{\partial r} = \frac{\partial T_\ominus}{\partial r} = 0$	—	$\frac{\partial C_i^L}{\partial r} = \frac{\partial T_L}{\partial r} = 0$	—	$\frac{\partial C_i^L}{\partial r} = \frac{\partial T_L}{\partial r} = 0$	—	$\frac{\partial T_S^S}{\partial r} = 0$	—
$r = R$, $0 < z < L_B$	Cocurrent	$\frac{\partial p_i^G}{\partial r} = 0$	—	$\frac{\partial C_i^L}{\partial r} = 0$	—	$\frac{\partial C_i^L}{\partial r} = 0$	—		—
		$-\lambda_r^G \frac{\partial T_\ominus}{\partial r} = h_{GW}(T_G - T_W)$		$-\lambda_r^L \frac{\partial T_L}{\partial r} = h_{LW}(T_L - T_W)$		$-\lambda_r^L \frac{\partial T_L}{\partial r} = h_{LW}(T_L - T_W)$		$-\lambda_r^S \frac{\partial T_S^S}{\partial r} = h_{SW}(T_S^S - T_W)$	
$\xi = 0$, $0 \leqslant z \leqslant L_B$, $0 \leqslant r \leqslant R$	Cocurrent/ countercurrent	—	—	—	—	—	—	—	$\frac{\partial C_{Si}^S}{\partial \xi} = \frac{\partial T_S}{\partial \xi} = 0$
$\xi = \frac{d_p}{2}$, $0 \leqslant z \leqslant L_B$, $0 \leqslant r \leqslant R$	Cocurrent/ countercurrent	—	—	—	—	—	—	—	$-D_{ei}^L \frac{\partial C_i^L}{\partial \xi} = f_w k_i^S a_S \left(C_{SLi}^S - C_i^L\right) + k_i^S \left(C_{SLi}^S - C_{Si}^L\right) = \rho_B \zeta \sum_{j=1}^{N_{Rl}} \upsilon_{ij}^L \eta_j^L r_j'^L \left(C_{SLi}^S, T_S^S\right)$
									$-D_{ei}^G \frac{\partial C_i^S}{\partial \xi} = (1 - f_w) k_i^{GS} a_S \left(C_{SGi}^S - C_i^G\right) = \rho_B \zeta \sum_{j=1}^{N_{Rg}} \upsilon_{ij}^G \eta_j^G r_j^G \left(C_{SGi}^S, T_S^S\right)$
									$(1 - f_w) h_{GS} a_S \left(T_S^S - T_G\right) + f_w h_{LS} a_S \left(T_S^S - T_L\right) = -\lambda_e^S \frac{\partial T_S}{\partial \xi}$

not saturated with H_2, that is, the initial H_2 concentration in oil is zero $\left(\left(C^L_{H_2}\right)_0 = 0\right)$ for $t \geqslant 0$ at $z = 0$ (3, 121).

When a high-purity hydrogen stream without gas recycle is used, such as in the case of some laboratory and bench-scale HDT reactors, or when the gas recycle has been subject to purification process in commercial units, values of partial pressure $\left(p_i^G\right)$ and liquid molar concentrations $\left(C_i^L\right)$ of H_2S, NH_3, and LHC at the entrance of the catalytic bed ($z = 0$ and $z = L_B$ for cocurrent and countercurrent operation, respectively) are equal or very close to zero. For commercial HDT reactors without high purification of gas recycle stream, values of partial pressures $\left(p_i^G\right)$ and liquid molar concentrations $\left(C_i^L\right)$ of H_2S, NH_3 and LHC at the entrance of the catalytic bed ($z = 0$) are different to 0 (152).

The axial and radial dispersion terms of mass and heat result in a second-order differential equation for all phases, consequently, two boundary conditions are necessary which according to Danckwerts (67) are:

- Danckwerts' boundary condition at $z = 0$:

$$-\varepsilon_f D_a^f \left.\frac{\partial\left(C_i^f\right)}{\partial z}\right|_{z=0^+} = u_f\left[\left(C_i^f\right)_0 - \left(C_i^f\right)_{z=0^+}\right], \text{ and} \tag{38}$$

$$-\varepsilon_f \lambda_a^f \left.\frac{\partial T_f}{\partial z}\right|_{z=0^+} = u_f \rho_f Cp_f\left[\left(T_f\right)_0 - \left(T_f\right)_{z=0^+}\right], \tag{39}$$

which can be simplified to

$$C_i^f = \left(C_i^f\right)_0; \quad T_f = \left(T_f\right)_0. \tag{40}$$

- These boundary conditions are true because the axial dispersion of mass and heat is relatively small and the concentration and temperature gradients at the reactor inlet are quite flat (106).
- Danckwerts' boundary condition at $z = L_B$:

$$\frac{\partial C_i^f}{\partial z} = \frac{\partial T_f}{\partial z} = 0. \tag{41}$$

- The following infinite type boundary condition:

$$z \to \infty \quad T_f \to T_W, \tag{42}$$

is the real condition at the outlet of the reactor, which is difficult to apply under most numerical methods. Because of this, many researchers prefer to use Danckwerts' boundary conditions where the temperature gradients at the

exit of the reactor are zero. It must be pointed out that unless the reactor is infinitely long, this exit condition will not be true because the fluid will not reach equilibrium with its surroundings. This lack of equilibrium at the exit would be even more pronounced at the high temperatures frequently experienced in TBRs. The boundary conditions proposed by Young and Finlayson (177) avoid this abnormality. They derived inlet and outlet conditions similar to those of Danckwerts for the case in which both axial and radial dispersion is present. However, the outlet condition was reported with a non-zero gradient which is reduced to the Danckwerts' form when radial dispersion is neglected. The boundary condition $\partial T_S^S/\partial z = 0$ for $z \geq L_B$ is a Danckwerts' type also, but as the solid phase is commonly non-existent for $z > L_B$, it is generally regarded as valid exit condition. For the same reason, as the reaction does not take place without the solid catalyst, the concentration gradients can be assumed to be zero at the exit. Therefore, the Danckwerts boundary conditions are used when there is no mass (or heat) dispersion outside the reactor (20, 104).

Boundary condition at $\xi = d_{pe}/2$ is sometimes considered to be $C_{fi}^S = C_{Sfi}^S$ (81, 130).

According to Chen et al. (106), the following boundary conditions will be applied for heat transfer in the thermowell:

$$\lambda_{TW}\frac{\partial T_{TW}}{\partial z} = h_{air}\left[(T_{TW})_0 - T_{room}\right];\ \text{at } z = 0, \tag{43}$$

$$-\lambda_{TW}\frac{\partial T_{TW}}{\partial z} = h_{air}\left[(T_{TW})_f - T_{room}\right];\ \text{at } z = L_B, \tag{44}$$

$$\frac{\partial T_{TW}}{\partial r} = 0;\ \text{at } r = 0, \text{ and} \tag{45}$$

$$\lambda_{TW}\frac{\partial T_{TW}}{\partial r} = h_{TW}\left(T_f - T_{TW}\right);\ \text{at } r = R_{TW}. \tag{46}$$

The resulting set of PDEs coupled with the respective initial and boundary conditions are then simultaneously solved using an appropriated numerical method (96).

D. Example of Simplification of the Generalized Model

Sometimes to simplify heat transfer modeling in HDT reactors, the three processes involved (heat transfer in solid, liquid and gas phase) can be lumped in only one equation with a pseudohomogeneous heat balance. In the following

part an example of how to obtain a pseudohomogeneous heat balance from the generalized heat balance presented in Table 6 is shown:

The general heat balance for the gas phase is:

$$\mathrm{HA1} = \mathrm{HA2} + \mathrm{HA3} + \mathrm{HA4} + \mathrm{HA5} + \mathrm{HA6} + \mathrm{HA7} + \mathrm{HA8}. \tag{47}$$

The general energy heat balance for the liquid phase is:

$$\mathrm{HB1} = \mathrm{HB2} + \mathrm{HB3} + \mathrm{HB4} + \mathrm{HB5} + \mathrm{HB6} + \mathrm{HB7} + \mathrm{HB8}. \tag{48}$$

Assuming no temperature gradient within the catalyst particles (isothermal catalyst), the general heat balance for the solid phase is:

$$\mathrm{HC1} = \mathrm{HC3} + \mathrm{HC4} + \mathrm{HC9} + \mathrm{HC10} + \mathrm{HC11}. \tag{49}$$

When modeling commercial HDT reactors it is generally accepted that axial dispersion can be omitted, then: HA3 = HB3 = HC3 = 0. If adiabatic operation is also assumed, then HA4 = HB4 = HC4 = 0 (isothermal reactor in the radial direction), and HA8 = HB8 = 0 (no heat transfer between fluid phase and reactor wall).

The pseudohomogeneous model is based on the fact that the temperature difference among the gas, liquid, and catalyst at any particular axial position of the reactor is negligible. Hence, $T_G = T_I = T_L = T_S^S = T$, and in consequence the following terms can be neglected: HA5 = HA7 = HB5 = HB7 = HC9 = HC10 = 0. The temperature gradients $(T_G - T_I)$ and $(T_I - T_L)$ in HA6 and HB6 terms are also neglected. The final heat balance equation for gas, liquid, and solid phase is then

$$\mathrm{HA1} + \mathrm{HB1} + \mathrm{HC1} = \mathrm{HA2} + \mathrm{HB2} + \mathrm{HC6'} + \mathrm{HB6'} + \mathrm{HC11}. \tag{50}$$

Eq. (50) in terms of model parameters for cocurrent operation gives

$$\begin{aligned}
&\varepsilon_G \rho_G Cp_G \tfrac{\partial T}{\partial t} + \varepsilon_L \rho_L Cp_L \tfrac{\partial T}{\partial t} + \varepsilon_S \rho_S Cp_S \tfrac{\partial T}{\partial t} = \\
&-u_G \rho_G Cp_G \tfrac{\partial T}{\partial z} - u_L \rho_L Cp_L \tfrac{\partial T}{\partial z} + \sum_{i=1}^{N_{CG}} \left\{ K_{Li} a_L \left(\tfrac{p_i^G}{H_i} - C_i^L \right) (-\Delta H_{vi}) \right\} + \\
&\sum_{i=1}^{N_{CG}} \left\{ K_{Li} a_L \left(\tfrac{p_i^G}{H_i} - C_i^L \right) (\Delta H_{vi}) \right\} + \rho_B \zeta \left[\begin{array}{l} \sum_{j=1}^{N_{RL}} \left(-\Delta H_{Rj}^L \right) \eta_j^L r'^L_j \left(C_{SLi}^S, T \right) \\ + \sum_{j=1}^{N_{RG}} \left(-\Delta H_{Rj}^G \right) \eta_j^G r'^G_j \left(C_{SGi}^S, T \right) \end{array} \right].
\end{aligned} \tag{51}$$

The final simplified pseudohomogeneous heat balance is:

$$(\varepsilon_G\rho_G Cp_G+\varepsilon_L\rho_L Cp_L+\varepsilon_S\rho_S Cp_S)\frac{\partial T}{\partial t}=-(u_G\rho_G Cp_G+u_L\rho_L Cp_L)\frac{\partial T}{\partial z}$$
$$+\rho_B\zeta\left[\sum_{j=1}^{N_{RL}}\left(-\Delta H_{Rj}^L\right)\eta_j^L r'^L_j\left(C_{SLi}^S,\,T\right)+\sum_{j=1}^{N_{RG}}\left(-\Delta H_{Rj}^G\right)\eta_j^G r'^G_j\left(C_{SGi}^S,\,T\right)\right]. \quad (52)$$

If catalyst wetting efficiency is also assumed to be complete, $f_w = 1$ (e.g. when properly designed liquid distributors and high liquid velocities in commercial reactors are used), therefore reactions occur only in the liquid phase, then Eq. (52) is rewritten as:

$$(\varepsilon_G\rho_G Cp_G+\varepsilon_L\rho_L Cp_L+\varepsilon_S\rho_S Cp_S)\frac{\partial T}{\partial t}=-(u_G\rho_G Cp_G+u_L\rho_L Cp_L)\frac{\partial T}{\partial z}$$
$$+\rho_B\zeta\sum_{j=1}^{N_{RL}}\left(-\Delta H_{Rj}^L\right)\eta_j^L r'^L_j\left(C_{SLi}^S,\,T\right). \quad (53)$$

According to Feyo De Azevedo et al. (20) some researchers have included the radiation effects in nonisothermal reactors in the radial direction (HA4 = HB4 = HC4 ≠ 0), by means of the effective radial thermal conductivity

$$\lambda_{er}=\left(\varepsilon_S\lambda_r^S+\varepsilon_L\lambda_r^L+\varepsilon_G\lambda_r^G\right)=(\lambda_{er})_0+\lambda_{rad}, \text{ and} \quad (54a)$$

$$\lambda_{rad}=4\psi_r\sigma d_{pe}T^3, \quad (54b)$$

where $(\lambda_{er})_0$ is the conductive plus convective contributions to the effective radial conductivity, and λ_{rad} is the radiant contribution, σ is the Stephan-Boltzmann constant and ψ_r is a radiant transfer factor defined as

$$\psi_r=\frac{2}{\frac{2}{e}-0.264}, \quad (55)$$

where e is the particle emissivity. Therefore, rearranging Eq. 54a as $\lambda_{er}(r) = (\lambda_{er})_0 + K_1[T(r)]^3$ (where $K_1 = 4\psi_r\sigma d_{pe}$), the pseudohomogeneous radial heat dispersion term (HA4+HB4+HC4 with $T_S^S = T_L = T_G = T$) is expressed as

$$\lambda_{er}\left(\frac{\partial^2 T}{\partial r^2}+\frac{1}{r}\frac{\partial T}{\partial r}\right)=\frac{1}{r}\frac{\partial}{\partial r}\left(r\lambda_{er}(r)\frac{\partial T}{\partial r}\right)=\lambda_{er}(r)\left(\frac{1}{r}\frac{\partial T}{\partial r}+\frac{\partial^2 T}{\partial r^2}\right)+\frac{\partial\lambda_{er}(r)}{\partial r}\frac{\partial T}{\partial r}$$
$$=\lambda_{er}(r)\left(\frac{1}{r}\frac{\partial T}{\partial r}+\frac{\partial^2 T}{\partial r^2}\right)+3K_1T^2\left(\frac{\partial T}{\partial r}\right)^2, \quad (56)$$

where the last term on the right side of Eq. (56) represents the radioactive heat transfer, and its exclusion may produce errors in estimation of some other heat transfer parameters.

IV. ESTIMATION OF MODEL PARAMETERS

In order to solve the set of ODEs (for steady-state regime) or the set of PDEs (for dynamic regime), it is necessary to evaluate several parameters and chemical properties of the system. Those parameters can be estimated with existing correlations, whose accuracy is of great importance for the whole robustness of the reactor model.

A. Effective Diffusivity

The description of steady state diffusion and reaction of a multicomponent liquid mixture in a porous catalyst particle requires the appropriate definition of the species fluxes to the particle. Fick's law for equimolar counterdiffusion through an ideal cylindrical pore is given by:

$$N_i^f = -D_{ei}^f \nabla C_{fi}^S, \tag{57}$$

where D_{ei}^f is the effective diffusivity, by means of which the structure (porosity and tortuosity) of the pore network inside the particle is taken into consideration into the modeling. Table 9 shows the Bosanquet's formula to estimate the effective diffusivity inside the catalyst particle (178), which consists of two diffusion contributions: Knudsen diffusivity $\left(D_{Ki}^f\right)$ and molecular diffusivity $\left(D_{Mi}^f\right)$. Both Bosanquet's formula and Fick's law can also be applied with sufficient accuracy to cases involving a narrow unimodal pore size distribution and very dilute mixtures. The restrictive factor $F(\lambda_g)$ accounts for additional friction between the solute and the pore walls. The exponent $\widehat{Z}$ is equal to 4 for $\lambda_g < 0.2$ (144). The tortuosity factor of the pore network, τ, is used in the calculation of D_{ei}^f because the pores are not oriented along the normal direction from the surface to the center of the catalyst particle, and its value generally varies between 3 and 7, but for HDT process it is commonly assumed to be equal to 4 (6, 119, 144, 180, 186). It is also possible to estimate the tortuosity factor assuming valid the upper bound correlation given by Weissberg (182) for a packing of random spheres as shown in Table 9.

B. Effectiveness Factor

The effectiveness factor of independent reactions can be defined as the ratio of the volumetric average of the reaction rate into the particle to the reaction rate at the surface of the particle as proposed by Thiele (187) and Zeldowich (188):

Table 9: Effective diffusivity estimation.

Parameter	Gas Phase	Liquid Phase
Molecular diffusivity coefficient (179–181)	$\frac{1}{D^G_{Mi}} = \frac{1}{1-y_i}\sum_{k\neq i}^{N_{CG}} \frac{y_k}{D_{i,k}}$	$D^L_{Mi} = 8.93\times 10^{-8}\frac{v_i^{0.267}T_L}{v_i^{0.433}\mu_L}$
Knudsen diffusivity coefficient (180)	$D^G_{Ki} = 9700 r_g\left(\frac{T_G}{MW_i}\right)^{0.5}$	$\frac{1}{D^L_{Ki}} \approx 0$
Effective diffusivity (178)	$D^f_{ei} = \frac{\epsilon_S}{\tau}\frac{1}{\frac{1}{D^f_{Mi}}+\frac{1}{D^f_{Ki}}}F(\lambda_g)$	
Restrictive factor (144)	$F(\lambda_g) = (1-\lambda_g)^{\widehat{z}}$	
Ratio of radius of gyration over pore radius (100, 150)	$\lambda_g = \frac{r_{solute}}{r_g}$	
Mean pore radius (49)	$r_g = \frac{2V_g}{S_g}$	
Tortuosity factor (182)	$\frac{1}{\tau} = \frac{\epsilon_S}{1-\frac{1}{2}\log(\epsilon_S)}$	
Binary diffusion coefficient[a] (179, 180)	$D_{i,k} = 0.0018583\sqrt{T_G^3\left(\frac{1}{MW_i}+\frac{1}{MW_k}\right)}\frac{1}{P\sigma_{ik}^2\Omega_D}$	
Dynamic liquid viscosity (183, 184)	$\mu_L = 3.141\times 10^{10}(T_L - 460)^{-3.444}(\log_{10}(API))^a$; $a = 10.313(\log_{10}(T_L - 460)) - 36.447$	
Molar volume of solute (i) in liquid phase and liquid solvent (L) (183, 184)	$v_i = 0.285(v_{Ci})^{1.048}$; $v_L = 0.285(v_{cL})^{1.048}$	
Solvent critical specific volume (185)	$v_{cL} = v^m_{cL}MW_L$; $v^m_{cL} = 7.5214\times 10^{-3}T^{0.2896}_{MeABP}d^{-0.7666}_{15.6}$	

[a] P at atm.

$$\eta_j^f = \frac{\frac{1}{V_p}\int r_j'^f\left(C_{fi}^S, T_S\right)dV_p}{r_j'^f\left(C_{Sfi}^S, T_S^S\right)}, \text{ and} \tag{58a}$$

$$\eta_j^f = \frac{r_j'^f\left(C_{fi}^S, T_S\right)}{r_j'^f\left(C_{Sfi}^S, T_S^S\right)} = \frac{\left(r_j'^f\right)_{obs}}{\left(r_j'^f\right)_{in}} \tag{58b}$$

Analytical solutions for Eqs. (58a) and (58b) are possible only for single reactions and zero and first order rate expressions. The different correlations used in the literature to estimate the catalyst effectiveness factor for isothermal and irreversible reactions are shown in Table 10.

For other kinetic models different to power-law approach, such as Langmuir-Hinshelwood-Hougen-Watson (**LHHW**) type kinetic expressions, there is not an analytical solution of Eq. (58a). Therefore, an alternative method to avoid the numerical integration of Eq. (58a) is the Bischoff generalized modulus approach (193), which enables the analytical solution to any type of rate equation and single reaction.

As it was previously mentioned, the effectiveness factor in commercial HDS catalysts has been reported to be in the range of 0.4–0.8 (6, 30, 37, 56, 109, 119, 180, 194).

The expressions for isothermal first-order reactions with irregular shape catalysts lead at steady state conditions to acceptable results with errors not exceeding 20% (56, 195). Bischoff (193) proposed a general modulus in order to predict the effectiveness factor for any reaction type within a relatively narrow region. If reactions of order less than one-half are excluded, the spread between all the various curves is about 15%. The mean deviation of values of η calculated from the empirical correlation proposed by Papayannakos and Georgiou (49) is less than 2.4% from those predicted with the normalized modulus for simple order reactions proposed by Froment and Bischoff (29) in the range $0.05 < \eta < 0.99$.

C. Global Gas-Liquid Mass Transfer

The gas-liquid interphase mass transfer flux is described in terms of the simple two-film theory:

$$\frac{1}{K_{Li}} = \frac{RT_G Z_{(P,\,T_G)}}{k_i^G H_i} + \frac{1}{k_i^L}. \tag{59}$$

Table 10: Catalyst effectiveness factor estimation.

Kinetic Model	Reaction Order	Shape	Thiele Modulus	Effectiveness Factor
Power-Law (28, 29, 189)	$n = 1$	Spheres and crushed	$\Phi_j^f = \frac{V_p}{S_p}\sqrt{\frac{k'^f_{in,\,j}\rho_S}{D^f_{ei}}}$	$\eta_j^f = \frac{3\Phi_j^f \coth\left(3\Phi_j^f\right)-1}{3\left(\Phi_j^f\right)^2}$
Power-Law (56, 190)	$n = 1$	Pellet, cylinder, 2-, 3-lobe, etc.	$0.5 > \Phi_j^f > 10$	$\eta_j^f = \frac{\tanh\left(\Phi_j^f\right)}{\Phi_j^f}$
Power-Law (49)	$2 \leqslant n \leqslant 3$	Any geometry	$\Phi_j^f = \frac{V_p}{S_p}\sqrt{\left(\frac{n+1}{2}\right)\frac{k'^f_{in,\,j}\left(C^S_{Sfi}\right)^{n-1}\rho_S}{D^f_{ei}}}$	$\eta_j^f = \frac{1}{\sqrt{\left(\Phi_j^f\right)^2+1}}$
Power-Law (56, 191, 192)	$n \geqslant 0$	Any geometry	$\Phi_j^f > 3$	$\eta_j^f = 1\Big/\Phi_j^f$
Power-Law (119)	$n \geqslant 0$	Any geometry	Supposed to be $\Phi_j^f > 3$	$\eta_j^f = \frac{2D^f_{ei}\left(S_p/V_p\right)^2}{(n+1)k'^f_{app,\,j}\left(C^S_{Sfi}\right)^{n-1}\rho_S}$
Langmuir-Hinshelwood (193)	–	Spheres and crushed	$\Phi_j^f = \frac{V_p\rho_S r'^f_j\left(C^S_{Sfi},\,T^S_S\right)}{S_p\sqrt{2}}\left[\int_{C_{i,\,eq}}^{C^S_{Sfi}} D^f_{ei}\rho_S r'^f_j\left(C^S_{fi},\,T^S_S\right)dC_i\right]^{-1/2}$	$\eta_j^f = \frac{3\Phi_j^f \coth\left(3\Phi_j^f\right)-1}{3\left(\Phi_j^f\right)^2}$
Langmuir-Hinshelwood (193)	–	Pellet, cylinder, 2-, 3-lobe, etc.	$\Phi_j^f = \frac{V_p\rho_S r'^f_j\left(C^S_{Sfi},\,T^S_S\right)}{S_p\sqrt{2}}\left[\int_{C_{i,\,eq}}^{C^S_{Sfi}} D^f_{ei}\rho_S r'^f_j\left(C^S_{fi},\,T^S_S\right)dC_i\right]^{-1/2}$	$\eta_j^f = \frac{\tanh\left(\Phi_j^f\right)}{\Phi_j^f}$

The overall external resistance to mass transfer (K_{Li}) is composed by the resistance to mass transfer in the gas $\left(k_i^G\right)$ and liquid $\left(k_i^L\right)$ films. Estimates of the compressibility factor Z sometimes give values close to 1; therefore, ideal gas law could be used (94).

For slightly soluble gases, such as H_2, the value of Henry's constant (H_i) exceeds unity and then mass transfer resistance in the gas film can be neglected (19). Therefore, the total mass transfer is approximately equal to the liquid side mass transfer coefficient as:

$$\frac{1}{K_{Li}} = \frac{1}{k_i^L}. \tag{60}$$

Liquid film mass transfer coefficient $\left(k_i^L\right)$ is calculated using correlations reported in Table 11.

D. Gas-Liquid Equilibrium

The gas-liquid equilibrium along the catalyst bed is represented in the mass balance equations by the Henry's law constant. The constants related to this law for different chemical species available in the system may be defined by the following two ways:

1. *Solubility Coefficients*

Employing solubility coefficients the following expression is used to estimate the Henry's constant:

$$H_i = \frac{v_N}{\lambda_i \rho_L}, \tag{61}$$

where λ_i stands for the component i solubility; and v_N is the molar volume at normal conditions.

Using this expression implies the knowledge of the gaseous components solubility in the liquid phase considering the process temperature effect. Korsten and Hoffman (109) have reported the next correlations to evaluate this parameter only for H_2 and H_2S:

$$\begin{aligned}\lambda_{H_2} = &-0.559729 - 0.42947 \times 10^{-3} T_L + 3.07539 \times 10^{-3} \frac{T_L}{\rho_L} \\ &+ 1.94593 \times 10^{-6} T_L^2 + 0.835783 \frac{1}{\rho_L^2},\end{aligned} \tag{62}$$

for hydrogen, and

Table 11: Correlations to estimate model parameters:

Parameter	*Symbol*	*Referentes*	*Parameter*	*Symbol*	*References*
Holdup Gas	ε_G	Calculated from Eq. 95	Density of the liquid phase	ρ_L	(185)
Holdup liquid	ε_L	(196–199)	Catalyst bulk density	ρ_B	Experimental
Bed void fraction	$\in_B$	(29, 200, 201)	Dynamic viscosity of liquid	μ_L	(184, 185, 233)
Catalyst wetting efficiency (or contacting effectiveness)	f_w (η_{CE})	(202, 203)	Dynamic viscosity of gas	μ_G	(185, 233)
Two-phase pressure drop	ΔP	(204, 205)	Diffusion coefficients for gases	D_{Mi}^G	(234)
Gas-liquid interfacial area	a_L	(206)	Diffusion coefficients for liquids	D_{Mi}^L	(181)
Gas-solid interfacial area	a_S	(60, 207)	Specific heat of gas phase	Cp_G	(235, 236)
Mass transfer gas-solid coefficient	k_i^{GS}	(208, 209)	Specific heat of liquid phase	Cp_L	(235, 237, 238)
Mass transfer liquid-solid coefficient	k_i^S	(7)[a],(209),(210)[b], (211–215)	Specific heat of solid phase	Cps	(238)
Mass transfer coefficient of liquid-side at G–L interface	k_i^L	(213, 216)	Gas-liquid heat transfer coefficient	h_{GL}	(40, 239)
Mass transfer coefficient of gas-side at G–L interface	k_i^G	(216),(217)[c],(218)	Liquid-solid heat transfer coefficient	h_{LS}	(239)[e]
Axial dispersion of gas	D_a^G	(69, 70, 219)	Chilton-Colburn *j*-factor for energy transfer (gas-solid)	j_H	(210, 240)
Axial dispersion of liquid	D_a^L	(39, 69, 70, 89)	Effective thermal conductivity radial	λ_{er}^f	(241)
Radial dispersion of gas	D_r^G	(220, 221)	Effective thermal conductivity axial	λ_{ea}^f	(242)[f],(243)
Radial dispersion of liquid	D_r^L	(220, 221)	Thermal conductivity of fluids	k_f	(230, 244)
Binary interaction parameter for H_2-Oil using PR EoS	$k_{H_2,Oil}$	(109, 222–226)	Heat of reaction	ΔH_R	(242)
Binary interaction parameter for H_2S-Oil using PR EoS	$k_{H_2S,Oil}$	(227–229)	Heat of vaporization/ condensation	ΔH_v	(231, 232)
Binary interaction parameter for NH_3-Oil using SRK EoS	$k_{NH_3,Oil}$	(230)[d]	Thiele modulus	Φ	(193)
Density of the gas phase	ρ_G	(231, 232)	Effectiveness factor	η	(29, 195)

[a] Choose those correlations for high pressure and temperature and trickle flow regime as found in industrial reactors. [b] Interval of Re numbers unknown. [c] Pulsing regime. [d] In absence of other data. [e] This analogy has to assume some conditions given by Bird et al. (210). [f] Analogy with axial mass Peclet number.

$$\lambda_{H_2S} = \exp(3.3670 - 0.008470 T_L), \tag{63}$$

for hydrogen sulfide.

However, this last correlation may be no adequate to evaluate the solubility of H_2S in oil fractions at the complete temperature range used in commercial units. In that case, it is possible to use an EoS to estimate this Henry's constant.

2. Equation of State

It is also possible to obtain the Henry's constant assuming local equilibrium at the liquid-gas interface:

$$H_i = \frac{P y_i}{C_{Tot}^L x_i} = \frac{P}{C_{Tot}^L} K_{eq,\,i}(x_i,\, y_i,\, T_I,\, P), \tag{64}$$

where equilibrium constant ($K_{eq,i}$) is calculated using the adequate EoS (Peng-Robinson (**PR**), Soave-Redlich-Kwong (**SRK**), t-van der Waals, Grayson-Streed, etc.). For this expression, it is necessary to calculate previously at each local point along the catalytic bed a two phase thermodynamic equilibrium in order to estimate the interface temperature, and the molar compositions in liquid and gas phases. The main advantage of this expression is that it takes into account the volatility of feedstock, however, it also increases too much the computing time.

Another way to calculate the Henry's constant of gaseous solute in a solvent is using the next thermodynamic assumption:

$$H_i = \lim_{x_i \to 0} \frac{f_i^L}{x_i} = \lim_{x_i \to 0} P \varphi_i^L, \tag{65}$$

where φ_i^L is the fugacity coefficient of gaseous compound i (solute) in the liquid phase (solvent), and its calculation using EoS is addressed below. The SRK and the PR equations of state are the most widely used in HDT process modeling, being defined by the next generalized expression:

$$P = \frac{RT_f}{v^f - b} - \frac{a}{(v^f + \delta_1 b)(v^f + \delta_2 b)}. \tag{66}$$

For pure compounds values of parameters a and b are given by

$$a = a_{ii} = a_i = a_{c,\,i} \alpha_i(T_f), \tag{67}$$

with

$$a_{c,\,i} = \Omega_a \frac{R^2 T_{c,\,i}^2}{P_{c,\,i}}, \tag{68}$$

and

$$b = b_i = \Omega_b \frac{R T_{c,\,i}}{P_{c,\,i}}. \tag{69}$$

The generalized temperature function $\alpha_i(T_f)$ was proposed by Soave (231) to be an equation of the form:

$$\alpha_i(T_f) = \left[1 + m_i\left(1 - \sqrt{\frac{T_f}{T_{c,\,i}}}\right)\right]^2, \tag{70}$$

with

$$m_i = M_0 + M_1\omega_i + M_2\omega_i^2. \tag{71}$$

When applied to mixtures, the classical mixing rules may be considered to evaluate the parameters a and b:

$$a = a_m = \sum_{i=1}^{N_{CL}} \sum_{k=1}^{N_{CL}} x_i x_k a_{ik}, \tag{72}$$

$$a_{ik} = a_{ki} = \sqrt{a_{ii}a_{kk}}(1 - k_{ik}), \text{ and} \tag{73}$$

$$b = b_m = \sum_{i=1}^{N_{CL}} x_i b_i, \tag{74}$$

where k_{ik} are the binary interaction parameters, which may be obtained from references reported in Table 11. It is important to point out, that quality of Henry's constant calculation depends enormously in the accuracy of these interaction parameters. The liquid phase fugacity coefficient can be derived from Eq. (66) to give:

$$\ln \varphi_i^L = \frac{b_i}{b}\left(Z^L - 1\right) - \ln\left(Z^L - B\right) - \frac{A}{B(\delta_2 - \delta_1)}\left(\frac{2\sum_{k=1}^{N_{CL}} x_k a_{ik}}{a} - \frac{b_i}{b}\right)\ln\left(\frac{Z^L + \delta_2 B}{Z^L + \delta_1 B}\right), \tag{75}$$

with

$$A = \frac{aP}{(RT_L)^2}, \text{ and} \tag{76}$$

$$B = \frac{bP}{RT_L}, \tag{77}$$

where Z^L is the compressibility factor of liquid phase at saturation obtained from the solution of Eq. (66) expressed in its cubic compressibility factor form:

$$A_Z\left(Z^L\right)^3 + B_Z\left(Z^L\right)^2 + C_Z\left(Z^L\right) + D_z = 0. \tag{78}$$

The values of the universal parameters (δ_1, δ_2, Ω_a, Ω_b, M_0, M_1, M_2, A_Z, B_Z, C_Z, and D_Z) are given in Table 12.

E. Heat Transfer Coefficients

Correlations employed for mass transfer can be used to calculate the parameters for energy transfer between phases by employing the Chilton-Colburn analogy (239). The Chilton-Colburn *j*-factor for mass transfer (j_D) is given by

$$j_D = \frac{Sh}{\mathrm{Re}_f\, Sc^{1/3}} = f\left(\mathrm{Re}_f, \textit{geometry}, \textit{boundary conditions}\right). \tag{79a}$$

Table 12: Parameters for Soave-Redlich-Kwong (SRK) and Peng-Robinson (PR) Equation of State (EoS).

	EoS	
Parameter	**SRK**	**PR**
δ_1	1	$1+\sqrt{2}$
δ_2	0	$1-\sqrt{2}$
Ω_a	0.42748	0.457236
Ω_b	0.08664	0.077796
M_0	0.48	0.37464
M_1	1.574	1.54226
M_2	−0.176	−0.26992
A_Z	1	1
B_Z	−1	−(1-B)
C_Z	A-B-B^2	A-2B-3B^2
D_Z	$-AB$	$-(AB$-B^2-$B^3)$

In order to evaluate, i.e., the liquid-solid mass transfer coefficients, Eq. (79a) must be expressed as

$$j_D = \frac{k_i^S}{u_L}\left(\frac{\mu_L}{\rho_L D_{M,i}^L}\right)^{2/3}. \qquad (79b)$$

On the other hand, the Chilton-Colburn *j*-factor for energy transfer (j_H) is given by

$$j_H = \frac{Nu}{\mathrm{Re}_f\,\mathrm{Pr}^{1/3}} = g\left(\mathrm{Re}_f, \textit{geometry}, \textit{boundary conditions}\right), \qquad (80a)$$

where $g(\mathrm{Re}_f$, *geometry, boundary conditions*) is a correlation that is function of Reynolds number of the respective phase f to be evaluated; some of these correlations are shown in Table 11. If one needs to estimate, i.e. the liquid-solid heat transfer coefficient, Eq. (80a) is rewritten in the following expression:

$$j_H = \frac{h_{LS}}{Cp_L u_L \rho_L}\left(\frac{Cp_L \mu_L}{k_L}\right)^{2/3}. \qquad (80b)$$

There are various correlations to estimate the mass transfer coefficients, Chilton-Colburn analogy is no usually employed to evaluate them. Whereas, due to the lack of correlations to estimate the heat transfer coefficients in the gas or liquid film side at the gas-liquid interface, and in the liquid film at the liquid-solid interface, it is common to use the Chilton-Colburn analogy, by equating Eqs. (79a) and (80a) ($j_D = j_H$), in order to estimate these coefficients. The physical and geometrical properties involved in the dimensionless numbers must be evaluated at conditions of reaction and for each phase in a heterogeneous reactor.

It is necessary, in order to use the Chilton-Colburn analogy, to consider the following conditions (210):

(i) constant physical properties;

(ii) small net mass transfer rates;

(iii) no chemical reaction;

(iv) no viscous dissipation heating;

(v) no absorption or emission of radian energy; and

(vi) no pressure diffusion, thermal diffusion or forced diffusion.

F. Theoretical Calculations of Some Parameters Relative to Catalyst Bed

Dilution of the catalyst bed with inert material is a common practice in experimental HDT reactors (173). The following simple formula is employed to

calculate the dilution factor:

$$\zeta = \frac{V_c}{V_c + V_i}, \tag{81}$$

where V_c is the catalyst volume; and V_i is the volume of inert particles, both obtained experimentally.

Equivalent particle diameter (d_{pe}), defined as the diameter of a sphere that has the same external surface (or volume) as the actual catalyst particle, is an important particle characteristic that depends on particle size and shape. For fixed beds with catalyst extrudates of commercial size, the equivalent particle diameter can be calculated according to Cooper et al. (245):

$$d_{pe} = 6\left(\frac{V_p}{S_p}\right) \Big/ \phi_S. \tag{82}$$

The calculation of external volume (V_p) and surface (S_p) of regular shapes (sphere, pellet, and cylinder) is done with the following equations:

- Sphere:

$$\begin{aligned} V_p &= \frac{4}{3}\pi\left(r_{sph}\right)^3 \\ S_p &= 4\pi\left(r_{sph}\right)^2 \end{aligned} \tag{83}$$

- Pellet:

$$\begin{aligned} V_p &= \pi r_c^2 d_p \\ S_p &= 2\pi r_c^2 + 2\pi r_c d_p \end{aligned} \tag{84}$$

- Cylinder:

$$\begin{aligned} V_p &= \pi r_c^2 l_c \\ S_p &= 2\pi r_c^2 + 2\pi r_c l_c \end{aligned} \tag{85}$$

For pellet, it should be remembered that it is a particle which has the same length and diameter ($l_p = d_p$), and its radius saw as a cylinder is the particle radius ($r_c = r_p$). For cylinder, its radius is also the particle radius, but $l_c \neq d_c$.

For the other lobe-shaped particles, Ancheyta et al. (186) developed the following general equations to determine V_p and S_p:

$$V_p = n_l\left(\pi r_c^2 l_p\right) - A_1 l_p, \text{ and}$$
$$S_p = n_l\left(2\pi r_c^2 + 2\pi r_c l_p\right) \pm 2A_1 - n_l A_2. \tag{86}$$

The values of parameters in Eq. (86) (A_1, A_2, n_l) are given elsewhere (186).

Bed void fraction (or bed porosity) for undiluted catalyst bed can be calculated with the following correlation reported by Froment and Bischoff (29), Haughey and Beveridge (200), and Carberry and Varma (201):

$$\epsilon_B = 0.38 + 0.073\left[1 + \frac{\left(d_t/d_{pe} - 2\right)^2}{\left(d_t/d_{pe}\right)^2}\right]. \tag{87}$$

This correlation was developed for undiluted packed beds of spheres; however, if the equivalent particle diameter concept is used, it can also be employed for non-sphere particles. Once bed void fraction is determined, particle density can be calculated as follows (242):

$$\rho_S = \rho_B/(1 - \epsilon_B). \tag{88}$$

Since the continuous models are based on the volume average form of the transport equations for multiphase systems, then equations expressing conservation of volume are (246):

$$\epsilon_B = \varepsilon_L + \varepsilon_G, \text{ and} \tag{89}$$

$$\varepsilon_L + \varepsilon_G + \varepsilon_S = 1. \tag{90}$$

Relationships between phase holdups inside the catalyst solid are given in the following expressions:

$$\epsilon_S = \varepsilon_{pL} + \varepsilon_{pG}, \text{ and} \tag{91}$$

$$\varepsilon_{pL} + \varepsilon_{pG} + \varepsilon_{pS} = 1. \tag{92}$$

The external surface area of catalyst particles per unit of reactor volume for PBRs can be calculated as:

$$a_S = \frac{6(1 - \epsilon_B)}{d_{pe}}. \tag{93}$$

Catalyst porosity ($\in_S$) may be calculated with the following equation from experimental data of total pore volume (V_g):

$$\in_S = \rho_S V_g. \tag{94}$$

In an extreme case where the experimental S_g parameter is not available in order to estimate the average pore radius, one can use the correlation proposed by Macé and Wei (247):

$$r_g = \frac{4\in_S}{S'_g}, \tag{95}$$

where

$$S'_g = 4\pi\rho_S \left(\frac{d_{pe}}{2}\right)^2 \in_S. \tag{96}$$

G. Concluding Remarks

Some parameters that account for bed characterization are experimentally measurable, some others are experimental or can be obtained through simulations, and some are empirical. Of course although it is better to obtain local porosity experimentally, measurements required the use of advanced techniques. In place to do that, computational calculations are preferred.

Most of empirical correlations for predicting liquid saturation, pressure drop and flow regimes are based on experiments performed at atmospheric conditions. Since industrial trickle-bed reactors are operated at high pressures and temperatures, the applicability of these correlations for such operating conditions needs to be investigated (129). The majority of correlations that have been developed on laboratory scale may not work for large scale reactors (operated at high pressure/temperature) due to significant changes in hydrodynamic characteristics with reactor scale (136). Although extensive studies in hydrodynamic correlations are available in the literature (7) it seems that many works in modeling reactors for petroleum fractions still employ the classical correlations, i.e. those derived from reasonable assumptions with simple expressions. Some researchers have employed the same correlations of previous papers without checking the accuracy of these expressions or the range in which they are applicable. On the other hand, although the benefit of using correlations based on neural networks has been reported, considerable data are necessary for employing this approach. In order to overcome this feature, an alternative is to create a data base with different types of crude oils and fractions in order to develop an online

program able to determine the various parameters involved in modeling of HDT reactor. Nowadays it is not available. The only valuable effort seems to be that of Larachi and Grandjean (248) who have developed a simulator based on neural networks for prediction of some hydrodynamic parameters for trickle-bed reactors. Although neural networks are continuously updated, which favors its use for parameter predictions, it is necessary to develop fundamental relationship taking advantage of novel techniques for characterization of hydrodynamic parameters.

The limitations of the various models reported in the technical literature are closely related to the number of parameters involved and to the reliability of the available data. Therefore, appropriate correlations for mass and energy transfer should be employed in order to calculate each one of the terms used in a model reactor, i.e., correlations developed under similar conditions such as same flow regime, pressure and temperature, assuming similar liquid system and porous particles. Generalized correlations for prediction of properties having a broad range of variation should be avoided when modeling a TBR in detail, because they could produce some miscalculations. Constant values assumed *a priori*, such as tortuosity factor, binary interaction parameters, heat of reaction, specific heat, etc., should be used as reference when experimental data are available. In order to simplify a TBR model, some researchers have ignored the low heat of some reactions because its contribution is not significant in the energy balance which seems to be a reasonable assumption.

Using different approaches for fluid dynamics, kinetics or thermodynamics can lead to very different conclusions in predictions of reactor performance. For instance Gunjal et al. (136) has reported 15% more conversion considering all parameters constant and only assuming uniform porosity, instead of non-uniform porosity. Akgerman et al. (85) has reported 24–38% higher conversions when considering volatiles with respect to nonvolatiles, and Inoue et al. (166) has predicted larger size of reactor employing *n*th kinetic model that when more accurate kinetic expression has been utilized. Another important finding is the consideration of thermowell in the energy balance for pilot plant as has been pointed out by Chen et al. (106). These are the reasons to account for detailed models which allow for both making accurate description of the chemical phenomena and for reliable preliminary calculations when designing a TBR reactor.

V. SUMMARY

Different alternatives for modeling HDT process have been presented in this work, which has been focused on detailed deterministic reactor model.

After revision of several approaches a complete reactor model to simulate the behavior of TBRs has been developed, since almost all the involved internal processes during HDT of oil fractions are taking into account, e.g., thermodynamics, chemical kinetics and transport phenomena. It is desirable to account for such a detailed model due to recent trends in miniaturization process, which in turn, must be scaled at commercial operation.

The election of the model complexity degree must be made considering the scope of the simulation and keeping in mind the inherent error caused when ignoring some terms of the model, however the omission of these terms must be based on the application of analytical or experimental criteria to assure that their effects on accuracy of the model prediction are minima (249). If the objective is to obtain a raw estimation of reactor dimensions as for the case of exploring a novel process, it is more appropriate to use the simplest model, e.g., steady-state 1D pseudohomogeneous plug-flow model. On other hand, if the model is to be used for research and development purposes, it is more recommendable to make use of a more complex model, e.g., dynamic 2D heterogeneous reactor model, in order to predict some important facts that could not be well-addressed with a simple model, such as hot spots, temperature run-away, catalyst deactivation, etc. For the development of reactor model structure to be used, it is prudent to propose initially all the terms involved, and thereafter to cancel some of them as the corresponding criteria to assess the validity of absence of their effects in the reactor behavior are fulfilled.

Many works have outlined the use of different simplifications of a general model, as it was presented here, to study particular phenomena. Unfortunately, the inclusion of all terms may lead to an almost intractable problem, as the time for obtaining a solution may not meet the requirements for routine design, optimization or control studies. This is the stage where the researcher must decide if it is convenient to develop a complex deterministic model or an alternative approach such as a neural network model.

As for estimation of physicochemical properties, it is observed that the majority of correlations employed for calculating hydrodynamics parameters have been obtained in reactors, whose dimensions are different from the laboratory scale reactor and commercial reactor. Hence, such correlations could not be applicable neither to pilot plant scale nor to large scale (i.e., industrial reactor). In such cases, simulations based on CFD can provide a method for estimating hydrodynamic behavior of any reactor scale.

Almost all scientific papers dealing with simulation claim a close agreement between their experimental data and simulation; however, those models are limited to specific feed and/or operational conditions. Several other features such as the effects by reactant mixture volatilization through catalyst bed, influence of different kinetic models, and hydrodynamics under typical

operation of TBRs for the various HDT process must be studied simultaneously in order to obtain accurate predictions of a reactor model.

It seems that reliable modeling and simulation of deep removing of impurities in HDT process is possible by investigating the typical characteristics of different feeds, where the identification of compound types with similar reactivity is the most important step and it is a trend that will be growing with the advent of new analytical techniques of characterization. Fundamental approaches on kinetics are necessary in order to separate the chemical phenomena from mass transfer phenomena. It is also necessary the development of accurate correlations for transport processes and thermodynamics, specifically for the interaction parameters involved in equations of state for NH_3, H_2S, H_2, and petroleum fractions. Novel and more robust thermodynamic approaches such a continuous thermodynamic should be investigated for HDT processes.

The limitations of the various models reported in the literature are closely related to the number of parameters involved and to the reliability of the available data. Therefore, appropriate correlations for mass and energy transfer should be employed in order to calculate each one of the terms present in a reactor model, i.e., correlations developed under similar conditions such as same flow regime, pressure, temperature, liquid system, porous particles, etc.

Recently, the modeling of processing of non-conventional crudes has gained the attention of the research community. Of course, it is more difficult to simulate a reactor model sustaining reactions of nonconventional crudes accurately than typical models that are employed for light petroleum fractions. Hence, it has been recognized that the simplified model for such novel processes can provide valuable information for preliminary design purposes.

It is advisable that computers-aided process modeling will continue in development and several alternative models can be devised as future tools for modeling TBR in the hydroprocessing of oil fractions for conventional light fractions an also for heavy crude oils.

NOMENCLATURE

a	Glaso's coefficient for viscosity correlation; energy parameter in equation of state
a_L	Gas-liquid interfacial area per unit reactor volume, cm^2_l/cm^3_r
a_S	Liquid (or gas)-solid interfacial area per unit reactor volume, cm^2_S/cm^3_r
A	Reduced parameter of energy parameter a
A_W	Bed-wall reactor heat transfer area, cm^2_r
A_Z	Coefficient of the cubic equation of state expressed in Z

A_1	Lateral area of the geometric shape between lobes, cm^2_S
A_2	Common area between each cylinder and each of the sides of the phase between lobes, cm^2_S
A', b'	Empirical constants for Bondi's correlation
API	API gravity
b	Volume parameter in equation of state
B	Reduced parameter of volume parameter b
B_Z	Coefficient of the cubic equation of state expressed in Z
C_Z	Coefficient of the cubic equation of state expressed in Z
C_i^I	Molar concentration of component i in the gas-liquid interface, mol_i/cm^3_L
C_i^L	Molar concentration of component i in the liquid phase, mol_i/cm^3_L
C_i^*	Concentration of compound i in the liquid in equilibrium with the gas phase, mol_i/cm^3_L
C_{fi}^S	Molar concentration of component i inside the solid filled with f phase, mol_i/cm^3_f
C_{Sfi}^S	Molar concentration of component i at surface of solid covered by f phase, mol_i/cm^3_f
Cp_f	Specific heat capacity of f phase, $J/(g_f \cdot K)$
Cp_{fi}	Specific heat capacity of component i in the f phase, $J/(mol_i \cdot K)$
d_p	Catalyst particle diameter, cm_S
d_{pe}	Equivalent particle diameter, cm_S
d_t	Reactor diameter, cm_r
$d_{15.6}$	Liquid specific gravity at 15.6°C and 1 atm, dimensionless
D_Z	Coefficient of the cubic equation of state expressed in Z
$D_{i,k}$	Fick's binary diffusion coefficient of components i and j, $cm^3_G/(cm_S \cdot s)$
D_{ei}^f	Effective fickian diffusivity of component i inside a porous catalyst, $cm^3_f/(cm_S \cdot s)$
D_{Ki}^f	Knudsen diffusion coefficient of component i in the f phase, $cm^3_f/(cm_S \cdot s)$
D_{Mi}^f	Molecular diffusion coefficient of component i in the f phase, $cm^3_f/(cm_S \cdot s)$
D_a^f	Mass axial dispersion coefficient of f phase, cm^2_r/s
D_r^f	Mass radial dispersion coefficient of f phase, cm^2_r/s
e	Particle emissivity, dimensionless
f_w	Catalyst wetting efficiency, $cm^2_{S,wet}/cm^2_S$
f_{St}	Fraction of liquid which is stagnant, dimensionless
f_i^L	Liquid phase fugacity of component i, MPa
F	Coefficient matrix for Stefan-Maxwell model
F_i	Molar flow rate of component i, mol_i/s
$F(\lambda_g)$	Restrictive factor due to friction between solute and pore walls, dimensionless
G_{mf}	Superficial mass flow velocity of f phase, $(g_f/cm^2_r \cdot s)$
h_{air}	Thermowell-atmosphere heat transfer coefficient, $J/(cm^2_{TW} \cdot s \cdot K)$
h_{GI}	Heat transfer coefficient at the gas side of the gas-liquid interface, $J/(cm^2_I \cdot s \cdot K)$
h_{GS}	Gas-solid heat transfer coefficient, $J/(cm^2_S \cdot s \cdot K)$
h_{GW}	Gas-wall reactor heat transfer coefficient, $J/(cm^2_W \cdot s \cdot K)$
h_{IL}	Heat transfer coefficient at the liquid side of the gas-liquid interface, $J/(cm^2_I \cdot s \cdot K)$
h_{LS}	Liquid-solid heat transfer coefficient, $J/(cm^2_S \cdot s \cdot K)$
h_{LW}	Liquid-wall reactor heat transfer coefficient, $J/(cm^2_W \cdot s \cdot K)$
h_{TW}	f phase-thermowell heat transfer coefficient, $J/(cm^2_{TW} \cdot s \cdot K)$
H_i	Henry's law coefficient of component i, $MPa \cdot cm^3_L/mol_i$
ΔH_{Rj}^f	Heat of reaction j in the f phase, J/mol_i
ΔH_{vi}	Heat of vaporization/condensation (or latent heat) of component i, J/mol_i
j_D	Chilton-Colburn j-factor for mass transfer, dimensionless

j_H Chilton-Colburn *j*-factor for heat transfer, dimensionless
k_{app} Apparent reaction rate constant (for first order reaction), s^{-1}
k_{in} Intrinsic reaction rate constant (for first order reaction), s^{-1}
k_{ik} Binary interaction parameter, dimensionless
k_L Thermal conductivity of liquid phase, $J/(cm_L \cdot s \cdot K)$
k_α, k_β First-order kinetic constants for reactive and refractory fraction respectively, 1/s
$(k)_{EH}$ Pseudokinetic rate constant referred to external holdup model, $(mol/cm^3)^{1-n}(1/s)$
$(k)_{AD}$ Pseudokinetic rate constant referred to apparent diffusivity model, $(mol/cm^3)^{1-n}(1/s)$
k_i^G Mass transfer coefficient from gas phase to gas-liquid interface, $cm^3_G/(cm^2_I \cdot s)$
k_i^{GS} Gas-solid mass transfer coefficient, $cm^3_G/(cm^2_S \cdot s)$
k_i^L Mass transfer coefficient from gas-liquid interface to liquid phase, $cm^3_L/(cm^2_I \cdot s)$
k_i^m Flowing-stagnant liquid mass transfer coefficient, $cm^3_L/(cm^2_S \cdot s)$
k_i^S Liquid-solid mass transfer coefficient, $cm^3_L/(cm^2_S \cdot s)$
k'^S_i Stagnant liquid-solid mass transfer coefficient, $cm^3_L/(cm^3_r \cdot s)$
$K_{eq,i}$ Liquid-vapor equilibrium constant of component *i*, dimensionless
K_i Adsorption equilibrium constant of component *i* on catalyst active sites, cm^3_L/mol_i
K_{Li} Overall G-L mass transfer coefficient of component *i* in the liquid phase, $cm^3_L/(cm^2_I \cdot s)$
K_{LSi} Overall L-S mass transfer coefficient of component *i* in the liquid phase, $cm^3_L/(cm^2_S \cdot s)$
K_1 Constant in Eq. (56)
l_c Length of cylinder, cm_S
l_p Length of catalyst particle, cm_S
L_B Length of catalyst bed, cm_r
LHSV Liquid hourly space velocity, $cm^3_L/(cm^3_{cat} \cdot h)$
m_i Slope parameter of component *i*
$M_{0,1,2}$ Universal constants
MW_i Molecular weight of component *i*, g_i/mol_i
MW_L Molecular weight of liquid phase, g/mol
n, m Reaction orders
n_l Number of lobes in lobe-shaped particles
N_i^f Molar flux of component *i* in the *f* phase, $mol_i/(cm^2_S \cdot s)$
N_{Cf} Number of components in the *f* phase
N_{Rf} Number of reactions in the *f* phase
p_i^G Partial pressure of component *i* in the bulk gas phase, MPa
p_i^l Partial pressure of component *i* in the gas-liquid interface, MPa
P Absolute reactor pressure, MPa
ΔP Two-phase pressure drop, MPa/cm_r
r Radial reactor coordinate, cm_r
r_c Radius of cylinder, cm_S
r_g Mean pore radius, cm_S
r_i Rate of disappearance of component *i*, $mol_i/(cm^3_L \cdot s)$
r_p Radius of particle, cm_S
r_{solute} Hydrodynamic molecular radius of the solute, cm_i
r_{sph} Radius of sphere, cm_S
$r_j^{'f}$ Rate of reaction *j* per unit of catalyst mass in the *f* phase, $mol_i/(g_S \cdot s)$
R Gas law constant, 8.314471 J/(mol·K)
R_{TW} Outer radius of thermowell, cm_{TW}

S_p	Total geometric external surface area of catalyst particle, cm^2_S
S_g	Specific external surface area of catalyst particle, cm^2_S/g_{cat}
S'_g	Surface area defined by Eq. (96), cm^2_S/g_{cat}
t	Time, s
T	Absolute temperature, K
u_f	Superficial velocity of f phase, $cm^3_f/(cm^2_r \cdot s)$
v_i	Molar volume of solute i at its normal boiling temperature, cm^3_i/mol_j
v_L	Molar volume of liquid solvent at its normal boiling temperature, cm^3_L/mol_L
v_N	Molar gas volume at standard conditions, Nl_G/mol_G
v^f	Molar volume of f phase, cm^3_f/mol_f
V	Reactor volume, cm^3_r
V_c	Bulk volume of catalyst, cm^3_{cat}
V_g	Total pore volume of catalyst particle, $cm^3_{(G+L)}/g_S$
V_i	Bulk volume of diluent, cm^3_{inert}
V_p	Total geometric volume of catalyst particle, cm^3_S
x_i	Mole fraction of the component i in the liquid phase, mol_i/mol_L
y_i	Mole fraction of the component i in the gas phase, mol_i/mol_G
z	Axial reactor coordinate, cm_r
Z	Compressibility factor, dimensionless
$\hat{Z}$	Constant employed in Bosanquet's formula, dimensionless

Greek Letters

α, β, γ	Empirical exponents
α_i	Generalized temperature function of component i
$\delta_{1,2}$	Universal constants in the generalized equation of state
$\in_B$	Catalyst bed void fraction or catalyst bed porosity, $cm^3_{(G+L)}/cm^3_r$
$\in_S$	Catalyst particle porosity, $cm^3_{(G+L)}/cm^3_S$
ε_f	External holdup of f phase, cm^3_f/cm^3_r
ε_{pf}	Holdup of f (= G or L) phase inside catalyst particle, cm^3_f/cm^3_S
ε_{pS}	Holdup of solid phase inside catalyst particle, cm^3_p/cm^3_S
ϕ_s	Shape factor (= surface area of a sphere of equal volume/surface area of the particle)
φ_i^L	Liquid phase fugacity coefficient of component i, dimensionless
ζ	Catalyst bed dilution factor, $cm^3_{cat}/(cm^3_{cat}+cm^3_{inert})$
η^*	Effectiveness factor of a partially external and internal wetted pellet, dimensionless
η_{CE}	External catalyst contacting efficiency, $cm^2_{S,wet}/cm^2_S$
η_E	External efficiency, dimensionless
η_G	Global reactor efficiency, dimensionless
η_i	Wetting efficiency inside catalyst particle, dimensionless
η_j^f	Catalyst effectiveness factor of reaction j in the f phase, dimensionless
$\eta_{TB,j}$	Overall catalyst effectiveness factor in a TBR, dimensionless
κ	Proportionality constant
λ	Extent of reaction, dimensionless
λ_i	Solubility coefficient of component i, $Nl\ i/(kg_L \cdot MPa)$
λ_{er}	Radial effective thermal conductivity, $J/(cm_r \cdot s \cdot K)$
λ_g	Hydrodynamic diameter of solute to pore diameter ratio, cm_i/cm_S
λ_{rad}	Radiant contribution, $J/(cm_r \cdot s \cdot K)$
λ_a^f	Axial f phase thermal conductivity, $J/(cm_r \cdot s \cdot K)$
λ_r^f	Radial f phase thermal conductivity, $J/(cm_r \cdot s \cdot K)$
λ_{TW}	Thermowell thermal conductivity, $J/(cm_{TW} \cdot s \cdot K)$
μ_f	Dynamic viscosity of f phase, cP
ν	Kinematic viscosity, cSt
v_{ci}	Critical specific volume of the gaseous compound i, cm^3/mol_i
v_{ci}	Solvent critical specific volume, cm^3_L/mol_L

v_L	Volumetric flow of liquid phase, cm^3_L/s
v^m_{cL}	Critical specific volume of liquid, ft^3_L/lb_M
v^f_{ij}	Stoichiometric coefficient of component *i* in reaction *j* in the *f* phase, dimensionless
ξ	Radial coordinate inside spherical catalyst particle, cm_S
ρ_B	Catalyst bulk (or bed) density, g_S/cm^3_{cat}
ρ_f	Density at process conditions of *f* phase, g_f/cm^3_f
σ	Surface tension, dyn/cm; Stephan-Boltzmann constant, 5.67×10^{-8} J/($m^2 \cdot s \cdot K^4$)
σ_c	Critical surface tension, dyn/cm
σ_{ik}	Collision diameter, Å
τ	Tortuosity factor for catalyst, cm_f/cm_S
$\tau_{1/2}$	Observed overall conversion half time, s
$\tau_{1/2,c}$	Conversion half time extrapolated to infinite liquid velocity, s
τ_L	Residence time or space time, h
Φ_T	Thiele modulus of an irregular particle, dimensionless
$\Phi_{TB,j}$	Modified Thiele modulus for TBRs, dimensionless
Φ^f_j	Thiele modulus of reaction *j* in the *f* phase, dimensionless
$\psi(u_L)$	Function of superficial liquid velocity that considers the degree of utilization of the catalyst due to hydrodynamic phenomena
ψ_r	Radiant transfer factor, dimensionless
ω	Empirical exponent; acentric factor, dimensionless
Ω_D	Collision integral, dimensionless
$\Omega_{a,b}$	Universal constants

Subscripts

app	Apparent
B	Referred to reactor catalytic bed
c	Referred to critical conditions
e	Effective
f	Phase (gas, liquid or solid); final or outlet condition
G	Gas phase
GO	Gas oil
H_2	Molecular hydrogen
H_2S	Hydrogen sulfide
i,k	Component index
in	Intrinsic
I	Gas-Liquid interface
j	Reaction index
L	Liquid phase
MeABP	Mean average boiling point
NH_3	Ammonia
O	Olefin
obs	Observed
p	Referred to catalyst particle
P	Referred to plug-flow
room	Referred to room conditions
S	Sulfur compound; solid phase; condition at external surface of solid catalyst particle
St	Condition at stagnant zone
Tot	Total
TW	Referred to thermowell
W	Referred to reactor wall
WN	Wild naphtha
0	Initial or inlet condition
*	Equilibrium condition

Superscripts

f Phase (gas, liquid or solid)
G Gas phase; gas side of the gas–liquid interface
I Gas-Liquid interface
L Liquid phase; liquid side of the gas–liquid interface
S Solid phase; liquid side of the liquid–solid interface; inside solid catalyst particle

Dimensionless Groups

Bo Bodenstein number, ud_{pe}/D
Nu Nusselt number, hd_{pe}/λ
Pe Peclet number, uL_B/D
Pr Prandtl number, $C_p\mu/\lambda$
Re Reynolds number, $uL\rho/\mu$ ($L = L_B$ or d_{pe})
Sc Schmidt number, ν/D
Sh Sherwood number, $k^f d_{pe}/D$

ACKNOWLEDGMENTS

The authors thank Instituto Mexicano del Petróleo for its financial support. F. S. M. and I. E. also thank CONACyT for financial support.

REFERENCES

[1] Kumar, V.R., Balaraman, K.S., Rao, V.S.R., Ananth, M.S. (1997) Modelling of Hydrotreating Process in a Trickle-Bed Reactor. *Pet. Sci. Technol.* 15 (1&2), 283–295.

[2] Chowdhury, R., Pedernera, E., Reimert, R. (2002) Trickle-Bed Reactor Model for Desulfurization and Dearomatization of Diesel. *AIChE J.*, 48 (1): 126–135.

[3] Mederos, F.S., Ancheyta, J. (2007) Mathematical Modeling and Simulation of Hydrotreating Reactors: Cocurrent versus Countercurrent Operations. *Appl. Catal. A General*, 332 (1): 8–21.

[4] Silveston, P.L., Hanika, J. (2004) Periodic Operation of Three-Phase Catalytic Reactors. *Can. J. Chem. Eng.*, 82 (6): 1105–1142.

[5] Paraskos, J.A., Frayer, J.A., Shah, Y.T. (1975) Effect of Holdup Incomplete Catalyst Wetting and Backmixing During Hydroprocessing in Trickle Bed Reactors. *Ind. Eng. Chem. Proc. Des. Dev.*, 14 (3): 315–322.

[6] Satterfield, C.N. (1975) Trickle-Bed Reactors. *AIChE J.*, 21 (2): 209–228.

[7] Dudukovic, M.P., Larachi, F., Mills, P.L. (2002) Multiphase Catalytic Reactors: A Perspective on Current Knowledge and Future Trends. *Catal. Rev. Sci. Eng.*, 44 (1): 123–246.

[8] Doraiswamy, L.K., Sharma, M.M. (1984) *Heterogeneous Reactions: Analysis, Examples, and Reactor Design*; John Wiley & Sons: New York, 1984; Vol. 2, 374 pp.

[9] Bhaskar, M., Valavarasu, G. (2002) Meenakshisundaram, A., Balaraman, K. S. Application of a Three Phase Heterogeneous Model to Analyse the Performance of a Pilot Plant Trickle Bed Reactor. *Pet. Sci. Technol.*, 20 (3&4): 251–268.

[10] Froment, G.F., Depauw, G.A., Vanrysselberghe, V. (1994) Kinetic Modeling and Reactor Simulation in Hydrodesulfurization of Oil Fractions. *Ind. Eng. Chem. Res.*, 33 (12): 2975–2988.

[11] Kemsley, J. (2003) Targeting Sulfur in Fuels for 2006. *C&EN*, 81: 40–41.

[12] Ali, M.F., Al-Malki, A., El-Ali, B., Martinie, G., Siddiqui, M.N. (2006) Deep Desulphurization of Gasoline and Diesel Fuels Using Non-Hydrogen Consuming Techniques. *Fuel*, 85, 1354–1363.

[13] Irvine, R.L., Varraveto, D.M. (1999) Adsorption Process for Removal of Nitrogen and Sulphur. *PTQ Summer*, 37–44.

[14] Lamourelle, A.P., Nelson, D.E., McKnight, J. (2001) Ultra Low Sulphur – Low Aromatic Diesel. *PTQ Summer*, 51–56.

[15] Palmer, R.E., Torrisi, S.P. (2004) Hydrotreater Revamps for ULSD Fuel. *PTQ Revamps & Operations*, February 7: 15–18.

[16] Feick, J., Quon, D. (1970) Mathematical Models for the Transient Behavior of a Packed Bed Reactor. *Can. J. Chem. Eng.*, 48: 205–211.

[17] Hofmann, H.P. (1978) Multiphase Catalytic Packed-Bed Reactors. *Catal. Rev. Sci. Eng.*, 17 (1): 71–117.

[18] Herskowitz, M., Smith, J.M. (1983) Trickle-Bed Reactors: A Review. *AIChE J.*, 29 (1): 1–18.

[19] Zhukova, T.B., Pisarenko, V.N., Kafarov, V.V. (1990) Modeling and Design of Industrial Reactors with a Stationary Bed of Catalyst and Two-Phase Gas-Liquid Flow–A Review. *Int. Chem. Eng.*, 30 (1): 57–102.

[20] Feyo De Azevedo, S., Romero-Ogawa, M.A., Wardle, A.P. (1990) Modelling of Tubular Fixed-Bed Catalytic Reactors: A Brief Review. *Trans. Inst. Chem. Eng.*, 68 (A): 483–502.

[21] Gianetto, A., Specchia, V. (1992) Trickle-Bed Reactors: State of Art and Perspectives. *Chem. Eng. Sci.*, 47 (13–14): 3197–3213.

[22] Al-Dahhan, M.H.; Larachi, F.; Dudukovic, M.P.; Laurent, A. (1997) High-Pressure Trickle-Bed Reactors: A Review. *Ind. Eng. Chem. Res.*, 36 (8): 3292–3314.

[23] Biardi, G.; Baldi, G. (1999) Three-Phase Catalytic Reactors. *Catal. Today*, 52 (2–3): 223–234.

[24] Andrigo, P.; Bagatin, R.; Pagani, G. (1999) Fixed Bed Reactors. *Catal. Today*, 52 (2–3): 197–221.

[25] Kundu, A., Nigam, K.D.P., Duquenne, A.M., Delmas, H. (2003) Recent Developments on Hydroprocessing Reactors. *Rev. Chem. Eng.*, 19 (6): 531–605.

[26] Shinnar, R. (1978) Process Control Resarch: In *An Evaluation of Present Status and Research Needs. ACS Symp. Series*, 72: 1.

[27] Deans, H.A., Lapidus, L. (1960) A Computational Model for Predicting and Correlating the Behavior of Fixed-Bed Reactors: I. Derivation of Model for Nonreactive Systems. *AIChE J.*, 6 (4): 656–663.

[28] Crine, M., Marchot, P., L'Homme, G.A. (1980) A Phenomenological Description of Trickle-Bed Reactors Application to the Hydrotreating of Petroleum Fractions. *Chem. Eng. Sci.*, 35 (1–2): 51–58.

[29] Froment, G.F, Bischoff, K.B. (1990) *Chemical Reactor Analysis and Design*; Wiley: New York; 654 pp.

[30] Iannibello, A., Marengo, S., Burgio, G., Baldi, G., Sicardi, S., Specchia, V. (1985) Modeling the Hydrotreating Reactions of a Heavy Residual Oil in a Pilot Trickle-Bed Reactor. *Ind. Eng. Chem. Proc. Des. Dev*, 24 (3), 531–537.

[31] Glasscock, D.A., Hale, J.C. (1994) Process Simulation: The Art and Science of Modeling. *Chem. Eng.*, 101 (11): 82–89.

[32] Froment, G.F. (1986) The Kinetics of Catalytic Processes: Importance in Reactor Simulation and *Design. App. Catal.*, 22 (1): 3–20.

[33] Muñoz, J.A.D., Alvarez, A., Ancheyta, J., Rodríguez, M.A. (2005) Marroquín, G. Process Heat Integration of a Heavy Crude Hydrotreatment Plant. *Catal. Today*, 109 (1–4): 214–218.

[34] Alvarez, A., Ancheyta, J. (2008) Simulation and Analysis of Different Quenching Alternatives for an Industrial Vacuum Gasoil Hydrotreater. *Chem. Eng. Sci.*, 63 (3): 662–673.

[35] Montagna, A., Shah, Y.T. (1975) Backmixing Effect in an Upflow Cocurrent Hydrodesulfurization Reactor. *Chem. Eng. J.*, 10 (1): 99–105.

[36] Sie, S. T., Krishna, R. (1998) Process Development and Scale Up: III. Scale-up and Scale-Down of Trickle Bed Processes. *Rev. Chem. Eng.* 14 (3): 203–252.

[37] Hofmann, H. (1977) Hydrodynamics, Transport Phenomena, and Mathematical Models in Trickle-Bed Reactors. *Int. Chem. Eng*, 17 (1): 19–28.

[38] Ancheyta, J. (2007) Reactors for Hydroprocessing. In *Hydroprocessing of Heavy Oils and Residua*; Ancheyta, J., Speight J. (eds.); Taylor & Francis: New York; 345 pp.

[39] Gierman, H. (1988) Design of Laboratory Hydrotreating Reactors Scaling Down of Trickle-Flow Reactors. *Appl. Catal.*, 43 (2): 277–286.

[40] Marroquín de la Rosa, J.O., Valencia López, J.J., Ochoa-Tapia, J.A., Viveros-García, T. (2002) Trickle-Bed Reactor Modeling for Diesel Hydrotreatment. Proc. 17th International Symposium on Chemical Reaction Engineering. ISCRE-17, Manuscript 285, Hong Kong, China, August 25–28.

[41] Ancheyta-Juárez, J., Aguilar-Rodríguez, E., Salazar-Sotelo, D., Betancourt-Rivera, G., Leiva-Nuncio, M. (1999) Hydrotreating of Straight Run Gas Oil–Light Cycle Oil Blends. *App. Catal. A General*, 180 (1–2): 195–205.

[42] Ancheyta, J., Angeles, M. J., Macías, M. J., Marroquín, G., Morales, R. (2002) Changes in Apparent Reaction Order and Activation Energy in the Hydrodesulfurization of Real Feedstocks. *Energy Fuels*, 16 (1): 189–193.

[43] Cecil, R.R., Mayer, F.Z., Cart, E.N. Jr. (1968) Fuel Oil Hydrodesulfurization Studies in Pilot Plant Reactors. Paper presented at the 61 AIChE Annual Meeting, Los Angeles, CA, Dec. 1–5.

[44] Henry, H.C., Gilbert, J.B. (1973) Scale Up of Pilot Data for Catalytic Hydroprocessing. *Ind. Eng. Chem. Proc. Des. Dev.*, 12 (3): 328–334.

[45] Smith, J.M. (1990) *Chemical Engineering Kinetics*; McGraw Hill: New York; 612 pp.

[46] Hill, C.G. (1977) *An Introduction to Chemical Engineering Kinetics & Reactor Design*; John Wiley & Sons: New York; 594 pp.

[47] Frye, C.G., Mosby, J.F. (1967) Kinetics of Hydrodesulfurization. *Chem. Eng. Prog*, 63 (9): 66–70.

[48] Hoekstra, G. (2007) The Effects of Gas-to-Oil Rate in Ultra Low Sulfur Diesel Hydrotreating. *Catal. Today*, 127 (1–4): 99–102.

[49] Papayannakos, N., Georgiou, G. (1988) Kinetics of Hydrogen Consumption During Catalytic Hydrodesulphurization of a Residue in a Trickle-Bed Reactor. *J. Chem. Eng. Jpn.*, 21 (3): 244–249.

[50] Ancheyta-Juárez, J., Maity, S.K., Betancourt-Rivera, G., Centeno-Nolasco, G., Rayo-Mayoral, P., Gómez-Pérez, M.T. (2001) Comparison of Different Ni-Mo/Alumina Catalysts on Hydrodemetallization of Maya Crude Oil. *App. Catal. A General*, 216 (1–2): 195–208.

[51] Pitault, I., Fongarland, P., Mitrovic, M., Ronze, D., Forissier, M. (2004) Choice of Laboratory Scale Reactors for HDT Kinetic Studies or Catalyst Tests. *Catal. Today*, 98 (1–2),: 31–42.

[52] Perego, C., Paratello, S. (1999) Experimental Methods in Catalytic Kinetics. *Catal. Today*, 52 (2–3): 133–145.

[53] Bondi, A. (1971) Handling Kinetics from Trickle-Phase Reactors. *Chem. Tech.*, 1: 185–188.

[54] Montagna, A.A., Shah, Y.T. (1975) The Role of Liquid Holdup, Effective Catalyst Wetting, and Backmixing on the Performance of a Trickle Bed Reactor for Residue Hydrodesulfurization. *Ind. Eng. Chem. Proc. Des. Dev.*, 14 (4): 479–483.

[55] Ross, L.D. (1965) Performance of Trickle Bed Reactors. *Chem. Eng. Prog.*, 61 (10): 77–82.

[56] Dudukovic, M.P. (1977) Catalyst Effectiveness Factor and Contacting Efficiency in Trickle-Bed Reactors. *AIChE J.*, 23 (6): 940–944.

[57] Mears, D.E. (1971) The Role of Axial Dispersion in Trickle-Flow Laboratory Reactors. *Chem. Eng. Sci.*, 26 (9): 1361–1366.

[58] Murphree, E.V., Voorhies, A. Jr., Mayer, F.X. (1964) Application of Contacting Studies to the Analysis of Reactor Performance. *Ind. Eng. Chem. Proc. Des. Dev.*, 3 (4): 381–386.

[59] Mears, D.E. (1974) The Role of Liquid Holdup and Effective Wetting in the Performance of Trickle-Bed Reactors. In *Proceedings of the 3rd Int. Symp. Chem. React. Eng. II*; Hulburt, H.M. (ed.); ACS Monograph Ser. No. 133, p. 218.

[60] Puranik, S.S., Vogelpohl, A. (1974) Effective Interfacial Area in Irrigated Packed Columns. *Chem. Eng. Sci.*, 29 (2): 501–507.

[61] Gianetto, A., Baldi, G., Specchia, V., Sicardi, S. (1978) Hydrodynamics and Solid-Liquid Contacting Effectiveness in Trickle-Bed Reactors. *AIChE J.*, 24 (6): 1087–1104.

[62] Callejas, M.A., Martínez, M.T. (2002) Evaluation of Kinetic and Hydrodynamic Models in the Hydroprocessing of a Trickle-Bed Reactor. *Energy Fuels*, 16 (3): 647–652.

[63] Iannibello, A., Marengo, S., Guerci, A., Baldi, G., Sicardi, S. (1983) Performance of a Pilot Trickle-Bed Reactor for Hydrotreating of Petroleum Fractions: Dynamic Analysis. *Ind. Eng. Chem. Proc. Des. Dev.*, 22 (4): 594–598.

[64] Mills, P.L., Dudukovic, M.P. (1981) Evaluation of Liquid-Solid Contacting in Trickle-Bed Reactors by Tracer Methods. *AIChE J.*, 27 (6): 893–904.

[65] Trejo, F., Ancheyta, J., Sánchez, S., Rodríguez, M.A. (2007) Comparison of Different Power-Law Kinetic Models for Hydrocracking of Asphalthenes. *Pet. Sci. Technol.*, 25 (1): 263–275.

[66] Danckwerts, P.V. (1953) Continuous Flow Systems. Distribution of Residence Times. *Chem. Eng. Sci.*, 2 (1): 1–13.

[67] Wehner, J.F., Wilhelm, R.H. (1956) Boundary Conditions of Flow Reactor. *Chem. Eng. Sci.*, 6 (2): 89–93.

[68] Burghardt, A., Zaleski, T. (1968) Longitudinal Dispersion at Small and Large Peclet Numbers in Chemical Flow Reactors. *Chem. Eng. Sci.*, 23 (6): 575–591.

[69] Hochman, J.M., Effron, E. (1969) Two-Phase Cocurrent Downflow in Packed Beds. *Ind. Eng. Chem. Fundam.*, 8 (1): 63–71.

[70] Sater, V.E., Levenspiel, O. (1966) Two-Phase Flow in Packed Beds–Evaluation of Axial Dispersion and Holdup by Moment Analysis. *Ind. Eng. Chem. Fundam.*, 5 (1): 86–92.

[71] Schwartz, J.G., Roberts, G.W. (1973) An Evaluation of Models for Liquid Backmixing in Trickle-Bed Reactors. *Ind. Eng. Chem. Proc. Des. Dev.*, 12 (3): 262–271.

[72] Deans, H.A. (1963) A Mathematical Model for Dispersion in the Direction of Flow in Porous Media. *Soc. Pet. Eng. J.*, 3 (1): 49–52.

[73] Buffham, B.A., Gibilaro, L.G., Rathor, M.N. (1970) A Probabilistic Time Delay Description of Flow in Packed Beds. *AIChE J.*, 16 (2): 218–223.

[74] Shah, Y.T., Paraskos, J.A. (1975) Criteria for Axial Dispersion Effects in Adiabatic Trickle Bed Hydroprocessing Reactors. *Chem. Eng. Sci.*, 30 (9):1169–1176.

[75] Tsamatsoulis, D., Koutoulas, E., Papayannakos, N. (1991) Improvement of Characteristic Reactions and Properties of a Heavy Residue by Catalytic Hydrotreatment. *Fuel*, 70 (6): 741–746.

[76] Callejas, M.A., Martínez, M.T. (1999) Hydroprocessing of a Maya Residue. Intrinsic Kinetics of Sulfur-, Nitrogen-, Nickel-, and Vanadium-Removal Reactions. *Energy Fuels*, 13 (3): 629–636.

[77] Ho, T.C. (2003) Property-Reactivity Correlation for HDS of Middle Distillates. *Appl. Cat. A General*, 244 (1): 115–128.

[78] Ho, T.C., Markley, G.E. (2004) Property-Reactivity Correlation for Hydrodesulfurization of Prehydrotreated Distillates. *Appl. Catal. A General*, 267 (1–2): 245–250.

[79] Ferdous, D., Dalai, A. K., Adjaye, J. (2006) Hydrodenitrogenation and Hydrodesulfurization of Heavy Gas Oil Using $NiMo/Al_2O_3$ Catalyst Containing Boron: Experimental and Kinetic Studies. *Ind. Eng. Chem. Res.*, 45 (2): 544–552.

[80] Jiménez, F., Kafarov, V., Nuñez, M. (2007) Modeling of Industrial Reactor for Hydrotreating of Vacuum Gas Oils—Simultaneous Hydrodesulfurization, Hydrodenitrogenation and Hydrodearomatization Reactions. *Chem. Eng. J.*, 134 (1–3): 200–208.

[81] Shokri, S., Marvast, M.A. (2007) Tajerian, M. Production of Ultra Low Sulfur Diesel: Simulation and Software Development. *Petroleum Coal*, 49 (2): 48–59.

[82] Berger, D., Landau, M.V., Herskowitz, M., Boger, Z. (1996) Deep Hydrodesulfurization of Atmospheric Gas Oil—Effects of Operating Conditions and Modelling by Artificial Neural Network Techniques. *Fuel*, 75 (7): 907–911.

[83] Shah, Y.T., Mhaskar, R.D., Paraskos, J.A. (1976) Optimum Quench Location for a Hydrodesulfurization Reactor with Time Varying Catalyst Activity. *Ind. Eng. Chem. Proc. Des. Dev.*, 15 (3): 400–406.

[84] Kodama, S., Nitta, H., Takatsuka, T., Yokoyama, T. (1980) Simulation of Residue Hydrodesulfurization Reaction Based on Catalyst Deactivation Model. *J. Japan Petrol. Inst.*, 23 (5): 310–320.

[85] Akgerman, A., Collins, G.M., Hook, B.D. (1985) Effect of Feed Volatility on Conversion in Trickle Bed Reactors. *Ind. Eng. Chem. Fundam.*, 24 (3), 398–401.

[86] Akgerman, A., Netherland, D.W. (1986) Effect of Equation of State on Prediction of Trickle Bed Reactor Model Performance. *Chem. Eng. Comm.*, 49 (1): 133–143.

[87] Döhler, W., Rupp, M. (1987) Comparison of Performance of an Industrial VGO-Treater with Reactor Model Predictions. *Chem. Eng. Technol.*, 10 (1): 349–352.

[88] Skala, D.U., Šaban, M.D., Orlovic, A.M., Meyn, V.W., Severin D. K., Rahimian, I.G.–H., Marjanovic, M.V. (1991) Hydrotreating of Used Oil: Prediction of

Industrial Trickle-Bed Operation from Pilot-Plant Data. *Ind. Eng. Chem. Res.*, 30 (9): 2059–2065.

[89] Tsamatsoulis, D., Papayannakos, N. (1998) Investigation of Intrinsic Hydrodesulphurization Kinetics of a VGO in a Trickle Bed Reactor with Backmixing Effects. *Chem. Eng. Sci.*, 53 (19): 3449–3458.

[90] Sau, M., Narasimhan, C.S.L., Verma, R.P. (1997) A Kinetic Model for Hydrodesulfurisation. Hydrotreatment and Hydrocracking of Oil Fractions. In *Stud. Surf. Sci. Catal.*; Froment, G.F., Delmon, B., Grange, P. (eds.); Elsevier Science B.V.: The Netherlands; vol. 106, p. 421.

[91] Cotta, R.M., Maciel Filho, R. (1996) Kinetic and Reactor Models for HDT of Middle Distillates. Presented at 5th World Congress of Chem. Eng., San Diego CA, USA, p. 1060.

[92] Lababidi, H. M. S., Shaban, H. I., Al-Radwan, S., Alper, E. (1998) Simulation of an Atmospheric Residue Desulfurization Unit by Quasi-Steady State Modeling. *Chem. Eng. Technol.*, 21 (2): 193–200.

[93] Cotta, R. M., Wolf-Maciel, M. R., Maciel Filho, R. (2000) A Cape of HDT Industrial Reactor for Middle Distillates. *Comput. Chem. Eng.*, 24 (2–7), 1731–1735.

[94] Mejdell, T., Myrstad, R., Morud, J., Rosvoll, J.S., Steiner, P., Blekkan, E.A. (2001) A New Kinetic Model for Hydrodesurfurization of Oil Products. In *Stud. Surf. Sci. Catal.*; Froment, G.F., Waugh, K.C. (eds.); Elsevier Science B.V.: The Netherlands; vol. 133, p. 189.

[95] Bellos, G.D., Papayannakos, N.G. (2003) The Use of a Three Phase Microreactor to Investigate HDS Kinetics. *Catal. Today*, 79–80 (1–4): 349–355.

[96] Melis, S., Erby, L., Sassu, L., Baratti, R. (2004) A Model for the Hydrogenation of Aromatic Compounds During Gasoil Hydroprocessing. *Chem. Eng. Sci.*, 59 (22–23): 5671–5677.

[97] Vargas-Villamil, F.D., Marroquín, J.O., de la Paz, C., Rodríguez, E. (2004) A Catalytic Distilliation Process for Light Gas Oil Hydrodesulfurization. *Chem. Eng. Process.*, 43: 1309–1316.

[98] Kam, E.K.T., Al-Shamali, M., Juraidan, M., Qabazard, H. (2005) A Hydroprocessing Multicatalyst Deactivation and Reactor Performance Model – Pilot-Plant Life Test Applications. *Energy Fuels*, 19 (3): 753–764.

[99] Sertiæ-Bionda, K., Gomzi, Z., Šariæ, T. (2005) Testing of Hydrodesulfurization Process in Small Trickle-Bed Reactor. *Chem. Eng. J.*, 106: 105–110.

[100] Toulhoat, H., Hudebine, D., Raybaud, P., Guillaume, D., Kressmann, S. (2005) THERMIDOR: A New Model for Combined Simulation of Operations and Optimization of Catalysts in Residues Hydroprocessing Units. *Catal. Today*, 109 (1–4): 135–153.

[101] Juraidan, M., Al-Shamali, M., Qabazard, H., Kam, E.K.T. (2006) A Refined Hydroprocessing Multicatalyst Deactivation and Reactor Performance Model—Pilot-Plant Accelerated Test Applications. *Energy Fuels*, 20 (4): 1354–1364.

[102] Botchwey, C., Dalai, A.K., Adjaye, J. (2006) Simulation of a Two-Stage Micro Trickle-Bed Hydrotreating Reactor using Athabasca Bitumen-Derived Heavy Gas Oil Over Commercial $NiMo/Al_2O_3$ Catalyst: Effect of H_2S on Hydrodesulfurization and Hydrodenitrogenation. *Int. J. Chem. Reactor Eng.*, 4 (A20): 1–15.

[103] Galiasso, T.R. (2006) Diesel Upgrading Into a Low Emissions Fuel. *Fuel Process. Tech.*, 87 (9): 759–767.

[104] Chao, Y.C., Chang, J.S. (1987) Dynamics of a Residue Hydrodesulfurization Trickle Bed Reactor System. *Chem. Eng. Comm.*, 56 (1–6): 285–309.

[105] Oh, M., Jang, E.J. (1997) Rigorous Modelling and Dynamic Simulation of an Industrial Naphtha Hydrodesulfurization Process. *J. Korean Inst. Chem. Eng. (in Korean)*, 35 (5): 791–798.

[106] Chen, J., Ring, Z., Dabros, T. (2001) Modeling and Simulation of a Fixed-Bed Pilot-Plant Hydrotreater. *Ind. Eng. Chem. Res.*, 40 (15): 3294–3300.

[107] Van Parijs, I.A., Froment, G.F. (1984) The Influence of Intraparticle Diffusional Limitations in Naphtha Hydrodesulfurization. I. *Chem. E. Symp. Ser.* 87: 319–327.

[108] Trambouze, P. (1990) Countercurrent Two-Phase Flow Fixed Bed Catalytic Reactors. *Chem. Eng. Sci.*, 45 (8): 2269–2275.

[109] Korsten, H., Hoffmann, U. (1996) Three-Phase Reactor Model for Hydrotreating in Pilot Trickle-Bed Reactors. *AIChE J.*, 42 (5): 1350–1360.

[110] Khadilkar, M.R., Mills, P.L., Dudukovic, M.P. (1999) Trickle-Bed Reactor Models for Systems with a Volatile Liquid Phase. *Chem. Eng. Sci.*, 54 (13–14): 2421–2431.

[111] van Hasselt, B.W., Lebens, P.J.M., Calis, H.P.A., Kapteijn, F., Sie, S. T., Moulijn, J.A., van den Bleek, C.M. (1999) A Numerical Comparison of Alternative Three-Phase Reactors with a Conventional Trickle-Bed Reactor. The Advantages of Countercurrent Flow for Hydrodesulfurization. *Chem. Eng. Sci.*, 54 (21): 4791–4799.

[112] Lopez, R., Dassori, C. G. (2001) Mathematical Modeling of a VGO Hydrotreating Reactor. *SPE Int.*, SPE 69499, 1–14.

[113] Vanrysselberghe, V., Froment, G.F. (2002) Hydrodesulfurization—Heterogeneous. Simulation of Hydrodesulfurization Reactors. In *Encyclopedia of Catalysis*; John Wiley & Sons, New York (Chapters).

[114] Avraam, D.G., Vasalos, I.A. (2003) HdPro: a Mathematical Model of Trickle-Bed Reactors for the Catalytic Hydroprocessing of Oil Feedstocks. *Catal. Today*, 79–80 (1–4): 275–283.

[115] Pedernera, E., Reimert, R., Nguyen, N.L., van Buren, V. (2003) Deep Desulfurization of Middle Distillates: Process Adaptation to Oil Fractions' Compositions. *Catal. Today*, 79–80: 371–381.

[116] Bhaskar, M., Valavarasu, G., Sairam, B., Balaraman, K. S., Balu, K. (2004) Three-Phase Reactor Model to Simulate the Performance of Pilot-Plant and Industrial Trickle-Bed Reactors Sustaining Hydrotreating Reactions. *Ind. Eng. Chem. Res.*, 43 (21), 6654–6669.

[117] Cheng, Z.-M., Fang, X.-C., Zeng, R.-H., Han, B.-P., Huang, L., Yuan, W.-K. (2004) Deep Removal of Sulfur and Aromatics from Diesel Through Two-Stage Concurrently and Countercurrently Operated Fixed-Bed Reactors. *Chem. Eng. Sci.*, 59 (22–23): 5465–5472.

[118] Froment, G.F. (2004) Modeling in the Development of Hydrotreatment Processes. *Catal. Today*, 98 (1–2): 43–54.

[119] Macías, M.J., Ancheyta, J. (2004) Simulation of an Isothermal Hydrodesulfurization Small Reactor with Different Catalyst Particle Shapes. *Catal. Today*, 98 (1–2): 243–252.

[120] Rodríguez, M.A., Ancheyta, J. (2004) Modeling of Hydrodesulfurization (HDS), Hydrodenitrogenation (HDN), and the Hydrogenation of Aromatics (HDA) in a Vacuum Gas Oil Hydrotreater. *Energy Fuels*, 18 (3): 789–794.

[121] Yamada, H., Goto, S. (2004) Advantages of Counter-current Operation for Hydrodesulfurization in Trickle Bed Reactors. *Korean J. Chem. Eng.*, 21 (4): 773–776.

[122] Al-Adwani, H.A.H., Lababidi, H.M.S., Alatiqi, I.M., Al-Dafferi, F.S. (2005) Optimization Study of Residuum Hydrotreating Processes. *Can. J. Chem. Eng.*, 83 (2): 281–290

[123] Jiménez, F., Núñez, M., Kafarov, V. (2005) Study and Modeling of Simultaneous Hydrodesulfurization, Hydrodenitrogenation and Hydrodearomatization on Vacuum Gas Oil Hydrotreatment. *Comp. Aided Chem. Eng.*, 20 (1): 619–624.

[124] Jiménez, F., Kafarov, V., Nuñez, M. (2006) Computer-Aided Modeling for Hydrodesulfurization, Hydrodenitrogenation and Hydrodearomatization Simultaneous Reactions in a Hydrotreating Industrial Process. *Comp. Aided Chem. Eng.*, 21 (1): 651–657.

[125] Jiménez, F., Ojeda, K., Sánchez, E., Karafov, V., Maciel Filho, R. (2007) Modeling of Trickle Bed Reactor for Hydrotreating of Vacuum Gas Oils: Effect of Kinetic Type on Reactor Modeling. *Comp. Aided Proc. Eng.*, ESCAPE17: 1–6.

[126] Broderick, D.H., Gates, B.C. (1981) Hydrogenolysis and Hydrogenation of Dibenzothiophene Catalyzed by Sulfided $CoO\text{-}MoO_3/\gamma\text{-}Al_2O_3$: The Reaction Kinetics. *AIChE J.*, 27 (4): 663–673.

[127] Mostoufi, N., Sotudeh-Gharebagh, R., Ahmadpour, M., Eyvani, J. (2005) Simulation of an Industrial Pyrolysis Gasoline Hydrogenation Unit. *Chem. Eng. Technol.*, 28 (2): 174–181.

[128] Stefanidis, G.D., Bellos, G.D., Papayannakos, N.G. (2005) An Improved Weighted Average Reactor Temperature Estimation for Simulation of Adiabatic Industrial Hydrotreaters. *Fuel Process. Technol.*, 86 (16): 1761–1775.

[129] Nguyen, N.L., Reimert, R., Hardy, E.H. (2006) Application of Magnetic Resonance Imaging (MRI) to Determine the Influence of Fluid Dynamics on Desulfurization in Bench Scale Reactors. *Chem. Eng. Technol.*, 29 (7): 820–827.

[130] Shokri, S., Zarrinpashne, S. (2006) A Mathematical Model For Calculation of Effectiveness Factor in Catalyst Pellets of Hydrotreating Process. *Petroleum Coal*, 48 (1): 27–33.

[131] Murali, C., Voolapalli, R.K., Ravichander, N., Gokak, D.T., Choudary, N.V. (2007) Trickle Bed Reactor Model to Simulate the Performance of Commercial Diesel Hydrotreating Unit. *Fuel*, 86 (7–8): 1176–1184.

[132] Verstraete, J.J., Le Lannic, K., Guibard, I. (2007) Modeling Fixed-Bed Residue Hydrotreatment Processes. *Chem. Eng. Sci.*, 62 (18–20): 5402–5408.

[133] Liu, Z., Zheng, Y., Wang, W., Zhang, Q., Jia, L.(2008) Simulation of Hydrotreating of Light Cycle Oil with a System Dynamics Model. *Appl. Catal. A General*, 339: 209–220.

[134] Liu, Z., Zhang, Q., Zheng, Y., Chen, J. (2008) Effects of Nitrogen and Aromatics on Hydrodesulfurization of Light Cycle Oil Predicted by a System Dynamics Model. *Energy Fuels*, 22 (2): 860–866.

[135] Dudukovic, M.P., Larachi, F., Mills, P.L. (1999) Multiphase Reactors – Revisited. *Chem. Eng. Sci.*, 54 (13–14): 1975–1995.

[136] Gunjal, P.R., Ranade, V.V. (2007) Modeling of Laboratory and Commercial Scale Hydro-Processing Reactors Using CFD. *Chem. Eng. Sci.*, 62 (18–20): 5512–5526.

[137] Sánchez, M., Shah, Y.T., Dassori, C.G. (1995) Multiphase Hydrotreating Reactor Modeling. Presented at the AIChE Spring Meeting, Houston, TX, March 19–24, Hydroprocessing III Session, Paper Number 42b.

[138] Guo, J., Jiang, Y., Al-Dahhan, M.H. (2008) Modeling of Trickle-Bed Reactors with Exothermic Reactions Using Cell Network Approach. *Chem. Eng. Sci.*, 63 (3): 751–764.

[139] Jakobsson, K., Hasanen, A., Aittamaa, J. (2004) Modelling of a Countercurrent Hydrogenation Process. *Trans. IChemE, Part A, Chem. Eng. Res. Des.*, 82 (A2): 203–207.

[140] Toppinen, S., Aittamaa, J., Salmi, T. (1996) Interfacial Mass Transfer in Trickle-Bed Reactor Modelling. *Chem. Eng. Sci.*, 51 (18): 4335–4345.

[141] Taylor, R., Kooijman, H.A., Hung, J.S. (1994) A Second Generation Nonequilibrium Model for Computer Simulation of Multicomponent Separation Processes. *Comput. Chem. Eng.*, 18: 205–217.

[142] Ojeda, J.A., Krishna, R. (2004) In-Situ Stripping of H_2S in Gasoil Hydrodesulphurization – Reactor Design Considerations. *Trans. IChemE, Part A, Chem. Eng. Res. Des.*, 82(A2): 208–214.

[143] Taylor, R., Krishna, R. (1993) *Multicomponent Mass Transfer*, Wiley Series in Chemical Engineering; Wiley: New York; 579 pp.

[144] Iliuta, I., Ring, Z., Larachi, F. (2006) Simulating Simultaneous Fines Deposition Under Catalytic Hydrodesulfurization in Hydrotreating Trickle Beds–Does Bed Plugging Affect HDS Performance? *Chem. Eng. Sci.*, 61 (4): 1321–1333.

[145] Carruthers, J.D., DiCamillo, D. (1988) Pilot Plant Testing of Hydrotreating Catalyst. Influence of Catalyst Condition, Bed Loading and Dilution. *Appl. Catal.*, 43 (2): 253–276.

[146] Furimsky, E., Massoth, F.E. (1999) Deactivation of Hydroprocessing Catalyst. *Catal. Today*, 52 (4): 381–495.

[147] Wärnå, J., Salmi, T. (1996) Dynamic Modelling of Catalytic Three Phase Reactors. *Comput. Chem. Eng.*, 20 (1): 39–47.

[148] Salmi, T., Wärnå, J., Toppinen, S., Rönnholm, M., Mikkola, J.P. (2000) Dynamic Modelling of Catalytic Three-Phase Reactors for Hydrogenation and Oxidation Processes. *Braz. J. Chem. Eng.*, 17 (4–7): 1023–1035.

[149] Hastaoglu, M.A., Jibril, B.E. (2003) Transient Modeling of Hydrodesulfurization in a Fixed-Bed Reactor. *Chem. Eng. Comm.*, 190 (2): 151–170.

[150] Vogelaar, B.M., Berger, R.J., Bezemer, B., Janssens J.-P., van Langeveld, A.D., Eijsbouts, S., Moulijn, J.A. (2006) Simulation of Coke and Metal Deposition in Catalyst Pellets Using a Non-Steady State Fixed Bed Reactor Model. *Chem. Eng. Sci.*, 61 (22): 7463–7478.

[151] Ho, T.C., Nguyen, D. (2006) Modeling of Competitive Adsorption of Nitrogen Species in Hydrodesulfurization. *Chem. Eng. Comm.*, 193 (4): 460–477.

[152] Mederos, F.S., Rodríguez, M.A., Ancheyta, J., Arce, E. (2006) Dynamic Modeling and Simulation of Catalytic Hydrotreating Reactors. *Energy Fuels*, 20 (3): 936–945.

[153] Tsamatsoulis, D., Papayannakos, N. (1995) Simulation of Non-Ideal Flow in a Trickle Bed Hydrotreater by the Cross-Flow Model. *Chem. Eng. Sci.*, 50 (23): 3685–3691.

[154] Lopez, R., Perez, J.R., Dassori, C.G., Ranson, A. (2001) Artificial Neural Networks Applied to the Operation of VGO Hydrotreaters. *SPE Int.*, SPE 69500: 1–10.

[155] Bollas, G.M., Papadokonstantakis, S., Michalopoulos, J., Arampatzis, G., Lappas, A.A., Vasalos, I.A., Lygeros, A. (2004) A Computer-Aided Tool for the Simulation and Optimization of the Combined HDS-FCC Processes. *Trans. IChemE, Part A, Chem. Eng. Res. Des.*, 82 (A7): 881–894.

[156] Bellos, G.D., Kallinikos, L.E., Gounaris, C.E., Papayannakos, N.G. (2005) Modelling of the Performance of Industrial HDS Reactors Using a Hybrid Neural Network Approach. *Chem. Eng. Process.*, 44: 505–515.

[157] Salvatore, L., Pires, B., Campos, M.C.M., De Souza Jr., M.B. (2005) A Hybrid Approach to Fault Detection and Diagnosis in a Diesel Fuel Hydrotreatment Process. *Trans. Eng. Comp. Tech.*, 7: 379–384.

[158] Zahedi, G., Fgaier, H., Jahanmiri, A., Al-Enezi, G. (2006) Artificial Neural Network Identification and Evaluation of Hydrotreater Plant. *Pet. Sci. Technol.*, 24 (12): 1447–1456.

[159] Lukec, I., Sertiæ-Bionda, K., Lukec, D. (2008) Prediction of Sulphur Content in the Industrial Hydrotreatment Process. *Fuel Proc. Tech.*, 89 (3): 292–300.

[160] Sutikno, T. (1999) Optimal HDS for Lower-Sulfur Gasoline Depends on Several Factors. *OGJ*, 97 (June): 55–59.

[161] Bellos, G.D., Gotsis, K.P., Galtier, P.A., Papayannakos, N.G. (2004) The Gas-Liquid Contacting Effects on Liquid Dispersion in Pilot Scale Upflow Hydrotreaters. *Chem. Eng. Sci.*, 59 (7): 1415–1422.

[162] Taylor, R., Krishna, R. (2000) Review Modelling Reactive Distillation. *Chem. Eng. Sci.*, 55 (22): 5183–5229.

[163] Joseph, B., Wang, F.H., Shieh, D.S.S. (1992) Exploratory Data Analysis: A Comparison of Statistical Methods with Artificial Neural Networks. *Comput. Chem. Eng.*, 16 (4): 413–423.

[164] Froment, G.F., Castaneda-Lopez, L.C., Marin-Rosas, C. (2008) Kinetic Modeling of the Hydrotreatment of Light Cycle Oil and Heavy Gas Oil using the Structural Contributions Approach. *Catal. Today*, 130(2–4): 446–454.

[165] Te, M., Fairbridge, C., Ring, Z. (2003) Various Approaches in Kinetics Modeling of Real Feedstock Hydrodesulfurization. *Pet. Sci. Technol.*, 21 (1&2): 157–181.

[166] Inoue, S., Takatsuka, T., Wada, Y., Hirohama, S., Ushida, T. (2000) Distribution Function Model for Deep Desulfurization of Diesel Fuel. *Fuel*, 79 (7): 843–849.

[167] Hu, M.C., Ring, Z., Briker, J., Te, M. (2002) Rigorous Hydrotreater Simulation. *PTQ* Spring: 85–91.

[168] Ho, T.C. (2008) Kinetic modeling of Large-Scale Reaction Systems. *Cat. Review*, 50 (3): 287–378.

[169] Chen, J., Wang, N., Mederos, F., Ancheyta, J. (2009) Vapor-Liquid Equilibrium Study in Trickle-Bed Reactors. *Ind. Eng. Chem. Res.*, 48 (3): 1096–1106.

[170] Cotterman, R.L., Bender, R., Prausnitz, J.M. (1985) Phase Equilibria for Mixtures Containing Very Many Components. Development and Application of Continuous Thermodynamics for Chemical Process Design. *Ind. Eng. Chem. Proc. Des. Dev.*, 24 (1): 194–203.

[171] Cotterman, R.L., Prausnitz, J.M. (1985) Flash Calculations for Continuous Mixtures Using an Equation of State. *Ind. Eng. Chem. Proc. Des. Dev.*, 24 (2): 434–443.

[172] Mueller, G.E. (1991) Prediction of Radial Porosity Distribution in Randomly Packed Fixed Beds of Uniformly Sized Spheres in Cylindrical Containers. *Chem. Eng. Sci.*, 46 (2): 706–708.

[173] Sie, S.T. (1996) Miniaturization of Hydroprocessing Catalyst Testing Systems: Theory and Practice. *AIChE J.*, 42 (12): 3498–3507.

[174] Fott, P., Schneider, P. (1984) Multicomponent Mass Transport with Complex Reaction in Porous Catalyst. In *Recent Advances in the Engineering Analysis of Chemically Reacting Systems*; Doraiswamy, L. K. (ed.); Wiley Eastern: New Delhi, 624 pp.

[175] Salmi, T., Romanainen, J. (1995) A Novel Exit Boundary Condition for the Axial Dispersion Model. *Chem. Eng. Process.*, 34: 359–366.

[176] Kumar, H., Froment, G.F. (2007) Mechanistic Kinetic Modeling of the Hydrocracking of Complex Feedstocks, Such as Vacuum Gas Oils. *Ind. Eng. Chem. Res.*, 46 (18): 5881–5897.

[177] Young, L.C., Finlayson, B.A. (1973) Axial Dispersion in Nonisothermal Packed Bed Chemical Reactors. *Ind. Eng. Chem. Fundam.*, 12 (4): 412–422.

[178] Bosanquet, C. H. (1944) British TA Report BR-507; September 27.

[179] Wilke, C.R., Lee, C.Y. (1955) Estimation of Diffusion Coefficients for Gases and Vapors. *Ind. Eng. Chem.*, 47 (6): 1253–1257.

[180] Satterfield, C.N. (1970) *Mass Transfer in Heterogeneous Catalysis:* MIT Press: Cambridge, MA; 267 pp.

[181] Tyn, M.T., Calus, W.F. (1975) Diffusion Coefficients in Dilute Binary Liquid Mixtures. *J. Chem. Eng. Data*, 20 (1): 106–109.

[182] Weissberg, H. (1963) Effective Difusión Coefficient in Porous Media. *J. Appl. Phys.*, 34: 2636–2639.

[183] Tyn, M.T., Calus, W.F. (1975) Estimating Liquid Molal Volume. *Processing*, 21 (4): 16–17.

[184] Glaso, O. (1980) Generalized Pressure-Volume-Temperature Correlations. *J. Petrol. Tech.*, 32 (5): 785–795.

[185] Ahmed, T. (1989) *Hydrocarbon Phase Behavior*; Gulf Publishing: Houston, TX; 424 pp.

[186] Ancheyta, J., Muñoz, J.A.D., Macías, M.J. (2005) Experimental and Theorical Determination of the Particle Size on Hydrotreating Catalysts of Different Shapes. *Catal. Today*, 109 (1–4): 120–127.

[187] Thiele, E.W. (1939) Relation Between Catalytic Activity and Size of Particle. *Ind. Eng. Chem.*, 31 (7): 916–920.

[188] Zeldovich, Y.B. (1939) On the Theory on Powders and Porous Substances. *Acta Phys. Chim.*, 10: 583.

[189] Ramachandran, P.A., Chaudhari, R.V. (1980) Predicting Performance of Three-Phase Catalytic Reactors. *Chem. Eng.*, 87 (24): 74–85.

[190] Aris, R. (1957) On Shape Factor for Irregular Particles-I. The Steady-State Problem. Diffusion and Reaction. *Chem. Eng. Sci.*, 6 (6): 262–268.

[191] Aris, R. (1965) A Normalization for the Thiele Modulus. *Ind. Eng. Chem. Fundam.*, 4 (2): 227–229.

[192] Aris, R. (1969) *Elementary Chemical Reactor Analysis*; Prentice Hall: New Jersey; 436 pp.

[193] Bischoff, K.B. (1965) Effectiveness Factors for General Reaction Rate Forms. *AIChE J.*, 11 (2): 351–355.

[194] Marroquín, G., Ancheyta, J., Esteban, C. (2005) A Batch Reactor Study to Determine Effectiveness Factors of Commercial HDS Catalyst. *Catal. Today*, 104: 70–75.

[195] Aris, R. (1975) *The Mathematical Theory of Diffusion and Reaction in Permeable Catalysts. The Theory of the Steady State*; Clarendon Press: Oxford; Vol. 1. 429 pp.

[196] Charpentier, J. C., Favier, M. (1975) Some Liquid Holdup Experimental Data in Trickle-Bed Reactors for Foaming and Nonfoaming Hydrocarbons. *AIChE J.*, 21 (6): 1213–1218.

[197] Satterfield, C.N. (1969) Mass Transfer Limitations in Trickle-Bed Reactor. *AIChE J.*, 15 (2): 226–234.

[198] Specchia, V., Baldi, G. (1977) Pressure Drop and Liquid Holdup for Two Phase Concurrent Flow in Packed Beds. *Chem. Eng. Sci.*, 32 (5): 515–523.

[199] Ellman, M.J., Midoux, N., Wild, G., Laurent, A., Charpentier, J.C. (1990) A New, Improved Liquid Hold-up Correlation for Trickle-Bed Reactors. *Chem. Eng. Sci.*, 45 (7): 1677–1684.

[200] Haughey, D.P., Beveridge, G.S. (1969) Structural Properties of Packed Beds—A Review. *Can. J. Chem. Eng.*, 47: 130–140.

[201] Carberry, J., Varma, A. (1987) *Chemical Reaction and Reactor Engineering. Chemical Industries/26*, Marcel Dekker: New York, 1069 pp.

[202] Al-Dahhan, M. H., Dudukovic, M. P. (1995) Catalyst Wetting Efficiency in Trickle-Bed Reactors at High Pressure. *Chem. Eng. Sci.*, 50 (15), 2377–2389.

[203] Ring, Z.E., Missen, R.W. (1991) Trickle-Bed Reactors: Tracer Study of Liquid Holdup and Wetting Efficiency at High Temperature and Pressure. *Can. J. Chem. Eng.*, 69: 1016–1020.

[204] Larkins, R.P., White, R.R., Jeffrey, D.W. (1961) Two-Phase Concurrent Flow in Packed Beds. *AIChE J.*, 7 (2): 231–239.

[205] Ellman, M. J., Midoux, N., Laurent, A., Charpentier, J.C. (1988) A New, Improved Pressure Drop Correlation for Trickle-Bed Reactors. *Chem. Eng. Sci.*, 43 (8): 2201–2206.

[206] Iliuta, I., Ortiz-Arroyo, A., Larachi, F., Grandjean, B.P.A., Wild, G. (1999) Hydrodynamics and Mass Transfer in Trickle-Bed Reactors: an Overview. *Chem. Eng. Sci.*, 54 (21): 5329–5337.

[207] Onda, K., Takeuchi, H., Koyama, Y. (1967) Effect of Packing Materials on the Wetted Surface Area. *Kagaku Kogaku (in Japanese)*, 31: 126–134.

[208] Petrovic, L. J., Thodos, G. (1968) Mass Transfer in the Flow of Gases Through Packed Beds. *Ind. Eng. Chem. Fundam.*, 7 (2): 274–280.

[209] Dwivedi, P.N., Upadhyay, S.N. (1977) Particle-Fluid Mass Transfer in Fixed and Fluidized Beds. *Ind. Eng. Chem. Proc. Des. Dev.*, 16 (2): 157–165.

[210] Bird, R.B., Stewart, W.E., Lightfoot, E.N. (2002) *Transport Phenomena*; John Wiley & Sons: New York, USA; 895 pp.

[211] Evans, G.C., Gerald, C.F. (1953) Mass Transfer from Benzoic Acid Granules to Water in Fixed and Fluidized Beds at Low Reynolds Numbers. *Chem. Eng. Prog.*, 49 (3): 135–140.

[212] Wilson, E.J., Geankoplis, C.J. (1966) Liquid Mass Transfer at Very Low Reynolds Numbers in Packed Beds. *Ind. Eng. Chem. Fundam.*, 5 (10): 9–14.

[213] Goto, S., Smith, J.M. (1975) Trickle-Bed Reactor Performance. Part I. Holdup and Mass Transfer Effects. *AIChE J.*, 21 (4): 706–713.

[214] Satterfield, C.N., Van Eek, M.W., Bliss, G.S. (1978) Liquid-Solid Mass Transfer in Packed Beds with Downward Concurrent Gas-Liquid Flow. *AIChE J.*, 24 (4): 709–717.

[215] Specchia, V., Baldi, G., Gianetto, A. (1978) Solid-Liquid Mass Transfer in Concurrent Two-Phase Flow Through Packed Beds. *Ind. Eng. Chem. Proc. Des. Dev.*, 17 (3): 362–367.

[216] Goto, S., Levec, J., Smith, J.M. (1975) Mass Transfer in Packed Beds with Two-Phase Flow. *Ind. Eng.Chem. Proc. Des. Dev.*, 14 (4): 473–478.

[217] Reiss, L.P. (1967) Cocurrent Gas-Liquid Contacting in Packed Columns. *Ind. Eng. Chem. Proc. Des. Dev.*, 6 (4): 486–499.

[218] Yaïci, W., Laurent, A., Midoux, N., Charpentier, J.C. (1988) Determination of Gas-Side Mass Transfer Coefficient in Trickle-Bed Reactors in Presence of an Aqueous or an Organic Liquid Phase. *Int. Chem. Eng.*, 28 (2): 299–305.

[219] Demaria, F., White, R.R. (1960) Transient Response Study of Gas Flowing Through Irrigated Packing. *AIChE J.*, 6 (3): 473–481.

[220] Fahien, R.W., Smith, J.M. (1955) Mass Transfer in Packed Beds. *AIChE J.*, 1 (1): 28–37.

[221] De Ligny, C.L. (1970) Coupling Between Diffusion and Convection in Radial Dispersion of Matter by Fluid Flow Through Packed Beds. *Chem. Eng. Sci.*, 25 (7): 1177–1181.

[222] Moysan, J.M., Huron, M.J., Paradowski, H, Vidal, J. (1983) Prediction of the Solubility of Hydrogen in Hydrocarbon Solvents Through Cubic Equations of State. *Chem. Eng. Sci.*, 38 (7): 1085–1092.

[223] Ronze, D., Fongarland, P., Pitault, I., Forissier, M. (2002) Hydrogen Solubility in Straight Run Gasoil. *Chem Eng. Sci.*, 57: 547–553.

[224] Riazi, M.R. (2005) *Characterization and Properties of Petroleum Fractions*; ASTM International Standards Worldwide: Philadelphia, USA; 407 pp.

[225] Lal, D., Otto, F.D., Mather, A.E. (1999) Solubility of Hydrogen in Athabasca Bitumen. *Fuel*, 78 (12): 1437–1441.

[226] Magoulas, K., Tassios, D. (1990) Thermophysical Properties of n-Alkanes from C1 to C20 and their Prediction for Higher Ones. *Fluid Phase Equilib.*, 56: 119–140.

[227] Feng, G.X., Mather, A.E. (1993) Solubility of H_2S in n-Hexadecane at Elevated Pressure. *Can. J. Chem. Eng.*, 71: 327–328.

[228] Feng, G.X., Mather, A.E. (1993) Solubility of H_2S in n-Dodecane. *Fluid Phase Equilib.*, 87 (2): 341–346.

[229] Carroll, J.J., Mather, A.E. (1995) A Generalized Correlation for the Peng-Robinson Interaction Coefficients for Paraffin-Hydrogen Sulfide Binary Systems. *Fluid Phase Equilib.*, 105 (2): 221–228.

[230] API. (1997) *Technical Data Book: Petroleum Refining*; Amer. Pet. Inst., Washington, DC; Chap. 8, pp. 8–56.

[231] Soave, G. (1972) Equilibrium Constants for a Modified Redlich-Kwong Equation of State. *Chem. Eng. Sci.*, 27 (6): 1197–1203.

[232] Peng, D.Y., Robinson, D.B. A New Two-Constant Equation of State. *Ind. Eng. Chem. Fundam.*, 15 (1): 59–64.

[233] Brulé, M.R., Starling, K.E. (1984) Thermophysical Properties of Complex Systems: Applications of Multiproperty Analysis. *Ind. Eng. Chem. Proc. Des. Dev.*, 23 (4): 833–845.

[234] Wilke, C. R., Chang, P. (1955) Correlation for Diffusion Coefficients in Dilute Solutions. *AIChE J.*, 1 (2): 264–270.

[235] Lee, B. I., Kesler, M.G. (1975) A Generalized Thermodynamic Correlation Based on Three-Parameter Corresponding States. *AIChE J.*, 21 (3): 510–527.

[236] Poling, E.B., Prausnitz, J.M., O'Connel, J.P. (2001) *The Properties of Gases and Liquids*. McGraw-Hill: New York; 865 pp.

[237] Lee, B.I., Kesler, M.G. (1976) Improve Prediction of Enthalpy of Fractions. *Hydrocarbon Process*, 3 (March): 153–158.

[238] Perry, R.H., Green, D.W., Maloney, J.O. (2004) *Perry's Chemical Engineers' Handbook*; McGraw-Hill: New York; pp 2–193.

[239] Chilton, T.H., Colburn, A.P. (1939) Mass Transfer (Absorption) Coefficients. *Ind. Eng. Chem.*, 26 (11): 1183–1187.

[240] Gupta, S.N., Chaube, R.B., Upadhyay, S.N. (1974) Fluid-Particle Heat Transfer in Fixed Bed and Fluidized Beds. *Chem. Eng. Sci.*, 29: 839–843.

[241] Hashimoto, K., Muroyama, K., Fujiyoshi, K., Nagata, S. (1976) Effective Radial Thermal Conductivity in Cocurrent Flow of Gas and Liquid Through Packed Bed. *Int. Chem. Eng.*, 16 (4): 720–727.

[242] Tarhan, M.O. (1983) *Catalytic Reactor Design*. McGraw-Hill: New York; 372 pp.

[243] Dixon, A.G. (1985) Thermal Resistance Models of Packed-Bed Effective Heat Transfer Parameters. *AIChE J.*, 31 (5): 826–834.

[244] Chung, T.-H., Ajlan, M., Lee, L.L., Starling, K.E. (1988) Generalized Multiparameter Correlation for Nonpolar and Polar Fluid Transport Properties. *Ind. Eng. Chem. Res.*, 27 (4): 671–679.

[245] Cooper, B.H., Donnis, B.B.L., Moyse, B. (1986) Hydroprocessing Conditions Affect Catalyst Shape Selection. *OGJ*, Dec. 8: 39–44.

[246] Whitaker, S. (1973) The Transport Equations for Multi-Phase Systems. *Chem. Eng. Sci.*, 28 (1): 139–147.

[247] Macé, O., Wei, J. (1991) Diffusion in Random Particle Models for Hydrodemetalation Catalysts. *Ind. Eng. Chem. Res.*, 30 (5): 909–918.

[248] Larachi, F., Grandjean, B.P.A. (2009) Excel Worksheet Simulators for Packed-Bed Reactors www.gch.ulaval.ca/bgrandjean/pbrsimul/pbrsimul.html (accessed January 17, 2009).

[249] Mederos, F.S., Ancheyta, J., Chen, J. (2009) Review on Criteria to Ensure Ideal Behaviors in Trickle-Bed Reactors. *Appl. Catal. A General*, 355 (1–2): 1–19.